VOL. 1 No. 4
AUGUST 1959

RNAL OF THE

LESS-COMMON METALS

AN INTERNATIONAL JOURNAL ON
THEIR CHEMISTRY AND METALLURGY

UNIVERSITY OF HA
LIBRARY
FEB 8 '61

S:
THBERTSON (Nottingham)
BROTHER (Manchester)

IAL ADVISORY BOARD:
RD (Paris)
E COOK (Birmingham)
OLY (Brussels)
NGHEUZIAN (Ottawa)
ETCHER (Harwell)
ONSER (Columbus, Ohio)
SEN (Frankfurt a.M.)
ELLI (Genoa)
MM (Münster)
OLL (Corvallis, Ore.)
RAY (Harwell)
OTNY (Vienna)
DGEON (Toronto)
WELL (Wembley)
LSTON (Hyattsville, Md.)
N ARKEL (Leyden)
ORNER (Melbourne)
ITEMA (Menlo Park, Calif.)

ELSEVIER

GENERAL INFORMATION

Types of contributions

(a) Original research work not previously published in other periodicals.
(b) Reviews on recent developments in various fields.
(c) Short communications.
(d) Bibliographical notes and book reviews.

Languages

Papers will be published in English, French or German.

Submission of papers

Papers should be sent to one of the following Editors:

Professor J. W. CUTHBERTSON (*Metallurgy*), Department of Metallurgy, The University, University Park, Nottingham, England.
Dr. F. FAIRBROTHER (*Chemistry*), The University of Manchester, Department of Chemistry, Manchester 13, England.

Authors should preferably submit two copies in double-spaced typing on pages of uniform size. Legends for figures should be typed on a separate page. The figures should be in a form suitable for reproduction, drawn in Indian ink on drawing paper or tracing paper, with lettering etc. in thin pencil. The sheets of drawing or tracing paper should preferably be of the same dimensions as those on which the article is typed. Photographs should be submitted as clear black and white prints on glossy paper.
All references should be given at the end of the paper. They should be numbered and the numbers should appear in the text at the appropriate places.
A summary of 50 to 200 words should be included. Authors of papers in French or German are encouraged to supply also a translation of the summary in English.

Reprints

Twenty-five reprints will be supplied free of charge. Additional reprints can be ordered at quoted prices. They must be ordered on order forms which are sent together with the proofs.

Publication

The *Journal of the Less-Common Metals* will have six issues to the volume, approx. 500 pages per volume.
Subscription price: £ 5.7.6 or $ 15.— or Dfl. 57.— per volume (post free).
For advertising rates apply to the publishers.

Subscriptions

Subscriptions should be sent to:

ELSEVIER PUBLISHING COMPANY, Spuistraat 110-112, Amsterdam-C., The Netherlands.

Just published

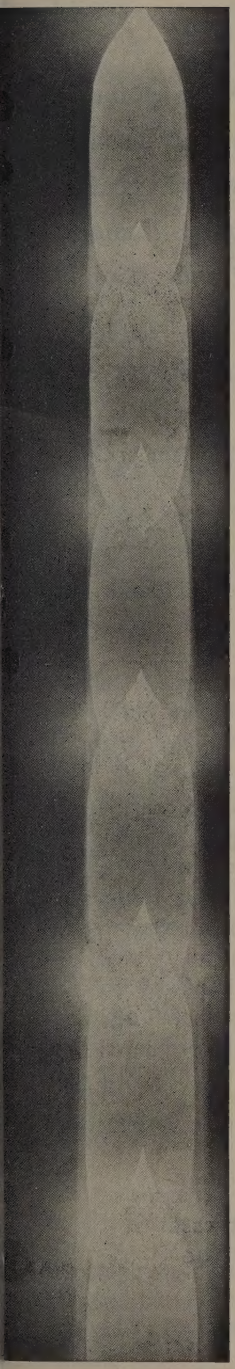

Rocket Propulsion

by

MARCEL BARRÈRE

Head of the Research Division of the Office National d'Études et de Recherches Aéronautiques (ONERA), Paris (France)

ANDRÉ JAUMOTTE

Professor at the University of Brussels (Belgium)

BAUDOUIN FRAEIJS DE VEUBEKE

Professor at the Universities of Liège and Louvain (Belgium)

JEAN VANDENKERCKHOVE

Lecturer at the Aeronautical Institute, University of Brussels (Belgium)

with a preface by **MAURICE ROY**

Member of the Académie des Sciences, General Director of ONERA, Paris (France)

and an introduction by **THEODORE VON KÁRMÁN**

President of the Advisory Group for Aeronautical Research and Development (AGARD)

6×9"
867 pages
71 tables
375 illus.
£ 6.15.0
Dfl. 70.00

Contents

Preface. Introduction. Rocket Propulsion Elements. Nozzle Theory and Characteristic Parameters. Aerothermochemistry of the Combustion Products. Solid Propellants. Internal Ballistics of Solid-Propellant Rockets. Design of Solid-Propellant Rockets. General Study of Liquid-Propellant Rockets. Experimental Techniques for Rocket Propulsion. Liquid Propellants. Combustion Instability in Liquid-Propellant Rockets. Elementary Problems of Over-all Rocket Performance. Variational Methods of Optimizing Rocket Performance. Author Index. Subject Index.

ELSEVIER PUBLISHING COMPANY

110–112 Spuistraat Amsterdam-C

internal stresses and fatigue in metals

Proceedings of a symposium held at the General Motors Research Laboratories, Warren, Mich., 1958

Edited by
Gerald M. Rassweiler
and
William L. Grube

$6\frac{1}{2} \times 9\frac{1}{2}$"
466 pages
229 illus.
1959
72 s.
$ 11.00
Dfl. 37.50

The severe demands of modern technology have focused attention on all types of metal failure, particularly fatigue. There is much phenomenological evidence that fatigue under some conditions is greatly influenced by internal, or "built-in", stresses. The symposium papers lay the groundwork for a better understanding of this relationship by examining the basic nature of internal stresses, fatigue, related phenomena, and their interactions. Special emphasis is placed on the role of lattice imperfections. Authorities in physics, metallurgy and engineering contribute a variety of viewpoints, extensive reviews, and important new research reports.

CONTENTS:

Part I Concepts and Significance of Internal Stresses
Part II Crystal Lattices, Imperfections, and Stresses
Part III Dislocations, Internal Stresses and Fatigue
Part IV Fatigue and Related Phenomena

ELSEVIER PUBLISHING COMPANY

110-112 Spuistraat Amsterdam-C

THE SOLUTION CHEMISTRY OF RHODIUM(III) IN 6 *N* HCl

A. M. KRISTJANSON AND M. LEDERER

Institut du Radium, Laboratoire Curie, Paris (France)

(Received December 28th, 1958)

SUMMARY

On the evidence of absorption spectra and adsorption on a Dowex-2 column rhodium chloride or rhodium hydroxide heated in 6 *N* HCl at 110° reaches equilibrium in approximately one hour. At equilibrium approx. 95% of the rhodium is in the form of hexachlororhodate(III), probably with a small amount of polynuclear chlororhodium complexes but apparently negligible amounts of aquo-chloro-complex anions. During the heating of rhodium hydroxide in 6 *N* HCl the intermediate formation of quite stable aquo-chloro complexes was demonstrated by isolation on Dowex-2 columns and determination of their absorption spectra.

The equilibria of the different aquo-chloro complexes of Rh(III) in solutions of HCl have been investigated by JØRGENSON[1] by spectrophotometry, by COZZI AND PANTANI[2] by polarographic methods and for the more dilute solutions (up to 1 *N*) by one of us[3] by paper electrophoresis and cation exchange chromatography.

From these studies it became evident that several species are always present in solutions up to 6 *N* HCl. The spectrophotometric data of JØRGENSON[1] indicated that at 6 *N* and over either a single species must exist or equilibrium is established instantaneously when a hexachlororhodate(III) is dissolved in 6 *N* (or over) HCl. KRAUS[4] reported that Rh(III) moves on Dowex-1 columns as a fast moving single dark red band. Our preliminary experiments with two commercial grade rhodium chloride samples and one pure grade ammonium chlororhodite showed that when these were dissolved in 6 *N* HCl, several bands were formed on Dowex-2 columns, usually one corresponding to the band described by KRAUS[4]. Standing several days at room temperature did not change the chromatograms of these solutions. It was thus thought of interest to carry out a detailed investigation of the behaviour of Rh(III) in 6 *N* HCl as this seemed the only concentration range for HCl in which analytical ion exchange separations would be possible.

EXPERIMENTAL

The absorption spectra of solutions were determined in the range 340 mμ to 650 mμ using 1 cm glass cells in a Jobin et Yvon spectrophotometer.

In some experiments solutions were heated in pyrex test-tubes in a boiling water-bath but in most of the experiments the solutions were heated under reflux (110°) in an all-pyrex apparatus.

References p. 254

Separations of ionic species were effected on Dowex-2 (200–400 mesh) anion-exchange columns which were 6 mm in diameter and approximately 10 cm in length. The eluting agent used was always 6 *N* HCl.

Rhodium chloride in 6 N HCl

Two commercial preparations of rhodium chloride were used, one that of "Prolabo" (Paris) the other "Caplain St. André" (Paris). Qualitatively the two samples of rhodium chloride showed the same properties in preliminary experiments but all the results reported here were obtained on the "Caplain St. André" preparation.

The samples of rhodium chloride used are dark-red solids which dissolve slowly in 6 *N* HCl. The solutions first obtained are orange-brown in colour and cloudy but on standing for one to two days at room temperature the solutions become clear and are a cherry-red colour. At room temperature the solutions are stable, the absorption spectrum of samples showing very little change on standing for a week at room temperature.

An aliquot of a solution of rhodium chloride in 6 *N* HCl on a Dowex-2 column eluted with 6 *N* HCl gives a fast moving red band (cerise-red in high concentration, pink-red in low concentration) and a red-brown band strongly adsorbed at the top of the column which is not eluted with 6 *N* HCl. The readily eluted red band was consistently found to pass through the column with just over two column volumes of

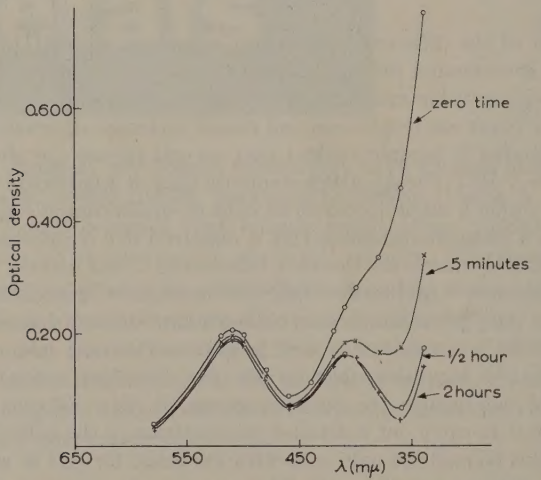

Fig. 1. Change in absorption spectrum of rhodium chloride in 6 *N* HCl with time of heating at 110°.

the eluting 6 *N* HCl. The absorption spectrum of this red band in 6 *N* HCl is in very good agreement with that reported for the hexachlororhodate(III) ion by JØRGENSEN[1].

On heating a solution of rhodium chloride in 6 *N* HCl under reflux (110°) a marked change in the absorption spectrum occurs. As shown in Fig. 1, the strong absorption in the region 340 mμ to 430 mμ decreases and the absorption spectrum

References p. 254

approaches very nearly to that of the hexachlororhodate(III) ion. Although there was a very slight change on heating from $^1/_2$ hour to 2 hours, other experiments showed no change in the spectrum on heating from 1 hour to 3 hours.

We have determined that solutions of hexachlororhodate(III) in 6 *N* HCl give absorption maxima at 512 mμ and 410 mμ (our spectrophotometer) and by dilution to various concentrations with 6 *N* HCl we have found that the variation of the optical density with concentration of $RhCl_6^{-3}$ at these two wave-lengths conforms very well to Beer's law. By isolating the red band of $RhCl_6^{-3}$ from a solution of rhodium chloride in 6 *N* HCl (aged 3 days at room temperature) on a Dowex-2 column and then isolating the $RhCl_6^{-3}$ from a sample of the same solution which had been refluxed 2 hours, we have calculated that approximately 70% of the rhodium in the solution of rhodium chloride (aged 3 days at room temperature) is in the form of hexachlororhodate(III).

An aliquot of a solution, which has been heated until its absorption spectrum is constant, gives only the fast-moving red band ($RhCl_6^{-3}$) on a Dowex-2 column. The absorption spectrum of the red band in 6 *N* HCl, however, is not quite identical with that of the heated solution of rhodium chloride in 6 *N* HCl from which it is obtained. Although we have observed that the spectrum of the red band in 6 *N* HCl remains unchanged over a week at room temperature, we repeatedly found that heating under reflux for 2 hours (in one experiment for 40 minutes) causes a slight but

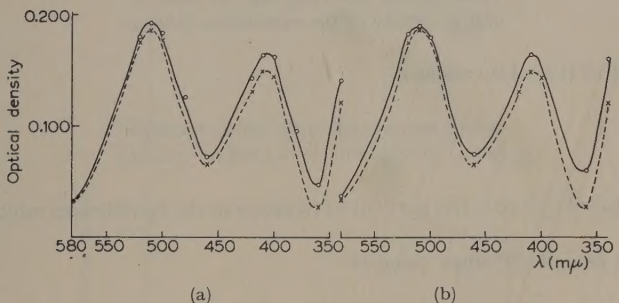

Fig. 2. Absorption spectra of Rh(III) solutions. (a) o——o $RhCl_3$ in 6 *N* HCl refluxed 2 h. 0.5 ml aliquot diluted to 5 ml. ×- - - -× 0.5 ml aliquot of refluxed solution above on Dowex column. Red band eluted with 6 *N* HCl and diluted to 5 ml. (b) ×- - - -× Red band in 6 *N* HCl from (a). o——o Above solution after refluxing for 40 min.

significant change in the spectrum. The spectrum of this heated solution of $RhCl_6^{-3}$ in 6 *N* HCl becomes identical in form with that of the original heated solution of rhodium chloride in 6 *N* HCl. These changes are illustrated in Fig. 2.

A determination of the per cent of rhodium as hexachlororhodate(III) in the equilibrium solutions in 6 *N* HCl at 110° can be made by one of the following methods. A solution of $RhCl_6^{-3}$ in 6 *N* HCl can be obtained by isolation on a Dowex-2 column and the optical density at the absorption maximum (512 mμ) determined for example on a 0.5 ml aliquot diluted to 5 ml. The solution of $RhCl_6^{-3}$ in 6 *N* HCl can then be

References p. 254

refluxed until equilibrium is reached, a 0.5 ml aliquot of the equilibrium solution placed on a Dowex-2 column, eluted with 6 *N* HCl and the red band of $RhCl_6^{-3}$ collected, diluted to 5 ml and its optical density determined. This final value represents the amount of $RhCl_6^{-3}$ in the equilibrium solution, the initial value represents the total rhodium in the equilibrium solution when it was present as $RhCl_6^{-3}$ so that the ratio

$$\frac{\text{optical density of the final } RhCl_6^{-3} \text{ solution}}{\text{optical density of the initial } RhCl_6^{-3} \text{ solution}} \times 100$$

is the per cent of rhodium as $RhCl_6^{-3}$ in the equilibrium solution. Alternatively if we have data for the optical density of a solution of $RhCl_6^{-3}$ and the equilibrium solution obtained by heating this solution of $RhCl_6^{-3}$, we can write this as a ratio

$$\frac{\text{optical density of the equilibrium solution}}{\text{optical density of the initial } RhCl_6^{-3} \text{ solution}}$$

Also if we have data for the optical density of an equilibrium solution and the optical density of the $RhCl_6^{-3}$ in this solution, when isolated on a Dowex-2 column, eluted with 6 *N* HCl and made up to the same volume as the equilibrium solution, we can write this as a ratio

$$\frac{\text{optical density of the final } RhCl_6^{-3} \text{ solution}}{\text{optical density of the equilibrium solution}}$$

The product of these two ratios is

$$\frac{\text{optical density of the final } RhCl_6^{-3} \text{ solution}}{\text{optical density of the initial } RhCl_6^{-3} \text{ solution}}$$

which multiplied by 100 is the per cent of rhodium in the equilibrium solution present as $RhCl_6^{-3}$.

From our data the average value of

$$\frac{\text{optical density of the equilibrium solution}}{\text{optical density of the initial } RhCl_6^{-3} \text{ solution}} = 1.02$$

based on four determinations varying between 1.01 and 1.04; the average value of

$$\frac{\text{optical density of the final } RhCl_6^{-3} \text{ solution}}{\text{optical density of the equilibrium solution}} = 0.93$$

based on five determinations varying from 0.87 to 0.99. The product of these two average values gives the result 0.95 indicating that, according to our calculations, 95% of the rhodium in the equilibrium mixture is present as hexachlororhodate(III). As no elaborate precautions were taken in measuring the volume of aliquots, final volume of diluted solutions etc., this value is liable to be in error by perhaps $\pm$ 5%.

A 0.02 *M* solution of rhodium chloride in 6 *N* HCl was heated under reflux for

References p. 254

2 hours. A 1.0 ml aliquot of this solution was evaporated to dryness in a pyrex beaker, cooled, then the solid redissolved in 10 ml of 6 *N* HCl to give an orange-red clear solution. A 0.5 ml aliquot of this solution on a Dowex-2 column gave the fast moving red band ($RhCl_6^{-3}$), but in addition gave an appreciable amount of a brown band at the top of the column which was not eluted by 6 *N* HCl. The spectrum of the remainder of the solution was taken on aging 1/2 hour, 24 hours and 72 hours. In Fig. 3 we have shown the spectrum of the original equilibrium solution of rhodium chloride in 6 *N* HCl along with the spectra obtained by evaporating the solution to dryness, dissolving the solid residue in 6 *N* HCl and allowing it to age 1/2 hour, 24 hours and 72 hours respectively. Our suggestion is that on heating to dryness there may be an appreciable conversion of hexachlororhodate(III) to dimeric or polymeric bridged-complexes, such as for example

$$H^+ + 2\ RhCl_6^{-3} \rightarrow HCl\uparrow + [Cl_5Rh - Cl - RhCl_5]^{-5}$$

$$2\ H^+ + 2\ RhCl_6^{-3} \rightarrow 2\ HCl\uparrow + [Cl_4Rh\langle^{Cl}_{Cl}\rangle RhCl_4]^{-4}$$

$$4\ H^+ + 3\ RhCl_6^{-3} \rightarrow 4\ HCl\uparrow + [Cl_4Rh\langle^{Cl}_{Cl}\rangle Rh\langle^{Cl}_{Cl}\rangle RhCl_4]^{-5}$$

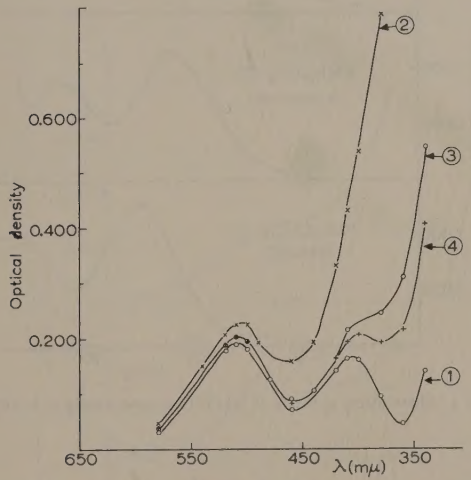

Fig. 3. Absorption spectra of Rh(III). Stability on aging at room temperature of a solution prepared by evaporating to dryness a solution of rhodium chloride in 6 *N* HCl and redissolving the dry residue in 6 *N* HCl. (1) Original solution of rhodium chloride in 6 *N* HCl. (2) Solution (1) evaporated to dryness, residue dissolved in 6 *N* HCl, solution aged 1/2 hour. (3) Solution aged 24 h. (4) Solution aged 72 h.

On aging in a dilute (0.002 *M*) solution there could be an appreciable conversion of polynuclear bridged-complexes to $RhCl_6^{-3}$ by the reverse of the reaction by which the bridged-complexes were formed.

References p. 254

Hexachlororhodate(III), Cu(II) chloride and Co(II) chloride in 6 *N* HCl can be readily separated on a Dowex-2 column, the $RhCl_6^{-3}$ being eluted first followed by Co(II) then by Cu(II). We also found that hexachlororhodate(III) is readily separated from ruthenium(III) chloride in 6 *N* HCl, the $RhCl_6^{-3}$ being readily eluted, the ruthenium(III) very slowly.

Rhodium hydroxide in 6 N HCl

Rhodium hydroxide was prepared from a solution of rhodium chloride in 2 *N* HCl by carefully adding 2 *N* NaOH until just basic. A slight excess of NaOH readily redissolves the precipitate. The rhodium hydroxide precipitates as a golden-yellow gelatinous precipitate which appears brown on centrifuging to a denser precipitate and on heating to dryness yields a brown solid. The precipitated rhodium hydroxide was repeatedly washed until the washings were neutral. Although the precipitate tended

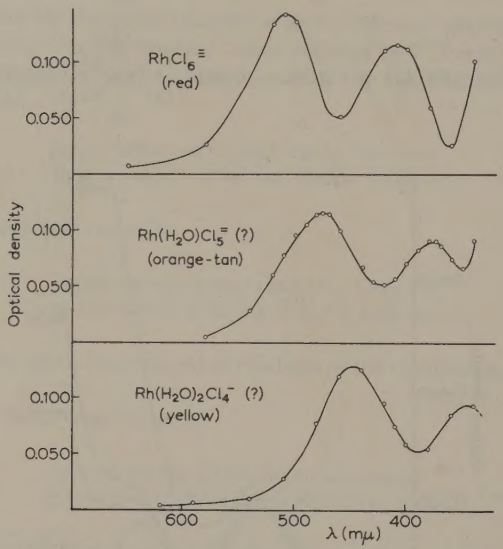

Fig. 4. Absorption spectra of Rh(III) complexes in 6 *N* HCl.

to become colloidal on washing it could be coagulated quite readily by heating in a boiling water-bath. The final washing gave a slight test for chloride, and a small portion of the solid, dissolved in nitric acid, also gave a slight test for chloride.

A precipitate of rhodium hydroxide, well centrifuged and the supernatant water poured off, dissolved very readily in 6 *N* HCl to give a yellow solution approximately 0.02 *M* in rhodium. On aging at room temperature for 2 days, the solution had become an orange-tan colour. The absorption spectrum taken at this time and ten days later showed very little change.

References p. 254

On a Dowex-2 column an aliquot of this orange-tan solution gave, on elution with 6 *N* HCl, a yellow colour which travelled with the eluting solvent, a very fast moving orange-tan band (which passed through the column with 1.4 column volumes of 6 *N* HCl), the red band of $RhCl_6^{-3}$ (which passed through the column with 2.4 column volumes of 6 *N* HCl) and a barely discernible, very slow-moving yellow band.

The orange-tan solution of rhodium hydroxide in 6 *N* HCl was heated in a boiling water-bath and samples taken at 1 h and 3 h. The solution had become red well before 1 h of heating and the absorption spectra on the 1 h sample and the 3 h sample showed only a small change, the spectra being very similar to those of the equilibrium solutions of rhodium chloride in 6 *N* HCl. An aliquot of the 1 h sample on a Dowex-2 column gave only the red band ($RhCl_6^{-3}$), but a yellow colour in the eluate followed later by a tan-coloured eluate was observed prior to elution of the red band. An aliquot of the 3 h sample on a Dowex-2 column gave the same results except that the intensity of yellow and tan colour in the eluate was appreciably less. The spectra of the yellow eluate (from the sample heated 1 h), the tan band and the red band (from an unheated sample) are shown in Fig. 4. From the regular shift in wave-length of the absorption maxima and minima we suggest that the yellow here is due to $Rh(H_2O)_2Cl_4^-$, the tan to $Rh(H_2O)Cl_5^{-2}$ and the red we have identified as $RhCl_6^{-3}$.

Another portion of the rhodium hydroxide precipitate was carefully heated in a pyrex test-tube until a solid brown paste was obtained. This solid dissolved quite

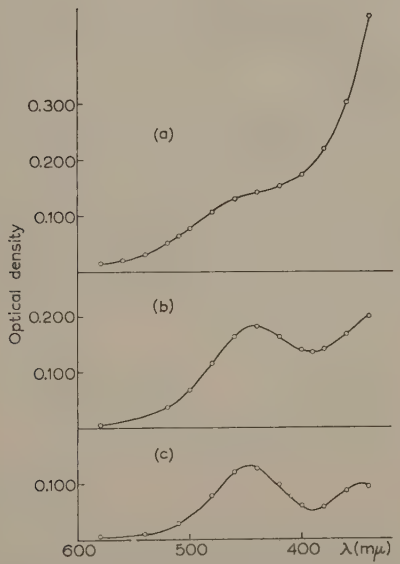

Fig. 5. Absorption spectra of eluate when a solution of rhodium hydroxide in 6 *N* HCl on a Dowex-2 column is eluted with just over 1 column volume of 6 *N* HCl. (a) Aged 1/4 h at room temperature. No adsorption on a Dowex-2 column. (b) Aged 2 days at room temperature. Weak red band ($RhCl_6^{-3}$) and strong tan band ($Rh(H_2O)Cl_5^{-2}$) on a Dowex-2 column. (c) Heated 1 h at 100°. Strong red band ($RhCl_6^{-3}$) and weak tan band ($Rh(H_2O)Cl_5^{-2}$) on a Dowex-2 column.

References p. 254

readily in 6 *N* HCl to yield a yellow solution approximately 0.02 *M* in rhodium. 15 min after the solution was prepared, its absorption spectrum was determined. An aliquot of the yellow solution on a Dowex-2 column passed through the column with the eluting solvent, the spectrum of the yellow eluate being unchanged as compared to that of the solution placed on the column. On aging for 1 day at room temperature, the solution became orange-tan in colour. The solution was heated on a water-bath and samples taken at 1 h and 3 h. As before, the solution became red on heating, the spectra of the heated solutions were essentially the same as in the experiment already described. On a Dowex-2 column, however, no yellow was observed in the eluate and a tan colour only very faintly.

In Fig. 5 we have presented the change in composition of a solution of rhodium hydroxide in 6 *N* HCl on aging as determined by the changes in the absorption spectrum and adsorption on a Dowex-2 column. One quarter of an hour after dissolution in 6 *N* HCl, the solution presumably consists of cationic and neutral species of the general formula $Rh(OH)_a(H_2O)_bCl_c^{-(3-b)}$ (where a + b + c = 6) with some $Rh(H_2O)_2Cl_4^-$ but no evidence for any $Rh(H_2O)Cl_5^{-2}$ or $RhCl_6^{-3}$. After 1 h heating at 100°, however, the solution contains chiefly $RhCl_6^{-3}$, some $Rh(H_2O)Cl_5^{-2}$, a small amount of $Rh(H_2O)_2Cl_4^-$, but evidently quite negligible amounts of other species.

Another sample of rhodium hydroxide was prepared and heated carefully to dryness to yield a brown solid. This product dissolved rather slowly, even with warming, in 6 *N* HCl to give a solution approximately 0.006 *M* in rhodium. The solution was heated under reflux (110°) and samples were taken at 1 h and 3 h. The absorption spectra of these two samples were alike and the same as samples of rhodium chloride in 6 *N* HCl heated under reflux to equilibrium.

Ammonium chlororhodate in 6 N HCl

The "pure grade" ammonium chlororhodite preparation used was obtained from Johnson and Matthey, London, samples of which dissolved in 6 *N* HCl to form orange-red solutions. The absorption spectrum of this solution differed considerably from that of hexachlororhodate(III) although it exhibited absorption maxima at 508 mμ and 405 mμ, shifted slightly from the absorption maxima of solutions of hexachlororhodate(III). An aliquot of this solution on a Dowex-2 column gave a fast-moving tan band and a red band which proved to be hexachlororhodate(III). The absorption

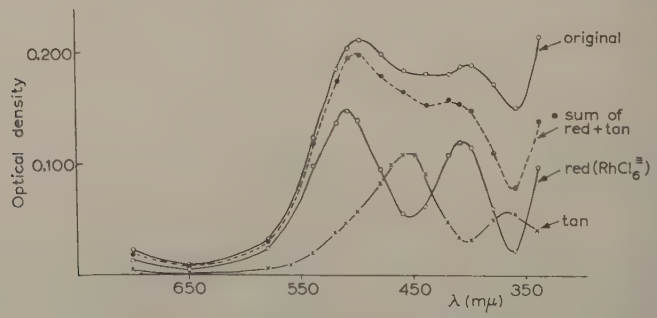

Fig. 6. Absorption spectra of $(NH_4)_3RhCl_6$.

References p. 254

maxima of the tan band in 6 *N* HCl were at 455 mμ and 368 mμ with an absorption minimum at 405 mμ. The absorption maxima are thus shifted to shorter wave-lengths than those of the tan band obtained from a solution of rhodium hydroxide in 6 *N* HCl, a shift one might expect as between $Rh(H_2O)Cl_5^{-2}$ and $Rh(NH_3)Cl_5^{-2}$. As seen in Fig. 6, the spectra of the red band and tan band do not quite add up to the original spectrum indicating that there may be traces of higher ammine complexes of rhodium present.

The solution of ammonium chlororhodite was refluxed 3 h and an aliquot of this solution now gave a barely visible tan band and a strong red band of hexachlororhodate(III). From the optical densities of the hexachlororhodate(III) at 512 mμ it was found that the amount of hexachlororhodate(III) had nearly doubled on refluxing.

CONCLUSIONS

Samples of a commercial preparation of rhodium chloride (Caplain St. André, Paris) on being dissolved in 6 *N* HCl and the solutions aged 2 days at room temperature form cherry-red solutions. The absorption spectra of these solutions show little change on aging at room temperature for periods up to a week at least. Approximately 70% of the rhodium in these solutions is present as hexachlororhodate(III), some portion or all of the remainder of the rhodium is present in a form which on a Dowex-2 column forms a strongly adsorbed red-brown band.

By evaporating to dryness a solution of rhodium chloride in 6 *N* HCl, an operation which might be expected to cause the formation of chloro-bridged complexes, and dissolving the dry residue in 6 *N* HCl, a solution is obtained with an absorption spectrum similar to that of rhodium chloride in 6 *N* HCl. This solution contains approximately 70% of its rhodium in the form of $RhCl_6^{-3}$ and an appreciable amount of a species which forms a strongly adsorbed red-brown band on a Dowex-2 column. The spectrum of this solution on aging changes appreciably, unlike the stable solutions of rhodium chloride in 6 *N* HCl. However, this may be a difference in degree rather than kind.

A solution of rhodium chloride in 6 *N* HCl, on refluxing at 110°, has reached an equilibrium state in 1 h as evidenced by a constant absorption spectrum. A precipitate of rhodium hydroxide, on dissolving in 6 *N* HCl and heating at reflux (110°), has been converted in 1 h to the same equilibrium solution as is reached on heating rhodium chloride in 6 *N* HCl. The rhodium hydroxide must pass through a large number of intermediate complexes before reaching $RhCl_6^{-3}$, evidence for some of which we have obtained. By adsorption on a Dowex-2 column in conjunction with the determination of absorption spectra, we have obtained rather concrete evidence for the series of successive reactions; rhodium hydroxide + 6 *N* HCl → cationic and neutral complexes → diaquotetrachlororhodate(III) → aquopentachlororhodate(III) → hexachlororhodate(III).

We consistently observed that on heating a solution of $RhCl_6^{-3}$ in 6 *N* HCl there was no detectable shift in the wave-length of the absorption maximum at 512 mμ, but there was a slight increase in optical density with a greater increase in optical density of the maximum at 410 mμ and an appreciable increase in optical density of the minimum at 358 mμ. All these changes are essentially the reverse of the changes which occur on the aging of the solution obtained by evaporating a solution of

References p. 254

hexachlororhodate(III) to dryness and dissolving the dry residue in 6 *N* HCl. If aquation to $Rh(H_2O)Cl_5^{-2}$ occurred, we would expect to observe a slight shift to shorter wave-length and a decrease in the optical density of the absorption maximum at 512 mμ rather than the observed slight increase. On the basis of these observations then we would suggest that on heating $RhCl_6^{-3}$ in 6 *N* HCl, a small amount of polynuclear rhodium complexes is formed and exists in equilibrium with hexachlororhodate(III).

A sample of "pure grade" ammonium chlororhodite was shown to have approximately one-half of its rhodium in the form of $RhCl_6^{-3}$. On refluxing in 6 *N* HCl for 3 h at 110°, the rhodium in the sample was largely converted to $RhCl_6^{-3}$ although there was still present, to a slight extent, another form of rhodium which was isolated on a Dowex-2 column. From the spectrum of this "other form" of rhodium and its behaviour on a Dowex-2 column we suggest that it is $Rh(NH_3)Cl_5^{-2}$. This experience suggests the difficulty of preparing pure ammonium chlororhodite without forming complexes such as $Rh(NH_3)Cl_5^{-2}$ and even higher ammine complexes.

Our experience has been that rhodium, either in the form of rhodium chloride or rhodium hydroxide, on refluxing in 6 *N* HCl for an hour is converted to a solution containing approximately 95% $RhCl_6^{-3}$. On a Dowex-2 column $RhCl_6^{-3}$ is eluted very readily, which suggests the feasibility of separating rhodium from other metals by refluxing a mixture of metal chlorides or hydroxides in 6 *N* HCl for 1 h, then separating on a Dowex-2 column. We have found that by this method rhodium is readily separated from cobalt, copper and ruthenium. If, as we have suggested, there are some polynuclear rhodium complexes in equilibrium with $RhCl_6^{-3}$, they probably would be strongly adsorbed on the Dowex-2 columns and complicate separations by this method.

REFERENCES

[1] C. K. Jørgenson, *Acta Chem. Scand.*, 10 (1956) 500.
[2] D. Cozzi and F. Pantani, *J. Inorg. & Nuclear Chem.*, 8 (1958) 385.
[3] M. Lederer, Paper presented to the *Congress on Analytical Chemistry, Moscow, December 1957.*
[4] K. A. Kraus and F. Nelson, *Peaceful Uses of Atomic Energy Conference, Geneva, 1955*, Vol. VII.

THE STUDY OF RHODIUM(III) COMPLEXES BY PAPER ELECTROPHORESIS AND ION EXCHANGE CHROMATOGRAPHY

IV. THE SOLUTION CHEMISTRY OF RHODIUM SULPHATES

S. K. SHUKLA AND M. LEDERER

Institut du Radium, Laboratoire Curie, Paris (France)

(Received December 5th, 1958)

SUMMARY

The solution chemistry of rhodium sulphate was investigated by paper electrophoresis. Conditions for the formation of the yellow and the red rhodium sulphates are discussed.

INTRODUCTION

Two forms of rhodium sulphate were reported by KRAUSS AND UMBACH[1], a yellow one and a red one. They were able to show that the yellow form behaved as if all of the sulphate were ionised and also that the Rh(III) precipitated on addition of KOH. The red form on the other hand had properties that indicated that complexation had occurred. For the complexed form the formula $Rh[Rh(SO_4)_3] \cdot 4$ or $6\ H_2O$ was proposed although it was left unexplained why KOH did not precipitate the first Rh(III).

JØRGENSEN[2] did not investigate the chemistry of rhodium sulphate in solution further than to take an absorption spectrum of a solution of rhodium, prepared from the metal and HNO_3–H_2SO_4 by boiling almost to dryness, for which he reported a maximum at 401 mμ and a shoulder at about 320 mμ.

In a previous communication one of us[3] observed that when $Rh(OH)_3$ is dissolved in H_2SO_4 and electrophorised in a mixture of Na_2SO_4–H_2SO_4 the major fraction is anionic. This band as well as the original solution were yellow.

Since paper electrophoresis had proved of use in investigating the chemistry of Rh(III) in dilute HCl and dilute $HClO_4$ solutions[4,5], a similar investigation of rhodium sulphate was undertaken and will be described here.

METHODS

Paper electrophoresis was carried out with the paper clamped between glass plates as described in previous communications[4–6]. Details of the electrolyte are given in each case. Unless otherwise stated 250 V were applied for 45 minutes. The rhodium could be detected on the paper by spraying with a mixture of $SnCl_2$–KI in HCl and subsequent heating under an infrared lamp.

References p. 262

EXPERIMENTAL

1. *Action of cold H_2SO_4 on rhodium hydroxide*

$Rh(OH)_3$ was dissolved in cold 0.5 *N* and *N* H_2SO_4. In both cases a yellow solution resulted. When electrophorised in either 0.5 *N* or *N* H_2SO_4, two bands were separated from the solution in 0.5 *N* H_2SO_4 and only a single band from the solution in *N* H_2SO_4. Fig. 1 shows these results as well as an electropherogram of the solution in *N* H_2SO_4 with 5% Na_2SO_4–0.1 *N* H_2SO_4 as electrolyte.

The cationic movement of all fractions when H_2SO_4 is used as electrolyte seems to confirm the observations of KRAUSS AND UMBACH[1] that the yellow form is cationic,

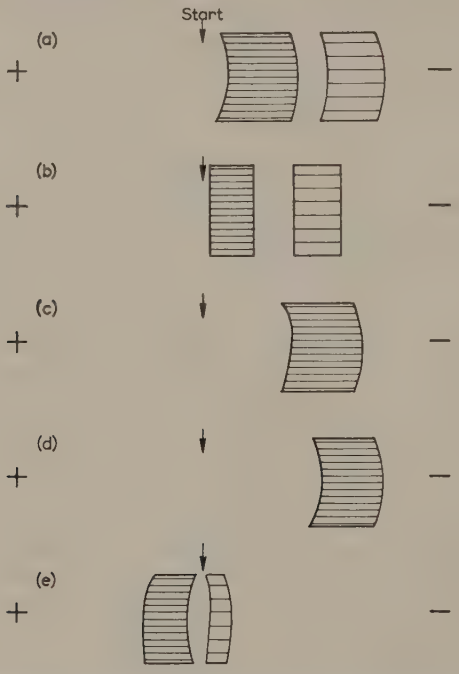

Fig. 1. Electropherograms of solutions of rhodium hydroxide in dilute sulphuric acid. Conditions: 250 V for 45 min. (a) a solution in 0.5 *N* H_2SO_4; electrolyte *N* H_2SO_4. (b) a solution in 0.5 *N* H_2SO_4; electrolyte 0.5 *N* H_2SO_4. (c) a solution in *N* H_2SO_4; electrolyte *N* H_2SO_4. (d) a solution in *N* H_2SO_4; electrolyte 0.5 *N* H_2SO_4. (e) a solution in *N* H_2SO_4; electrolyte 5% Na_2SO_4 + 0.1 *N* H_2SO_4.

i.e. $Rh(H_2O)_6^{+3}$. The presence of a second slower band in the solution in 0.5 *N* H_2SO_4 is probably due to the formation of hydroxy-sulphates, since in other systems the ions $RhOH^{+2}$ and $Rh(OH)_2^{+}$ have been observed when only dilute solutions of acids were used for dissolving $Rh(OH)_3$. The anionic behaviour in presence of Na_2SO_4 will be discussed below.

2. *The properties of solid rhodium sulphate (yellow)*

Solid yellow rhodium sulphate was prepared by dissolving freshly precipitated wash-

ed $Rh(OH)_3$ in cold N H_2SO_4 and evaporating the solution in a vacuum desiccator over conc. sulphuric acid. Before dissolving in H_2SO_4 a portion of the rhodium hydroxide was dissolved in perchloric acid and electrophorised in perchloric acid. One single band was obtained, indicating the absence of coprecipitated Cl^- in the precipitate (for details see ref. [5]).

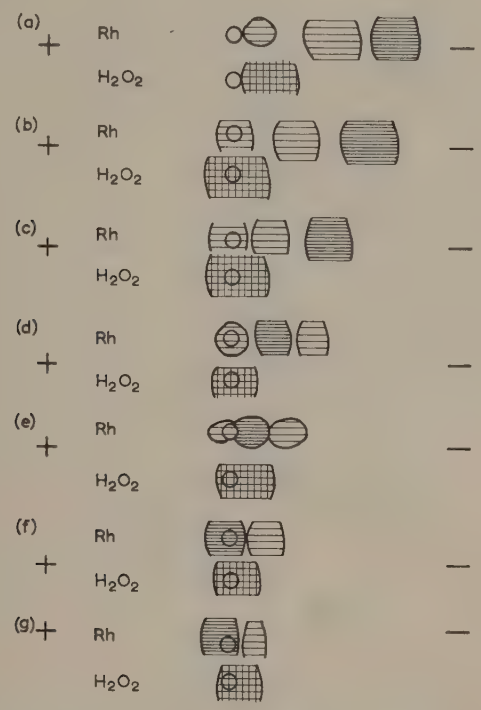

Fig. 2. Electropherograms of solutions of solid yellow rhodium sulphate and hydrogen peroxide on the same paper. Conditions: 250 V for 45 min. Electrolyte: (a) N H_2SO_4. (b) 0.9 N H_2SO_4 + 0.1 N Na_2SO_4. (c) 0.7 N H_2SO_4 + 0.3 N Na_2SO_4. (d) 0.5 N H_2SO_4 + 0.5 N Na_2SO_4. (e) 0.3 N H_2SO_4 + 0.7 N Na_2SO_4. (f) 0.1 N H_2SO_4 + 0.9 N Na_2SO_4. (g) N Na_2SO_4.

The preparation of course contains appreciable amounts of excess H_2SO_4. On dissolving in water a yellow solution was obtained which when electrophorised in N H_2SO_4 yielded several bands as shown in Fig. 2(a).

It appears thus that even under the mild conditions of a vacuum evaporation at room temperature some complexation occurs and rhodium sulphate prepared in this manner cannot be considered as pure rhodium(III) hexaquo sulphate.

. Some experiments on the anionic movement of the yellow sulphate

As shown in Fig. 1 the same yellow form may move cationically and anionically depending on the composition of the electrolyte. Fig. 2 shows the behaviour of a

References p. 262

solution of solid rhodium sulphate (yellow) as described in (2) when varying amounts of Na_2SO_4 and H_2SO_4 are used to prepare an electrolyte of normality = 1.

A spot of hydrogen peroxide was run side by side with the rhodium salt to indicate the electro-osmotic movement which varies with the electrolyte. However, the migration of the rhodium bands does become progressively more anionic as the

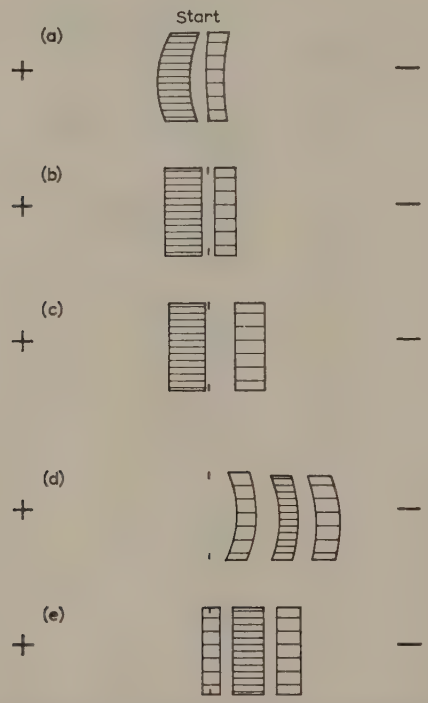

Fig. 3. Electropherograms of solutions of rhodium hydroxide in N H_2SO_4. Conditions: 250 V for 45 min. Electrolyte : (a) 0.9 N Na_2SO_4 + 0.1 N H_2SO_4. (b) 0.9 N K_2SO_4 + 0.1 N H_2SO_4. (c) 0.9 N $(NH_4)_2SO_4$ + 0.1 N H_2SO_4. (d) 0.9 N $MgSO_4$ + 0.1 N H_2SO_4. (e) 0.9 N $ZnSO_4$ + 0.1 N H_2SO_4

H^+ ions are replaced by Na^+ ions. An inversion of sequences occurs at the high Na concentrations where the minor (partially complexed) bands are not affected very much, while the main (hexaquo) band shows a distinct anionic movement.

According to BASOLO AND PEARSON[7] this anionic movement of a cationic ion may be attributed to ion pair formation, which seems to be particularly strong in the case of sulphates. Fig. 3 shows another series of experiments in which we investigated the effect of varying the cation of the electrolyte from Na to K, NH_4, Mg or Zn. Ion pair formation could be observed in the case of K and NH_4 but not with Zn or Mg. We should like to draw attention to the fact that in these cases ion pair formation seems to be limited to those sulphates that form alums in the solid state. Violet Cr(III)

References p. 262

sulphate behaves in paper electrophoresis identically to Rh(III) sulphate as shown in Fig. 4. The amount of ion pair formation in Na_2SO_4 seems to be identical.

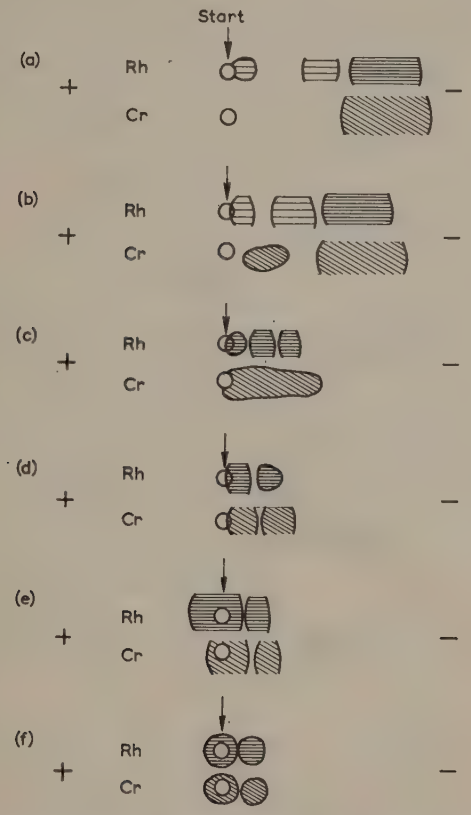

Fig. 4. Electropherograms of solutions of solid yellow rhodium sulphate and of violet chromium sulphate. Conditions: 250 V for 45 min. Electrolyte: (a) N H_2SO_4. (b) 0.7 N H_2SO_4 + 0.3 N Na_2SO_4. (c) 0.5 N H_2SO_4 + 0.5 N Na_2SO_4. (d) 0.3 N H_2SO_4 + 0.7 N Na_2SO_4. (e) 0.1 N H_2SO_4 + 0.9 N Na_2SO_4. (f) N Na_2SO_4.

4. *Effect of boiling on a yellow solution of rhodium sulphate*

A solution of rhodium hydroxide in N H_2SO_4 (*i.e.* the yellow form) was boiled in a test tube over a naked flame for five minutes, cooled and electrophorised in N H_2SO_4. Fig. 5. shows the electropherograms before and after heating. The single cationic band of the original solution is transformed into slower cationic bands. Thus boiling lowers the charge on the hexaquo rhodium(III) ion. Coordination of sulphate groups is most likely in N H_2SO_4.

References p. 262

5. *Experiments with the red form of rhodium sulphate*

According to GAVIS AND SIENKO[8] the red form of rhodium sulphate may be prepared by evaporating a solution of the yellow form on a water-bath. By paper electrophoresis such a preparation was found by us to be a mixture of various complexes.

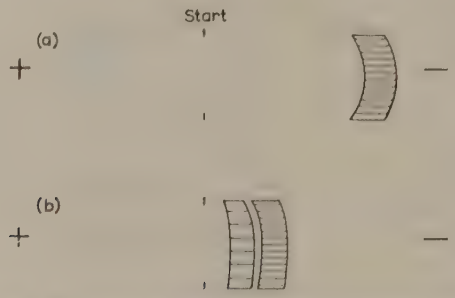

Fig. 5. Electropherograms of a solution of rhodium hydroxide in N H_2SO_4. (a) cold solution; (b) after boiling for 5 min. Conditions: 250 V for 45 min; electrolyte N H_2SO_4.

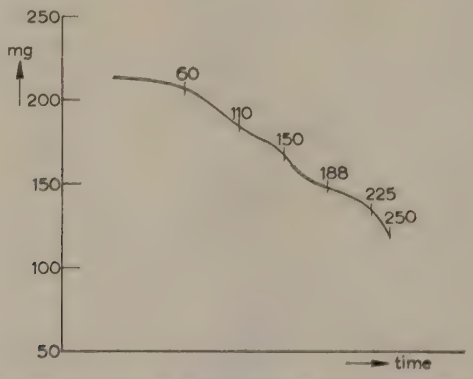

Fig. 6. Thermolysis curve showing the effect of heating on solid yellow rhodium sulphate.

To get an approximate idea of the temperature necessary for a complete transformation we heated a sample on a thermobalance. As shown in Fig. 6 the loss of water occurs in two definite steps, one at 110°, another at about 190°. The amount lost at the second step (30%) corresponds approximately to the water of crystallisation of $Rh_2(SO_4)_3$ 14 H_2O, which has a water content of 33.7%. The loss above 190° is presumably due to sulphuric acid which is still present in our starting product. Heating was discontinued at 250° to avoid decomposition. The dark green brittle compound so formed dissolved readily in water and on electrophoresis in N H_2SO_4 yielded one single rather elongated anionic band. Cationic and neutral bands were absent.

The stability of this solution at room temperature was then examined by electrophorising samples at different intervals for 14 days. Simultaneously a solution o

References p. 262

yellow rhodium sulphate (originally with three cationic bands) was electrophorised at various intervals. The results as shown in Fig. 7 indicate that both tend to establish an equilibrium mixture, although very slowly. The stability of a solution of rhodium hydroxide in N H_2SO_4 is considerably greater than that of the solid yellow rhodium sulphate. A solution allowed to age at room temperature for nine months did not show more than one cationic band, *i.e.* did not change noticeably.

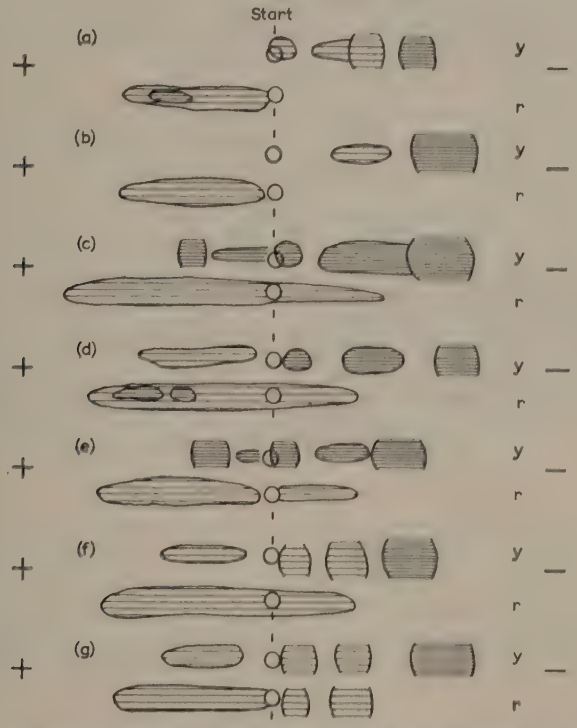

Fig. 7. Influence of aging of yellow and red rhodium sulphate solutions on their electropherograms. Conditions: 250 V for 45 min; electrolyte N H_2SO_4. Aging for: (a) 0 h (fresh solution). (b) 3 h. (c) 18 h. (d) 3 days. (e) 4 days. (f) 6 days. (g) 14 days.

CONCLUSIONS

Our paper electrophoretic study has shown the following behaviour of rhodium(III) sulphate.

1. The yellow rhodium sulphate, in which the Rh(III) is cationic, can be prepared by dissolving freshly precipitated $Rh(OH)_3$ in N H_2SO_4. In 0.5 N H_2SO_4 several presumably basic cations are formed.

When a solution of rhodium sulphate in N H_2SO_4 is heated or evaporated to crystallisation considerable complexation occurs, yielding a mixture of cationically

References p. 262

moving complexes. Solutions that are left at room temperature are stable for months.

2. Ion pair formation seems to occur in solutions of yellow rhodium sulphate containing Na, K or NH_4 sulphates. Depending on the concentration of the alkali sulphate, ion pair formation may produce anionic movement of the yellow rhodium sulphate.

3. Pure red (trisulphato) rhodium sulphate cannot be obtained by heating on the water-bath but may be prepared by heating to 250°. The solution of the red rhodium sulphate so prepared shows first a single anionic band. On standing it tends to form an equilibrium mixture similar to an aged yellow solution which however after 14 days still contains high amounts of anionic rhodium.

ACKNOWLEDGEMENT

The authors are indebted to Prof. CLÉMENT DUVAL for advice and permission to carry out the work with the thermobalance in his laboratory.

REFERENCES

1 F. KRAUSS AND H. UMBACH, *Z. anorg. u. allgem. Chem.*, 180 (1929) 42.
2 C. K. JØRGENSEN, *Acta Chem. Scand.*, 10 (1956) 500.
3 M. LEDERER, *J. Chromatog.*, 1 (1958) 279.
4 M. LEDERER, *Paper presented to the Congress of Analytical Chemistry*, Moscow, Dec. 1957.
5 S. K. SHUKLA, *J. Chromatog.*, 1 (1958) 457.
6 M. LEDERER AND F. L. WARD, *Anal. Chim. Acta*, 6 (1952) 355.
7 F. BASOLO AND R. G. PEARSON, *A Study of Metal Complexes in Solution*, John Wiley and Sons, Inc., New York, 1958.
8 J. GAVIS AND M. J. SIENKO, *J. Am. Chem. Soc.*, 77 (1955) 4983.

REACTIONS OF ORTHO-ESTERS OF TITANIUM

PART I. REACTIONS BETWEEN ISOPROPYL TITANATE AND ACETYL BROMIDE

I. D. VERMA AND R. C. MEHROTRA

Department of Chemistry, University of Gorakhpur (India)

(Received May 21st, 1959)

SUMMARY

The reaction between titanium isopropoxide and acetyl bromide has been studied and the following compounds, $TiBr(OPr^i)_3$, $TiBr_2(OPr^i)_2 \cdot 0.5\ CH_3COOPr^i$, $TiBr_3(OPr^i) \cdot CH_3COOPr^i$ and $TiBr_4 \cdot CH_3COOPr^i$ have been isolated. The tri- and tetra-bromide derivatives sublime with their ester of addition. The great ease with which these compounds exchange their radicals has been demonstrated by the reaction between dibromide and excess tetra-isopropoxide, whereby the monobromide crystallized out in quantitative yield. The monobromides and dibromides react with butanols or butyl acetates, to give products in which the alkoxy groups have been replaced. A number of normal and secondary butoxide derivatives have been isolated, but side-reactions occur in the case of tertiary butoxides, yielding decomposition products. It was shown that the reaction between $TiBr_4 \cdot CH_3COOPr^i$ and excess isopropanol produces $TiBr_2(OPr^i)_2$.

Much work has been carried out on the chloride-alkoxides of titanium[1,2] since the reaction between titanium tetrachloride and alcohols was described by JENNINGS, WARDLAW AND WAY[3]. The only references in the literature however concerning the titanium bromide-alkoxides are the preparation of titanium dibromide di-isopropoxide, by the action of hydrogen bromide on titanium isopropoxide[4] and the formation of $(RO)_2TiBr_2 \cdot ROH$[2,5] by the bromination of $Ti(OR)_4$ in ether and by the action of $TiBr_4$ on $Ti(OEt)_4$ (R = Et, Bu etc).

It was therefore considered worthwhile to find a more convenient and easily controllable method for the preparation of the bromide-alkoxides of titanium. For this purpose acetyl bromide was chosen to effect the replacement of alkoxide radicals.

The reaction between titanium alkoxides and acetyl chloride has been studied by BRADLEY, HANCOCK AND WARDLAW[1]. The analogous reactions between acetyl bromide and titanium isopropoxide were investigated and the products indicated by the following equations could be prepared in quantitative yields by using stoichiometric amounts of the reactants:

$$Ti(OPr^i)_4 + CH_3COBr \longrightarrow TiBr(OPr^i)_3 + CH_3COOPr^i$$

$$Ti(OPr^i)_4 + 2\ CH_3COBr \longrightarrow TiBr_2(OPr^i)_2 \cdot 0.5 CH_3COOPr^i + 1.5\ CH_3COOPr^i$$

$$Ti(OPr^i)_4 + 3\ CH_3COBr \longrightarrow TiBr_3 \cdot OPr^i \cdot CH_3COOPr^i + 2\ CH_3COOPr^i$$

$$Ti(OPr^i)_4 + 4\ CH_3COBr^* \longrightarrow TiBr_4 \cdot CH_3COOPr^i + 3\ CH_3COOPr^i$$

* Or more than 4 moles

References p. 268

These reactions were exothermic and were carried out in benzene solution. The products were isolated by evaporating the solvent under reduced pressure (1–2 mm) at 30–40°. The tendency to bind a molecule of isopropyl acetate of crystallization increases as the Br:Ti ratio in the compound increases, and so much so that the tri and tetra-bromide derivatives appear to sublime along with their ester of addition. These compounds are of particular interest since they may be examples of 5-coördination compounds of titanium. The mono and di-bromide derivatives can be crystallized from isopropanol in which case they appear to bind weakly some isopropanol of crystallization; on drying at 30–40° the products correspond in analyses to $TiBr(OPr^i)_3 \cdot 0.5Pr^iOH$ and $TiBr_2(OPr^i)_2 \cdot 0.5Pr^iOH$. These compounds could be distilled at 100.5°/1.5 mm and 85°/2.5 mm respectively, the distillates solidifying to pale yellow crystalline solids corresponding in analyses to $TiBr(OPr^i)_3$ and $TiBr_2(OPr^i)_2$.

As in the case of the reactions between zirconium alkoxides and acetyl chloride[6], the stoichiometric nature of the reactions indicated a ready exchange of radicals. This was confirmed by refluxing titanium dibromide di-isopropoxide with excess titanium isopropoxide, whereby titanium monobromide tri-isopropoxide crystallized out in quantitative yield.

Furthermore, the reactions of mono and di-bromide derivatives, prepared as above, with higher alcohols[7] or esters[8] of higher alcohols, indicated a ready alcohol or ester interchangeability, thus providing convenient methods for preparing the corresponding derivatives containing the higher alkoxy groups:

$$TiBr(OPr^i)_3 + 3\ BuOH \longrightarrow TiBr(OBu)_3 + 3\ Pr^iOH$$
$$TiBr_2(OPr^i)_2 + 2\ BuOH \longrightarrow TiBr_2(OBu)_2 + 2\ Pr^iOH$$
$$TiBr(OPr^i)_3 + 3\ BuOAc \longrightarrow TiBr(OBu)_3 + 3\ Pr^iOAc$$
$$TiBr_2(OPr^i)_2 + 2\ BuOAc \longrightarrow TiBr_2(OBu)_2 + 2\ Pr^iOAc$$

It was further found that the above interchange reactions are straightforward and can be forced to completion by fractionation in the case of primary and secondary alcohols or their acetates. However, side-reactions occur when the bromide-alkoxides are treated with *tert.*-butanol or *tert.*-butyl acetate, decomposition products being precipitated. This is analogous to the behaviour of the chloride-alkoxides of zirconium[9].

Titanium tetrabromide containing isopropyl acetate of addition has also been found to react with isopropanol to give the dibromide di-isopropoxide:

$$TiBr_4 \cdot CH_3COOPr^i + 2\ Pr^iOH \longrightarrow TiBr_2(OPr^i)_2 + CH_3COOPr^i + 2\ HBr$$

This is of interest in view of the similar reaction between titanium tetrachloride and alcohols and also of the reverse reaction of titanium isopropoxide with hydrogen bromide[4].

EXPERIMENTAL

Apparatus

The reactions were carried out in an all-glass apparatus, with ground joints and with rigid exclusion of moisture. A 60 cm column, packed with Raschig rings and fitted to a total-condensation variable take-off still-head, was used for fractionation.

References p. 268

Materials

Titanium isopropoxide (Peter Spence) was purified by distillation under reduced pressure (b.p. 80°/2 mm). Found: Ti, 16.88%; OPr^i, 83.0%. Calc. for $Ti(OPr^i)_4$: Ti, 16.85%; OPr^i, 83.15%.

Benzene (B.D.H. AnalaR) was first dried over sodium wire and then dried azeotropically with ethanol, over the column.

Acetyl bromide was carefully fractionated, the fraction distilling at 80.5° being collected.

Isopropanol was dried over aluminium isopropoxide and then distilled over zirconium isopropoxide. The *n-*, *sec.-* and *tert.*-butanols were dried over the corresponding sodium butoxides and carefully fractionated (b.p. 117.5°, 100° and 82.9° respectively). The corresponding esters were also purified by careful fractionation.

Analytical methods

Titanium was estimated as dioxide by ignition of the hydroxide obtained by precipitation with dilute ammonia. Bromide was estimated as silver bromide.

Reaction between titanium isopropoxide and acetyl bromide (molar ratio 1 : 1)

Acetyl bromide (5.4 g) was distilled into a solution of titanium isopropoxide (12 g) in benzene (47 g). An exothermic reaction occurred and the light yellow solution thus obtained was refluxed at 110° for an hour. The product was dried at 40°/1.5 mm. A light yellow, fairly mobile, liquid (13.06 g) was obtained. Found: Ti, 16.43%; Br, 29.52%; Ti : Br, 1 : 1.07. Calc. for $TiBr(OPr^i)_3$: Ti, 15.7%; Br, 26.33%.

Isopropanol (30 ml) was added to the above monobromide (12.8 g); an exothermic reaction occurred and the reaction mixture turned into a pale yellow solid mass. This was gently refluxed at 90° and the clear yellow solution thus obtained was set aside for crystallization. The mother liquor was decanted off and the crystals dried at 30°/1.5 mm. Pale yellow crystals (11 g) were obtained, which were soluble in water. Found: Ti, 13.94%; Br, 23.52%; Ti:Br, 1 : 1.01. $TiBr(OPr^i)_3 \cdot 0.5Pr^iOH$ requires: Ti, 14.3%: Br, 23.89%. The compound distilled at 100.5°/1.5 mm, the distillate solidifying to a light yellow crystalline mass. Found: Ti, 15.65%; Br, 26.30%. $TiBr(OPr^i)_3$ requires: Ti, 15.70%; Br, 26.33%.

Reaction between titanium isopropoxide and acetyl bromide (molar ratio 1 : 2)

Titanium isopropoxide (6.3 g), acetyl bromide (5.6 g) and benzene (55 g) were refluxed together at 90° for 2 hours. The product was dried at 40°/1.5 mm. A deep red liquid (9.4 g) was obtained, which developed a few needle-shaped crystals on prolonged standing. Found: Ti, 12.47%, Br, 42.78%; Ti : Br, 1 : 2.05. $TiBr_2(OPr^i)_2 \cdot 0.5CH_3COOPr^i$ requires: Ti, 12.71%; Br, 42.44%.

The above dibromide (9 g) was dissolved in isopropanol and the solution left to crystallize at 5°. The glistening white crystals obtained were dried at 35°/1.5 mm and yielded a bright yellow micro-crystalline powder (3.6 g). Found: Ti, 13.11%; Br, 42.25%; Ti : Br, 1 : 1.94. $TiBr_2(OPr^i)_2 \cdot 0.5Pr^iOH$ requires: Ti, 13.46%; Br, 44.94%. The compound was soluble in cold water and distilled at 85°/2.5 mm, giving a light yellow solid on cooling. Found: Ti, 14.62%; Br, 49.00%. $TiBr_2(OPr^i)_2$ requires: Ti, 14.7%; Br, 49.08%.

References p. 268

Reaction between $TiBr_2(OPr^i)_2$ and excess titanium isopropoxide

Titanium isopropoxide (2.2 g), the dibromide (1.5 g) and isopropanol (13.9 g) were stirred vigorously. The dibromide reacted slowly with titanium isopropoxide and a white finely divided suspension was obtained. The supernatant liquid was decanted off along with some solid and the residue was dried at 50°/5 mm. A pale yellow solid (2.8 g) was obtained. Found: Ti, 15.7%; Br, 23.03%; Ti : Br, 1 : 0.88. Calc. for $TiBr(OPr^i)_3 \cdot 0.5Pr^iOH$: Ti 14.3%, Br 23.89%.

Reaction between titanium isopropoxide and acetyl bromide (molar ratio 1 : 3)

Titanium isopropoxide (7.7 g), acetyl bromide (9.6 g) and benzene (43 g) were refluxed for 2 hours. The product was dried at 60°/1.5 mm. A brown solid (11.3 g) was obtained, which fumed strongly in air and readily dissolved in cold water. Found: Ti, 11.32%; Br, 52.41%; Ti : Br, 1 : 2.77. $TiBr_3(OPr^i) \cdot CH_3COOPr^i$ requires: Ti, 10.67%; Br, 53.46%. The compound sublimed at approximately 105°/1 mm to give a deep red solid, which was highly to sensitive moisture. Found: Ti, 11.4% Br, 54.84%; Ti : Br, 1 : 2.98.

Reaction between titanium isopropoxide and acetyl bromide (molar ratio 1 : 4)

Titanium isopropoxide (10.2 g), acetyl bromide (17.6 g) and benzene (43 g) were refluxed for 3 hours at 90°. The product was dried at 50°/1.5 mm. The dark coloured fuming lumps thus obtained, dissolved readily in cold water yielding a solution with a characteristic sweet smell. Found: Ti, 9.88%; Br, 51.4%; Ti : Br, 1 : 3.088. The product was purified by sublimation at 95°/1.5 mm. The deep red, moisture-sensitive, sublimate also dissolved readily in cold water. Found: Ti, 10.9%; Br, 68.42%; Ti : Br, 1 : 3.75. $TiBr_4 \cdot CH_3COOPr^i$ requires: Ti, 10.1%; Br, 68.08%. A brown residue was left in the flask after sublimation. Found: Ti, 16.87%; Br, 50.58%, Ti : Br, 1 : 1.78.

Alcohol and ester-interchange experiments

For alcohol and ester-interchange experiments (summarized in Tables I and II) the general procedure was the same; brief details will therefore be given in one instance only, the reaction of titanium dibromide di-isopropoxide (2.7 g) and *sec.*-butyl acetate (60 g). The reactants were refluxed at 140–150° under the column, and a fraction was collected at 89° (b.p. of isopropyl acetate). Towards the end, the reaction appeared to become slow and the distillate was collected at a reflux ratio (1:20) until the b.p. became constant (112.50°). The product was dried at 60°/2 mm. A bright yellow powder was obtained. Found: Ti, 11.7%; Br, 39.01%; $TiBr_2(O\text{-}sec.\text{-}Bu)_2 \cdot 0.5 sec.\text{-}BuOAc$ requires: Ti, 11.62%; Br, 38.82%.

On heating at 120–130°/0.5 mm for 1 hour, a slight loss in weight occurred. Found: Ti, 13.61%; Br, 45.4%. Calc. for $TiBr_2(O\text{-}sec.\text{-}Bu)_2$: Ti, 13.53%; Br, 45.19%.

For alcohol interchange experiments, the reaction between bromide alkoxide and butanol (*n*, *sec.* or *tert.*) was carried out in benzene, nearly double the theoretically required amount of butanol being used; the azeotrope was initially collected at 71–72°. Finally, the excess benzene was fractionated at a very high reflux ratio (1 : 20) in order to push the last stages of the reaction to completion. On being freed

References p. 268

of the volatile fractions at 50–60°/1–2 mm, the product appeared to retain 0.4–0.5 mole of butanol of addition, but this was lost on drying at 120–130°/1–2 mm.

In the attempts to interchange the alkoxy group by treatment with *tert.*-butyl acetate or *tert.*-butanol, the reaction appeared to proceed smoothly in the beginning. Soon a dirty yellow solid began to deposit on the sides of the reaction flask (*cf.* the reaction of zirconium chloride isopropoxide with *tert.*-butanol[9]). Bromide could be clearly detected in the distillate which, however, did not give any noticeable test for olefin (a possible decomposition product). Attempts were made to repeat the experiments under as mild conditions as possible, but to a varying extent degradation occurred in all the experiments, and the Br : Ti ratio in the products was lower than that in the starting bromide isopropoxide. Although the reaction could be represented by either of the general mechanisms proposed earlier[9] for the reaction between zirconium chloride isopropoxide and *tert.*-butanol, much more detailed work is necessary before a definite mechanism can be put forward.

TABLE I

REACTIONS OF $TiBr(OPr^i)_3$ WITH BUTANOL OR BUTYL ACETATE

Titanium bromide isopropoxide $TiBr(OPr^i)_3$ *g*	*Butyl alcohol (n-, sec.-, or tert.-BuOH) g*	*Benzene g*	*Butyl acetate (n-, sec.- or tert.-BuOAc)*	*Analyses of products**	
				%Ti	*%Br*
2.1	4.4 (*n*)	60	—	13.90	23.00
1.9	4.0 (*sec.*)	65	—	13.87	23.01
2.0	2.6 (*tert.*)	60	—	14.82	21.94
2.2	—	—	70 (*n*)	13.85	23.02
2.4	—	—	65 (*sec.*)	13.86	23.06
2.1	—	—	60 (*tert.*)	16.00	20.3

* $TiBr(OBu)_3$ requires: Ti, 13.80%; Br, 23.04%.

TABLE II

REACTIONS OF $TiBr_2(OPr^i)_2$ WITH BUTANOL OR BUTYL ACETATE

Titanium bromide isopropoxide $TiBr_2(OPr^i)_2$ *g*	*Butyl alcohol (n-, sec.- or tert.-BuOH) g*	*Benzene g*	*Butyl acetate (n-, sec.- or tert.-BuOAc) g*	*Analyses of products**	
				%Ti	*%Br*
2.2	3.5 (*n*)	70	—	13.52	45.2
2.4	4.1 (*sec.*)	72	—	13.60	45.1
2.3	2.5 (*tert.*)	65	—	15.93	36.7
2.5	—	—	65 (*n*)	13.55	45.2
2.7	—	—	60 (*sec.*)	13.61	45.4
2.5	—	—	60 (*tert.*)	17.5	29.6

* $TiBr_2(OBu)_2$ requires: Ti, 13.53%; Br, 45.19%.

Reaction between titanium tetrabromide containing isopropyl acetate of addition, and excess isopropanol

$TiBr_4CH_3COOPr^i$ (1 g) and isopropanol (8 g) were refluxed at 100° for 2 hours. The reaction mixture was concentrated under reduced pressure and left to crystal-

References p. 268

lize at 5°. The crystals were dried at 40°/1.5 mm. A light yellow micro-crystalline solid was obtained (0.3 g). Found: Ti, 13.41%; Br, 44.97%; Ti : Br, 1 : 2.01. Calc. for $TiBr_2(OPr^i)_2 \cdot 0.5Pr^iOH$: Ti, 13.46%; Br, 44.9%.[7]

ACKNOWLEDGEMENTS

The authors are grateful to Messrs. Peter Spence Ltd., Widnes, Lancashire, for a gift of titanium isopropoxide used in these investigations. One of us (I. D. V.) is indebted to the U.P. Scientific Research Committee for a scholarship, during the tenure of which this work was carried out.

REFERENCES

1 D. C. Bradley, D. C. Hancock and W. Wardlaw, *J. Chem. Soc.*, (1952) 2773.
2 A. N. Nesmeyanov, R. K. Freidlina and O. V. Nogina, *Izvest. Akad. Nauk S.S.S.R., Otdel. Khim. Nauk*, (1951) 518.
3 J. S. Jennings, W. Wardlaw and W. J. R. Way, *J. Chem. Soc.*, (1936) 637.
4 R. C. Mehrotra, *J. Indian Chem. Soc.*, 32 (1955) 761.
5 A. N. Nesmeyanov, E. M. Brainina and R. K. Freidlina, *Izvest. Akad. Nauk S.S.S.R., Otdel. Khim. Nauk*, (1955) 838.
6 D. C. Bradley, F. M. A. Halim, R. C. Mehrotra and W. Wardlaw, *J. Chem. Soc.*, (1952) 4609.
7 D. C. Bradley, R. C. Mehrotra and W. Wardlaw, *J. Chem. Soc.*, (1952) 2027, 4204 and 5020.
8 R. C. Mehrotra, *J. Am. Chem. Soc.*, 76 (1954) 2266.
9 D. C. Bradley, F. M. A. Halim, R. C. Mehrotra and W. Wardlaw, *J. Chem. Soc.*, (1952) 4960.

THE FABRICATION AND PROPERTIES OF RUTHENIUM

D. W. RHYS

The Mond Nickel Company Ltd., Research and Development Department, London (Great Britain)

(Received May 22nd, 1959)

SUMMARY

Sintered powder compacts were the best starting material for the fabrication of strip and rod, but purity, powder preparation and sintering conditions required careful control if satisfactory products were to be obtained. Control of these variables was followed by hardness, density and metallographic examination. Ruthenium developed directional properties during working and these were not removed by annealing. Single crystal ruthenium prepared by floating zone electron bombardment melting had good initial ductility but work hardened very rapidly; annealing of worked single crystals produced brittle polycrystalline material. During zone refining of ruthenium major purification occurred by evaporation.

The properties of ruthenium with particular reference to its ductility and possible applications are discussed.

INTRODUCTION

In the periodic classification of the elements, ruthenium is the first member of the second series of the Group 8 transition elements having as its horizontal neighbours technetium (Group 7) and rhodium, and as its vertical neighbours iron and osmium. It is one of the six platinum metals which in the periodic system are divided into two triad groups, the light group comprising ruthenium, rhodium and palladium, and the heavy group, osmium, iridium and platinum.

Comparison of the physical and metallurgical properties of ruthenium, its immediate neighbours and fellow members of the platinum group indicate that it is most closely allied to osmium and this vertical relationship is largely what might be expected and is also found with other members of the Group 8 metals.

At room temperature ruthenium has a close packed hexagonal type structure, with a small axial ratio, the values of lattice parameters being $a = 2.7003$ Å, $c = 4.2730$ Å, $c/a = 1.5824$. The density of the metal calculated from these parameters and an atomic weight of 101.7 is 12.43 grams/c.c. The melting point of the metal has not been determined accurately, but is usually recorded as 2500°C and the boiling point is estimated as 4230°C.

There is very little published information on the working technology of ruthenium, which is normally considered as a non-ductile metal. C. S. SIVIL[1] states that the metal has never been worked although according to A. JOLY[2] the metal, which is brittle when cold is slightly malleable at a dull red heat.

References p. 291

Metallurgically ruthenium is seldom employed in the elemental form, and this is due, not so much to its rarity as to the difficulties of fabrication. The melting point of ruthenium is too high for it to be conveniently cast into useful shapes and its lack of ductility prevents it being worked to such forms as strip and wire; consequently fabrication is possible only by pressing and sintering, with the inherent limitations of this technique.

Ruthenium is most often used as a hardener for platinum or palladium, and in this respect is particularly effective, the platinum–5% ruthenium alloy having properties comparable with the platinum-10% iridium alloy. It is also employed in certain hard alloys used for tipping the nibs of fountain pens. Minor additions of ruthenium, of the order of 0.1% have been used to refine the grain size and improve the mechanical properties of gold- and silver-base casting alloys, particularly those used in dentistry.

Ruthenium is resistant to attack by all mineral acids including aqua regia. On the other hand it has relatively poor resistance to high temperature oxidation, attack occurring by formation of a volatile oxide with resultant wasting of the

TABLE I

OXIDATION OF RUTHENIUM RODS 1.0 in. × 0.20 in. DIAMETER IN STILL AIR

Temperature (°C)	*Time (hours)*	*Loss in weight (percent)*	*Loss in weight (percent/hour)*
900	90	0.41	0.0045
1000	90	2.06	0.027
1100	90	7.11	0.079
1200	90	20.33	0.226
1300	90	67.75	0.753
1400	90	100.0	> 1.0
1500	61	98.23	1.64

metal. Figures indicating the rate of oxidation of ruthenium in still air are given in Table I. Possibilities of using ruthenium under oxidising conditions are therefore limited to moderately low temperatures. The rate of oxidation of ruthenium at high temperatures is, however, considerably less than the corresponding rate for molybdenum, and it is possible that it might be used in applications where oxidising conditions are too severe for use of this metal. The high-temperature strength of ruthenium has not yet been determined but is possibly of the same order as that of molybdenum.

Ruthenium might also be used to a greater extent in the field of electrical contacts where its resistance to tarnish at room temperature under the most adverse conditions would be of importance.

Ruthenium has the lowest neutron capture cross section of all the platinum metals, which coupled with its high resistance to corrosion in liquid media could be of interest in nuclear engineering.

Another useful attribute of ruthenium is its resistance to attack by the liquid metals, lead and bismuth. While the solubility of ruthenium in liquid lead is known to be small, no reliable figures are available. The solubility of ruthenium in liquid bismuth has been determined as 0.029% at 700°C and 0.106% at 1200°C.

References p. 291

REFINING OF RUTHENIUM

The refining of ruthenium has been described in some detail by JOHNSON AND ATKINSON[3] and also by GILCHRIST[4]. Ruthenium always occurs in association with the other platinum metals, and the main processes are concerned essentially with separation from other members of this group.

The concentrate of platinum metal is treated with aqua regia which dissolves platinum, palladium and any gold present. The residue is smelted with litharge and reducing fluxes to give a lead alloy from which lead and silver are dissolved by treatment with nitric acid, leaving a residue of rhodium, ruthenium, osmium and iridium. This residue is fused with potassium bisulphate and the cake treated with water; the rhodium is taken into solution, the insoluble portion retaining ruthenium, osmium and iridium. This is now fused with a mixture of potassium hydroxide and potassium nitrate which converts the ruthenium and osmium to the water-soluble potassium ruthenate and potassium osmate, leaving a residue of iridium.

TABLE II

SPECTROGRAPHIC ANALYSIS OF RUTHENIUM POWDERS

Ruthenium batch reference	*Impurity (per cent)*					
	Palladium	*Osmium*	*Rhodium*	*Silver*	*Nickel*	*Iron*
A	0.005	0.01	0.002	>0.0001	0.001	0.003
B	0.002	0.02	0.002	>0.0001	0.001	0.008
C	0.001	0.01	0.002	>0.0001	0.0006	0.007
D	0.002	0.14	0.001	>0.0001	0.006	0.005
E	0.001	0.01	0.002	>0.0001	0.0006	0.001
F	0.002	0.01	—	>0.0001	0.0025	0.001
G	0.002	0.02	0.001	—	0.003	0.001
H	<0.001	<0.01	0.001	0.0001	0.0001	0.0015
I	<0.001	<0.01	0.001	>0.0001	0.0001	0.002
K	<0.001	<0.01	0.003	>0.0001	0.0012	0.007

Traces of copper, lead, aluminium and manganese detected in all samples in varying amounts. Concentration not known but estimated as greater than 0.0001%.
Traces of tin in varying amounts detected in all samples except I and K. Estimated limit of detection 0.0001%.
Traces of silicon detected in unestimated quantities in all samples except H.
Gold was only sought in samples I and K and was detected in both samples in quantities greater than 0.0001%.
Not detected in any sample : platinum, iridium, arsenic, cadmium, gallium, germanium, mercury, indium, potassium, sodium, phosphorus, tantalum, thallium, vanadium and zinc.

Osmium is separated from the solution at this stage, if present in appreciable amount, by strongly acidifying with nitric acid and boiling, when it distils as volatile osmium tetroxide; the ruthenium solution is then made strongly alkaline, heated, and a stream of chlorine passed through it causing the ruthenium to distil as the tetroxide which is collected in a solution of hydrochloric acid, from which ruthenium chloride can be obtained by evaporation.

Ruthenium chloride is converted to the metal by ignition and reduction either

References p. 291

directly, or after treatment and conversion to ammonium ruthenium chloride. In the preparation of solid ruthenium by powder metallurgical methods, the mode of preparation of the ruthenium powder may be of some importance as described later.

INVESTIGATIONS OF THE WORKING TECHNOLOGY OF RUTHENIUM

1. *Purity*

The lack of ductility of ruthenium has been attributed by SIVIL[1] to its crystal form, but this explanation by itself is unlikely since other hexagonal metals of similar axial ratio have proved reasonably amenable to forming operations. A contributory cause of the poor results obtained in working ruthenium may be the presence of impurities and in the present investigation of a suitable technology for working the metal, several batches of ruthenium powder of different purities were examined. With three exceptions these ruthenium powders represented material that had been refined by conventional processes, and variation in purity was such as may occur from batch to batch processed under similar conditions. In one of the other batches (I) additional oxidation treatments with nitric acid were given in order to remove further osmium, and in the other two (H and K) the ruthenium tetroxide distillation was also repeated with the object of lowering the concentration of other impurities.

Spectrographic analysis of these samples of ruthenium are given in Table II. Unfortunately, spectrographic standards were not available for a number of elements, among them elements such as silicon, which might have an important influence on the ductility of ruthenium.

2. *Powder metallurgy — Preparation of powders*

Powder was produced from ruthenium chloride solution by four methods:

(a) The ruthenium chloride solution was evaporated and was then ignited in air at 500°C followed by reduction in hydrogen at 600°C with a final ignition at 900°C and subsequent cooling under hydrogen. Batch A was prepared by this method.

(b) Ammonium ruthenium chloride was precipitated from the chloride solution by addition of ammonium chloride. The filtered and dried salt was ignited in air at 500°C followed by reduction in hydrogen at 600°C with a final ignition at 900°C and subsequent cooling under hydrogen. Batch C was prepared by this method.

(c) Ammonium ruthenium chloride prepared as for (b) was ignited in air at 450°C followed by reduction in hydrogen at 450°C and a final ignition at 600°C and subsequent cooling under hydrogen. Batches B, D, E, F and G were prepared by this method.

(d) Ammonium ruthenium chloride prepared as for (b) was ignited in air at 400°C and subsequently ignited at 500°C and cooled in hydrogen. Batches H, I and K were prepared by this method.

Sieve analyses of the powders obtained by these four methods are given in Table III. No sub-sieve size analysis was made though it is probable that this analysis would in actual fact be of greater importance in determining the behaviour of the powders on pressing and sintering, as it was normally found preferable to use the minus 330 mesh powder for the preparation of compacts, and these sieved powders varied markedly between batches, in respect to compacting qualities.

Shadow photographs of some of the powders are shown in Figures 1–4.

References p. 291

3. *Powder metallurgy – Pressing of compacts*

Compacts were pressed by two methods, first the conventional method employing a steel die and plunger, and secondly by pressure applied hydrostatically using a rubber bag as described by DAVIS, DENSEM AND RENDALL[5]. For any but the smallest

TABLE III

SIEVE ANALYSIS OF RUTHENIUM POWDERS

Batch reference	*Method of preparation*	*Larger than 60 mesh*	*60–100 mesh*	*100–160 mesh*	*160–200 mesh*	*200–240 mesh*	*240–330 mesh*	*Finer than 330 mesh*
A	Ignition of ruthenium chloride at 900°C.	Nil	21%	13%	3%	2%	1%	60%
B	Ignition of ammonium ruthenium chloride at 600°C.	Nil	10%	Nil	2%	2%	6%	80%
C	Ignition of ammonium ruthenium chloride at 900°C.	Nil	21%	13%	3%	2%	1%	60%
H	Ignition of ammonium ruthenium chloride at 500°C.	Nil	Nil	1%	Nil	Nil	1%	98%

compacts pressed in a steel die, it was found essential to employ a binder, and for this purpose 5% weight of camphor was the most satisfactory additive: the pressure employed was also somewhat critical and of the order of 25 ton/sq.in. Hydrostatically pressed compacts did not require a binder; a pressure of 25 ton/sq.in. was employed in the preparation of all these compacts.

The approximate sizes of compact normally produced were, in the green state: steel die pressings 2 in. × 0.5 in. × 0.5 in., weighing about 60 grams, and hydrostatic pressings 6 in. × 0.4 in. diameter, weighing 50–80 grams.

4. *Powder metallurgy – Sintering*

Sintering temperatures up to 2200°C were used, though in the majority of experiments a maximum temperature of 1500°C was employed. For temperatures up to 1600°C heating was carried out in resistance furnaces using alumina tubes, but for higher temperatures self heating of the compacts by passage of current through them was employed. Four sintering atmospheres were used:

(a) Bottle hydrogen.

(b) Vacuum produced by a two-stage rotary pump (About 0.005 mm mercury, Pirani gauge reading).

(c) Vacuum produced by an oil-diffusion pump (Less than 0.0001 mm mercury, Pirani gauge reading).

(d) Vacuum produced by mercury diffusion pump with liquid air trap (Less than 0.00005 mm mercury, Phillips gauge reading).

References p. 291

Fig. 1. Reference A.

Fig. 2. Reference B.

Fig. 3. Reference C.

Fig. 4. Reference D.

Photomicrographs of synthetic mixtures of erythrosin powders (× 750)

Atmospheres (a), (b) and (c) were used when sintering was performed in alumina tube furnaces, and atmosphere (d) when sintering was by self heating.

5. *Powder metallurgy – Mechanical working*

Mechanical working operations on sintered ruthenium compacts were attempted between room temperature and 1800°C, the modes of deformation employed including pressing, hammering, swaging, strip rolling and rod rolling. In the hot working experiments heating was either in a resistance furnace using air, hydrogen, or nitrogen–hydrogen mixtures or by torch heating using an oxy–coal gas flame. Experiments were also made in which the compacts were enclosed in evacuated platinum envelopes for hot working operations.

6. *Powder metallurgy – Effect of various factors on mechanical working characteristics*

It was observed that the mode of preparation of the ruthenium powder had a marked effect on the compacting properties where this was carried out in steel dies, and that if compaction was made using an unsuitable powder there was considerable risk of splitting on release of pressure or during the subsequent sintering process. Powder prepared by sieving through minus 330 mesh was much more suitable for the preparation of compacts than powder containing coarse particles, but using ruthenium Batch C, which had been prepared by the ignition of ammonium ruthenium chloride at 900°C, it was found difficult to produce sound compacts by the die and plunger method on either sieved or unsieved powders. Powder prepared by ignition of ruthenium chloride at this temperature, or ammonium ruthenium chloride at the lower temperatures, was suitable for pressing, and as the low-temperature ignited material gave a better yield of fine powder, this was the normal method of preparation employed. Compacting qualities did not appear to be affected appreciably either by powder size or mode of preparation, when hydrostatic pressing was employed.

The workability of compacts varied considerably according to the batch of powder used, and there is little doubt that the purity of the metal has a considerable effect on its working properties, though it is not clear which particular impurities have an adverse effect. The compacts prepared from batches H, I and K were the most amenable to forging and rolling operations, and these references were those in which extra refining treatments had been given. Batches A and B were next in order of merit and references F and C were only of slightly inferior quality provided a good compact could be obtained during the pressing and sintering stages of the latter. On the other hand batches D and G were entirely unsuitable for working, failure occurring by cracking at very early stages in the forging operations. Batch D had a high osmium content but other impurities as indicated by spectrographic analysis were not appreciably higher than with more satisfactory references, while Batch G did not appear to have a higher level of impurities than some references of reasonably satisfactory quality. The difference in workability of the batches to which additional purification treatments had been given and other batches is however very marked, though apart from the absence of detectable quantities of osmium, there is only a general slightly lower level of other impurities. It is difficult to imagine that osmium, a closely allied element to ruthenium should have a marked effect on its ductility when present in trace quantities only.

The sintering atmosphere was also found to have an important bearing on the

References p. 291

workability of the compacts obtained. There was comparatively little difference between the workability of compacts sintered in bottle hydrogen, and in the vacuum, about 0.005 mm mercury pressure, produced by a two-stage rotary pump, but considerably improved workability was obtained if sintering took place in a vacuum produced by a diffusion pump, about 0.0001 mm mercury pressure.

The temperature of sintering did not appear to have an important effect on workability provided it was in excess of 1450°C; rate of heating to sintering temperature, and time of soaking also appeared unimportant though these aspects were not fully investigated for temperatures above 1600°C.

The temperature of hot working of compacts was not critical and a temperature as low as 1200°C could be used throughout hot working operations, though results were somewhat more satisfactory if during the early stages of forging, the temperature was in the region of 1450-1500°C. There appeared to be no special advantage

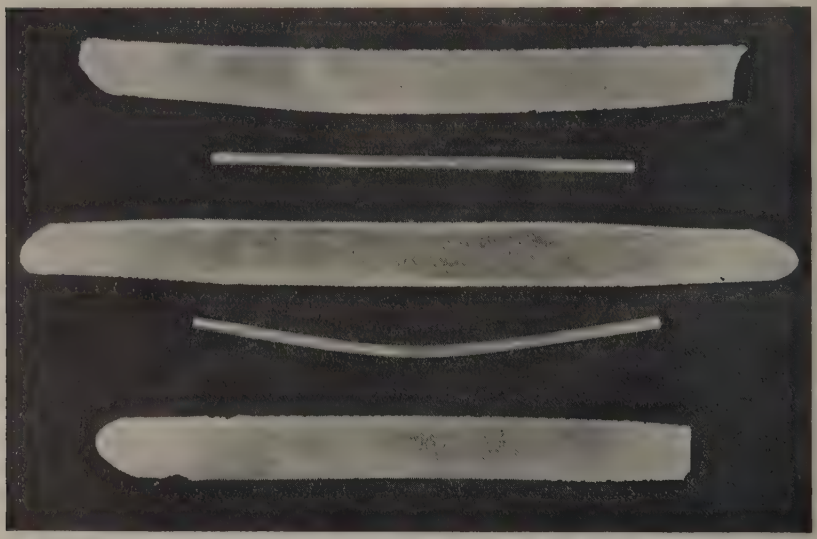

Fig. 5. Examples of hot rolled ruthenium strip 0.020 in. thickness, and swaged rods 0.20 in. diameter (× 3/8 approx.).

in working at temperatures as high as 1800°C. Workability was not dependent on the furnace atmospheres used during forging, air, hydrogen, and hydrogen-nitrogen mixtures being employed without noticeable difference. It was however, advantageous to give one or two intermediate anneals in vacuo at 1500°C during hot working.

Ruthenium enclosed in evacuated platinum envelopes forged and rolled rather more readily than metal exposed to atmosphere during hot working. However, the cold ductility of the platinum-clad ruthenium produced by this method was no greater than that of material produced without cladding.

Cold working was achieved in two circumstances only, first in pressing small sintered

References p. 291

discs having a thickness to diameter ratio of less than 0.4, and secondly in rolling thin strip prepared by hot working. In both instances reductions not much greater than 10% could be obtained between anneals without cracking of the metal, and after a total of 50 per cent reduction further annealing failed to restore any degree of cold ductility. Despite the small amount of reduction, cold-worked ruthenium recrystallised after annealing at 1200°C though usually vacuum heat treatment at 1500°C was employed for softening treatment.

No attempts were made to roll at elevated temperatures below that of recrystallisation.

Using suitably prepared compacts it was possible, on a laboratory scale, using hot followed by cold-rolling to produce ruthenium strip 0.010 in. in thickness, the

Fig. 6. Single crystal bar of ruthenium 3/8 in. diameter, prepared by electron bombardment zone melting. Bent by hand through nearly 180° (× 3/8 approx.).

resultant material however tending to be extremely brittle. Strip 0.02 in. in thickness, produced by hot rolling only, was considerably more ductile, though it could not be considered satisfactory in this respect. The minimum diameters obtained in rod specimens were 0.130 – 0.150 in., produced by hot swaging. Swaging to sizes below this diameter resulted in torsional fracture of the ruthenium. Fig. 5 illustrates some examples of forged and rolled ruthenium.

7. *Melted ruthenium*

In addition to its high melting point, ruthenium suffers from a similar disadvantage to silver, palladium, and rhodium in dissolving large quantities of oxygen when liquid and rejecting it on solidification. The most satisfactory methods of melting ruthenium appear therefore to be in argon or vacuum arc furnaces.

References p. 291

In the argon arc melting of ruthenium an argon pressure of 20 cm mercury was used, and the argon was 'gettered' by melting a titanium button before melting the ruthenium. In some instances the ruthenium was melted as many as thirty times with intermediate 'gettering' in order to remove all traces of reactive gases. The ruthenium employed had been presintered in vacuo.

Argon-arc melted ruthenium was forged in a similar manner to the powder compacts, but in no instance was a comparable degree of workability obtained. It was found however that the workability of the repurified ruthenium was superior to to that of other samples and that it was possible, with difficulty, to produce strip and rod.

8. *Zone-melted ruthenium*

Zone-melted ruthenium was prepared by the floating zone melting technique using electron bombardment as described by LEVER, CALVERLEY AND DAVIS[6]. The ruthenium samples used in this preparation were either swaged bars prepared from sintered compacts or bars prepared by vacuum sintering. Bars prepared by the zone-melting technique were single crystals and could be bent with little force through a right angle over a comparatively small radius, whereas bars of similar size prepared by other methods were extremely hard and relatively brittle. Fig. 6 shows a single crystal bar 3/8 in. diameter bent by hand without mechanical aid. The zone-melted ruthenium rods could be cold worked by about 10% reduction in area but on annealing became polycrystalline and very brittle at room temperature.

PROPERTIES OF RUTHENIUM BEARING ON WORKING TECHNOLOGY

1. *Allotropy*

According to JAEGER AND ROSENBOHM[7-10] ruthenium undergoes an allotropic change $\alpha \rightarrow \beta$ at 1035°C and further changes $\beta \rightarrow \gamma$ and $\gamma \rightarrow \delta$ at 1190 – 1200°C and 1500°C respectively. On the other hand CRANGLE AND HALL[11] showed that lattice parameters increased in a regular manner up to 1300°C.

Thermal analysis carried out between room temperature and 1600°C failed to indicate any allotropic changes, nor was there any evidence of such changes from metallographic examination. Further confirmation that no changes occur may be deduced from the fact that the zone-melted metal solidifies as a single crystal, and is retained as such at room temperatures.

2. *Density of sintered compacts*

Density measurements on some vacuum sintered compacts are given in Table IV. The densities of compacts varied considerably thoughin general it was not possible to relate them to sintering variables. Frequently densities of compacts producede from the same batch by nominally identical methods showed considerable variation. As a general rule density was independent of sintering temperature, provided this exceeded the minimum value of 1450 – 1500°C. The maximum density obtained on a sintered compact was 11.88, corresponding to 95.6% theoretical. Low density values were obtained on ruthenium given extra refining treatments especially batch H, the minimum value 9.44 corresponding to 76% theoretical, and it is with those batches of ruthenium alone that there is evidence that increased sintering tempera-

References p. 291

ture above 1500°C has any effect on density. These specially purified ruthenium powders, prepared by ignition at a lower temperature than other batches, were considerably more bulky, and it is possible this may have had an important influence.

TABLE IV

DENSITY OF SINTERED RUTHENIUM COMPACTS

Compact No.	*Batch reference*	*Type of compact* *	*Vacuum (mm Hg)*	*Sintering temp. (°C)*	*Time to reach sintering temp. (hours)*	*Time at sintering temp. (hours)*	*Density (gram/c.c.)*	*Percent theoretical density*
1	A	X	0.007	1500	26	0	11.72	94.3
2	A	X	0.008	1500	50	0	11.70	94.1
3	A	X	0.008	1600	26	0	11.43	92.0
4	A	X	0.0002	1500	52	0	11.22	90.3
5	B	X	0.008	1600	26	0	11.27	90.7
6	B	X	0.008	1600	26	0	11.38	91.5
7	B	X	0.0002	1500	24	0	11.88	93.1
8	B	X	0.008	1450	6	10	11.29	90.8
9	B	X	0.0002	1500	52	0	11.57	93.1
10	C	X	0.0002	1500	8	16	11.29	90.8
11	C	X	0.0002	1500	25	0	11.18	89.9
12	C	X	0.0002	1500	7	0	11.43	91.9
13	D	X	0.0002	1500	22	0	11.64	93.6
14	D	X	0.0002	1500	8	8	11.54	92.8
15	D	X	0.0002	1550	10	14	11.28	90.7
16	E	X	0.0002	1500	8	8	11.70	94.1
17	E	X	0.0002	1550	8	8	11.71	94.2
18	E	X	0.0002	1500	16	72	11.38	91.5
19	E	X	0.0002	1550	16	72	11.38	91.5
20	F	X	0.0002	1500	16	72	11.55	92.9
21	F	X	0.0002	1500	8	16	11.39	91.6
22	C	Y	0.0001	1450	2	0	11.54	92.8
23	C	Y	0.0001	1500	3	0	11.49	92.4
24	C	Y	0.0001	1500	10	7	10.49	88.4
25	C	Y	0.0001	1500	1¾	0	11.83	95.2
26	C	Y	0.0001	1500	35	66	11.24	90.4
27	F	Y	0.0001	1450	1¾	0	10.55	84.9
28	F	Y	0.0001	1500	2	0	11.02	88.7
29	F	Y	0.0001	1500	25	0	11.02	88.7
30	F	Y	0.0001	1500	42	52	11.83	95.2
31	G	Y	0.0001	1450	314	0	11.41	91.8
32	G	Y	0.0001	1500	4	16	11.42	91.9
33	H	X	0.0001	1500	6	2	9.71	78.1
34	H	X	0.0001	1500	6	2	9.69	78.0
35	H	Y	0.0001	1500	6	2	10.36	83.3
36	H	X	0.0001	1500	6	16	9.44	76.0
37	H	X	0.0001	1500	6	16	9.55	76.8
38	C	Y	0.00001	1900	1	1	11.13	89.5
39	G	Y	0.00001	2100	2	1	11.57	93.1
40	H	Y	0.00001	2100	2	1	11.24	90.4
41	I	X	0.0001	1500	6	6	11.01	88.6
42	I	X	0.0001	1500	6	6	10.94	88.0
43	I	X	0.00001	2200	2	1	11.43	91.9
44	I	Y	0.0001	1500	2	0	10.72	86.2
45	I	Y	0.00001	2000	2	0	10.72	86.2
46	K	X	0.0001	1500	3	1	10.68	85.9
47	K	X	0.0001	1500	3	1	10.81	87.0

* Pressed in steel die: X. Hydrostatically pressed: Y.

References p. 291

3. *Grain size of sintered compacts*

The grain size of sintered compacts was markedly affected by the degree of vacuum used for sintering. Figures 7 and 8 illustrate the grain size of compacts identical in all respects other than in one instance the pressure was 0.005 mm mercury and in the other 0.0001 mm mercury. For similar processing cycles the grain size of compacts prepared from the specially purified ruthenium was on average slightly larger than

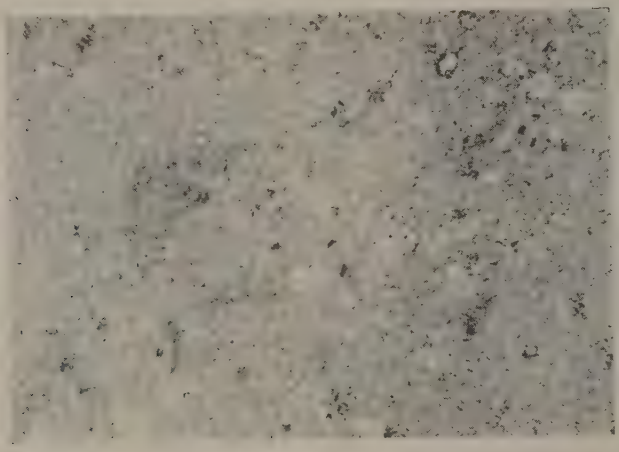

Fig. 7. 0.005 mm Hg pressure.

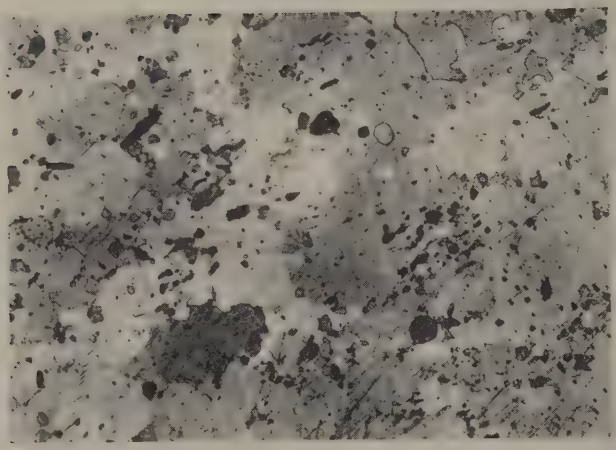

Fig. 8. 0.0001 mm Hg pressure.

Figs. 7–8. Identical ruthenium compacts sintered for 72 hours at 1500°C using different degrees of vacuum (× 100).

References p. 291

compacts from the normal production material, but other variables appeared to play a more important role than putity and it is possible that the difference observed in this instance may be due in part to initial particle size. The time taken to raise to sintering temperature appeared to have a more important influence on grain size than either sintering temperature or time at sintering temperature, and when this was slow there was sometimes considerable grain growth and variation in grain size, the coarser grains being located near the surface as though produced by some concentration gradient in this area (Fig. 9). These effects were not always reproducible however.

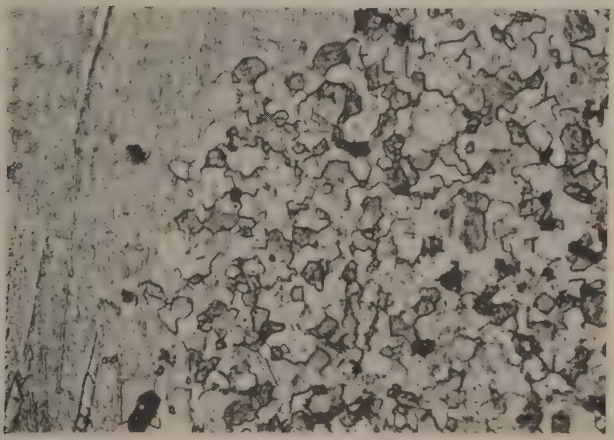

Fig. 9. Irregular grain size produced near surface of sintered compact by raising slowly to sintering temperture. The compact was sintered in vacuo (0.0002 mm Hg) for 96 hours before raising slowly to final sintering temperature of 1500°C (× 1000).

f. Hardness of sintered compacts

The hardness of sintered compacts exhibited a large scatter not only between lifferent compacts but between individual readings on the same compact. For ll hardness measurements recorded in Table V, at least ten impressions were nade and the results are given as maximum, minimum and mean. In all compacts ised for workability tests the mean hardness was approximately the same in all irections, but it was possible to produce compacts in which the hardness varied ccording to the direction of applied pressure during compaction.

The low hardness values recorded with compacts prepared from batches H, I and K, re worthy of note, though it is not known whether these were a function of purity lone. Other variables that were observed to have an influence on hardness values ere the sintering atmosphere (the higher the vacuum, the lower the hardness) and ie time taken to raise to the sintering temperature (the slower the heating rate the igher the hardness).

Apart from the greater ductility of compacts prepared from the specially treated

eferences p. 291

ruthenium, some of which were considerably softer than normal, no significant relationship appeared to exist between hardness and workability of compacts.

ARGON-ARC MELTED RUTHENIUM

The maximum density obtained with argon-arc melted ruthenium was 12.39 which is over 99.5% theoretical, and most ruthenium specimens melted by this technique had densities approximating to this figure. The grains in the ingot produced by this method were large, and columnar in character. Hardness values exhibited a wide scatter, much greater even than on sintered material, and if the indenter coincided with a grain boundary the resultant impression was so distorted as to render measurement impossible.

TABLE V

HARDNESS OF SINTERED COMPACTS

*Compact No.**	*Hardness – D.P.N.*		
	Max.	*Min.*	*Mean*
1	345	294	320
2	335	299	317
3	256	240	248
4	235	135	179
5	232	163	205
6	224	184	203
8	219	198	209
9	230	182	208
10	170	130	151
11	190	153	161
13	290	210	256
14	287	217	247
19	250	195	224
21	358	313	332
22	183	177	179
23	194	170	178
24	290	232	270
25	191	156	174
26	193	176	184
27	239	219	202
28	271	243	252
29	282	281	282
30	315	293	302
31	289	157	229
32	229	221	226
33	113	79	91
35	128	120	122
37	129	89	104
38	262	200	221
39	229	206	216
40	124	95	108
41	220	175	201
43	182	136	154
45	151	130	139
46	209	169	185
47	221	180	199

* For processing details, see Table 3.

References p. 291

An interesting feature of the hardness measurements was that the mean hardness on the ingot surface was much greater than on a section through the ingot, see Table VI, and although the surface hardness could be reduced by vacuum annealing it retained a higher value than that of the section. Repeated arc melting with intermediate 'gettering' of the argon with titanium had a negligible effect on the hardness values.

TABLE VI

HARDNESS OF ARGON ARC MELTED RUTHENIUM

Treatment	*Hardness D.P.N. (surface)*			*Hardness D.P.N. (section)*		
	Max.	*Min.*	*Mean*	*Max.*	*Min.*	*Mean*
As melted	452	307	377	275	169	209
Annealed in vacuo at 1500°C for 200 hours.	320	257	291	275	175	210
Remelted 5 times with intermediate 'gettering'	381	302	336	290	201	241
Remelted 10 times with intermediate 'gettering'	444	290	375	305	185	231
Remelted 20 times with intermediate 'gettering'	415	221	305	289	175	226
Remelted 30 times with intermediate 'gettering'	421	299	373	380	197	248

SINGLE CRYSTAL RUTHENIUM

Although comparatively little work was done on single crystal ruthenium, one observation on an orientated crystal is of interest as illustrating the anisotropy of the metal.

Hardness measurements on a plane corresponding to a prismatic face of the crystal give a mean hardness value of 480 D.P.N. but when the crystal was rotated through 90° about its sixfold axis of symmetry, hardness of the new face was only 227 D.P.N.

PROPERTIES OF WORKED RUTHENIUM

Because of difficulties in working ruthenium ingots prepared by melting, all investigations on the properties of worked ruthenium were performed on material prepared from sintered compacts.

The density of sintered compacts increased fairly rapidly during the early stages of hot forging, and more slowly during later stages. At about 60% reduction the density was in the range 12.1 – 12.2 (97 – 98% theoretical) and forged bars tended towards these values independently of the initial density of the compact. The maximum value of density obtained on any worked compact was 12.31 (99.0% theoretical) after 80% reduction, and on this material further working failed to produce any

References p. 291

TABLE VII

PROPERTIES OF HOT WORKED RUTHENIUM COMPACTS

Compact No.	Working procedure: Method of working	Working procedure: Temp. (°C)	Working procedure: Thickness (in.)	Working procedure: Total reduction (per cent)	Working procedure: Annealing temp. (°C)	Hardness (D.P.N.): Longitudinal section	Hardness (D.P.N.): Cross section	Density (gram c.c.)
	Forged	1400	0.25	45	1500	395	270	11.96
4	,,	1400/1350	0.16	64	700	—	—	12.12
	,,	1450/1260	0.127	73	1500	405	257	12.13
	Rolled	1500	0.099	79	1500	409	278	—
6	Forged	1450/1200	0.167	63	1500	397	280	12.12
	Rolled	1800	0.026	94	1500	434	—	—
8	Forged	1500/1260	0.180	64	1500	405	258	12.12
	Rolled	1800	0.023	95	1500	438	—	12.16
10	Forged	1800	0.338q.	50	1500	334	294	12.29
	Swaged	1800	0.178 round	90	1500	427	354	—
18	Forged	1800	0.136	71	1500	399	260	12.24
	Rolled	1800	0.050	89	1500	415	270	12.25
19	Forged	1500	0.168	65	1500	450	—	12.07
	Swaged	1800	0.022	95	1500	455	—	—
48	Forged and Swaged	1800	0.275 round	66	1500	—	—	12.18
49	Forged and Swaged	1500	0.172 round	90	1500	390	308	12.24
50	Forged and Swaged	1800	0.172 round	90	1500	397	298	12.24
34	Forged	1500	0.150	66	1500	—	220	12.12
	Rolled	1500	0.019	95	1500	307	232	—
47	Forged	1500	0.160	64	1500	—	263	12.23

TABLE VIII

THE EFFECT OF COLD WORK ON SURFACE HARDNESS OF RUTHENIUM

Cold work (per cent)	Surface hardness (D.P.N.)
0 (Annealed strip)	320
2	367
5	445
11	535

References p. 291

density increase. This density figure is appreciably lower than that obtained on arc melted ruthenium, 12.39 (99.5% theoretical).

The hardness of worked and annealed bars was invariably higher than that of the original sintered compacts and in addition the hardness of longitudinal sections was always greater than of transverse sections, an indication that some preferred orientation was maintained even after annealing. Nevertheless, X-ray diffraction patterns suggested that preferred orientation was slight; its nature and extent were not determined. Hardness figures for a number of hot-worked compacts of ruthenium are given in Table VII.

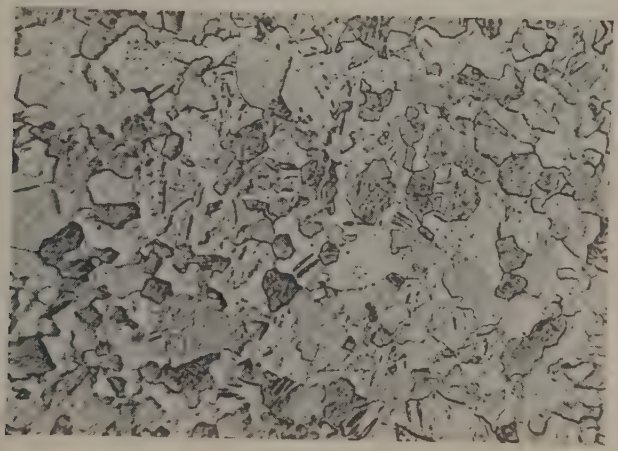

Fig. 10. Sintered compact.

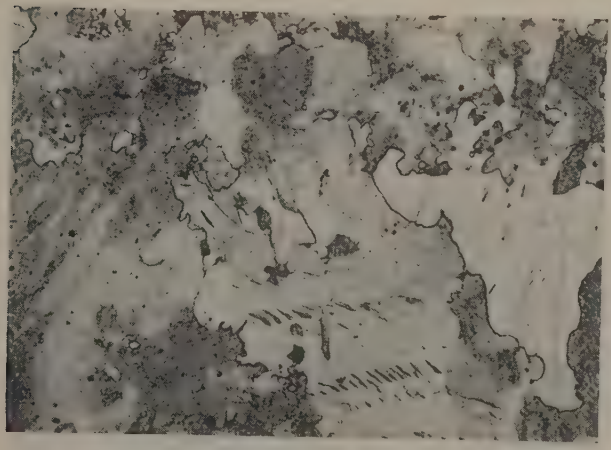

Fig. 11. Forged compact.

Figs. 10–11. Comparison of grain size of ruthenium compact, as sintered, and after 50% reduction in cross sectional area by forging at 1500°C (× 500).

References p. 291

Hardness increased rapidly on cold working, as illustrated in Table VIII. The annealing temperature of either hot-worked or cold-worked metal was found to be approximately 1200°C, maximum reduction in hardness being quickly obtained at all higher temperatures, and recrystallisation being evident from metallographic examination.

It has not so far proved possible to maintain the normal very fine grain structure of sintered compacts during working operations though grain growth was not very pronounced. Figures 10 and 11 illustrate the typical increase in grain size which occurred during working.

Forged ruthenium bars were relatively brittle even after high-temperature annealing. They could be bent plastically only over a large radius. Hot rolled and annealed ruthenium strip, 0.02 in. thick, could be bent plastically through an angle of 90° over a radius of about 1 in. and subsequently bent in the reverse direction in a similar manner. Bending of the strip over this radius to an angle much greater than 90° produced brittle fracture. Cold-rolled and annealed strip could not be deformed to this extent, fracture occurring after only very small plastic deformation.

Ruthenium samples could not be cut with the saw, nor could they be filed. Machining proved impracticable though the metal could be shaped by grinding, using carborundum discs. Tensile test pieces ground to shape from flat-rolled, and annealed strip, 0.02 in. thick, had a tensile strength of approximately 25 ton/sq.in. at room temperature along the direction of rolling, the metal breaking with small reduction in area and an elongation of about 5%.

MODES OF DEFORMATION

Ruthenium appears to deform both by slip and by twinning. Fig. 12 shows slip planes adjacent to a hardness impression on a ruthenium single crystal, while Fig. 13 shows deformation by both mechanisms in the same crystal in a plane at right

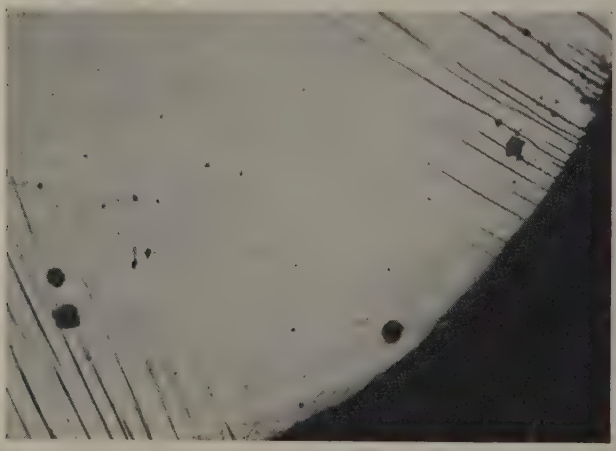

Fig. 12. Deformation by slip at hardness impression on ruthenium single crystal (× 500).

References p. 291

angles to that for the first impression. Such evidence as is available indicates that slip occurs on the prismatic $(10\bar{1}0)$ planes. In certain circumstances room temperature cleavage of a ruthenium single crystal was found to occur on basal planes.

BAIRD AND GEACH[12] recently investigated modes of deformation and were unable to observe traces of basal (0001) slip. Their results indicate that deformation occurs by slip on $(10\bar{1}0)$ and twinning on $(11\bar{2}1)$, $(11\bar{2}3)$, $(10\bar{1}1)$ and occasionally $(10\bar{1}2)$ planes. Traces of cleavage cracks were observed parallel to $(10\bar{1}1)$ planes and cracking

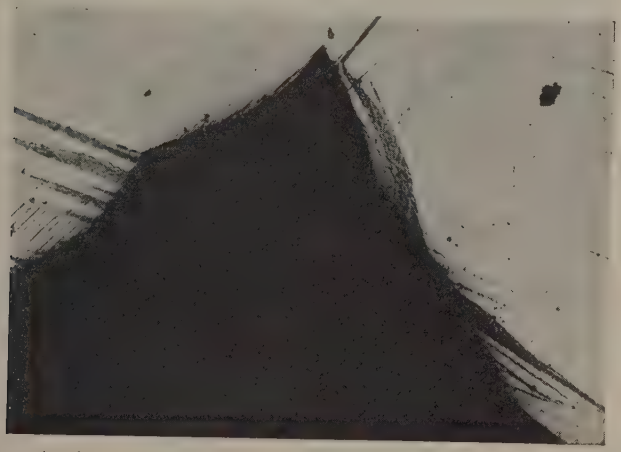

Fig. 13. Deformation by twinning and slip at hardness impression on ruthenium single crystal (× 500).

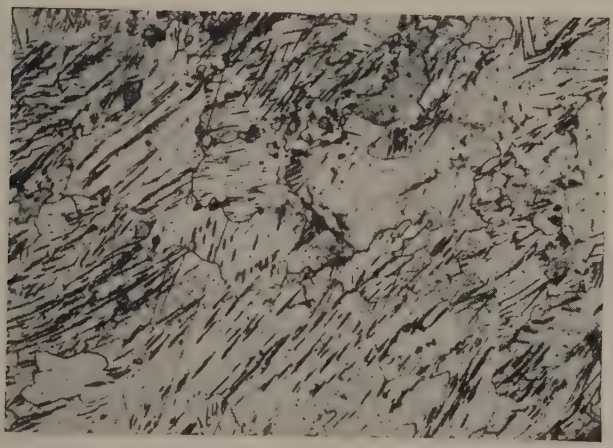

Fig. 14. Deformation twins produced by grinding and polishing ruthenium surface. Etched in sodium hypochlorite (× 500).

References p. 291

was once observed between a $(10\bar{1}1)$ twin and the matrix. Some of their evidence also indicates cleavage on basal planes.

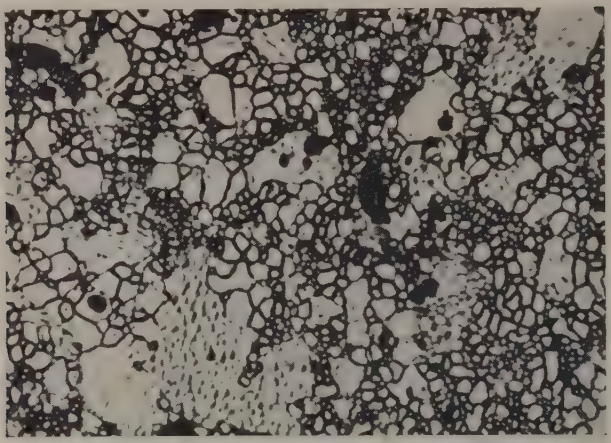

Fig. 15. Recrystallisation of surface layer produced by thermally etching polished ruthenium surface (× 500).

METALLOGRAPHY OF RUTHENIUM

Ruthenium was prepared for metallographic examination using standard laboratory methods of grinding and polishing, involving final lapping on soft cloth with quarter micron diamond dust; etching was carried out by immersion in concentrated sodium hypochlorite solution. This method of preparation was not satisfactory, as disturbance of the surface during grinding and polishing results in the production of a large number of deformation twins, Fig. 14. These could be eliminated by a vacuum anneal, at 1200°C or higher, after polishing, but the resultant recrystallisation produces an entirely false impression of the grain size of the metal, Fig. 15 shows the same area as in Fig. 14.

GAS ANALYSIS

Little is known concerning gas content of ruthenium specimens, and nothing concerning the effect this might have on workability.

The gas content of a ruthenium compact sintered for 7 days at 1500°C in vacuo (0.0001 mm mercury pressure) was determined as:*

Oxygen	—	0.02	weight–%
Nitrogen	—	0.003	weight–%
Hydrogen	—	0.00002	weight–%

* Gas analysis of sintered ruthenium given by courtesy of the British Non-Ferrous Metals Research Association, who performed this analysis.

References p. 291

and of an argon-arc melted sample remelted five times in gettered argon

Oxygen	—	0.0035	weight–%
Nitrogen	—	0.001	weight–%
Hydrogen	—	0.0001	weight–%

ALLRED, HIMES AND GOERING[13] have reported 0.0063 weight–% oxygen in ruthenium vacuum sintered at 2200°C and 0.0007 weight–% oxygen in ruthenium melted by electron bombardment.

TABLE IX

SPECTROGRAPHIC ANALYSIS OF ZONE MELTED RUTHENIUM BAR[a]

Impurity element	*Original bar*	*First zone*	*End zone*
Palladium	0.001%	0.0001%	0.0003%
Rhodium	0.002%	<0.001%	0.001%
Osmium	<0.01%	<0.01%	<0.01%
Gold	About 0.0002%	<0.0001%	<0.0001%
Silver	<0.0001%	>0.0001%	>0.0001%
Aluminium[b]	Trace	Faint trace	Trace
Cobalt[b]	Trace	Not detected	Not detected
Chromium[b]	Faint trace	Not detected	Not detected
Copper[b]	Trace	Trace	Trace
Iron	0.10%	<0.001%	0.01%
Titanium[b]	Trace	Faint trace	Trace
Manganese[b]	Trace	Not detected	Faint trace
Nickel	0.0003%	Not detected <0.0001%	0.0001%
Silicon[b]	Trace	Trace	Trace
Tungsten[b]	Faint trace	Very faint trace	Trace

[a] Melted 14 times at 15 cm/hour.

[b] Standards for these elements are not available. Probable limits of detection of aluminium, cobalt, chromium, copper and manganese about 0.0001%.

ZONE REFINING

Since purity appears to have an important bearing on the ductility of ruthenium it is a fairly obvious development that zone refining of the metal should be carried out in order to improve its workability. The amount of work done on this aspect to date is, however, very slight and has been confined to attempts to segregate impurities in the ends of melted bars.

In these zone purification experiments the floating zone technique previously described has been employed. Results of spectrographic analysis are given in Table IX of the original metal and first and end zones after fourteen passes on a zoned length of 200 mm using a zone width of 4 mm and a speed of traverse of 2.5 mm/min.

Nearly all the impurities present in ruthenium would be expected to lower the melting point of the metal and hence during zoning should be eliminated from the

References p. 291

first zone and concentrated at the end zone. In actual fact both melted zones contain a lower concentration of impurity elements than the original bar, an indication that the major part of the purification occurred by volatilization.

The removal of individual impurities has been investigated by additions of 0.1% rhodium and 0.1% nickel separately and together to ruthenium bars. For these two elements the rate of evaporation in electron bombardment melting greatly exceeds any effect due to zone refining. Results on bars zone melted six times are given in Table X.

TABLE X

ZONE REFINING OF RUTHENIUM ALLOYS

Alloy	*Concentration of alloying element in zoned bar per cent*					
	1st zone		*Bar centre*		*End zone*	
	Nickel	*Rhodium*	*Nickel*	*Rhodium*	*Nickel*	*Rhodium*
Ruthenium–0.1% nickel	0.0002	<0.001	<0.0001	<0.001	0.0001	<0.001
Ruthenium–0.1% rhodium	—	0.009	—	0.012	—	0.019
Ruthenium–0.1% nickel–0.1% rhodium	<0.0001	0.003	<0.0001	0.001	0.001	>0.025

CONCLUSIONS

The experiments described have been designed to investigate the possibility of forming ruthenium using techniques such as might normally be used in the fabrication of a high melting point metal. A number of factors that might be expected to have an influence on the ductility of the metal have been examined but these investigations have not been exhaustive.

Ruthenium in the purity at which it is at present available is a metal that is relatively non ductile, but the improvement in ductility that can be obtained by the selection of refined powder of high purity coupled with control of processing conditions indicate that the metal itself is not inherently brittle. Unfortunately no knowledge of the nature or concentration of impurities producing brittleness can be ascribed with certainty.

Ruthenium, at present, can be produced only in small quantities in fabricated forms and there is considerable limitation to the gauges of rod and strip that can be produced. The metal may however be considered as one of low ductility rather than in its former status of a brittle metal, and as improved ductility appears to be a function of purity, it is likely that the production of a truly ductile ruthenium will depend on improved methods of refining and on new methods for analysis for trace element impurities.

By analogy with other metals it might be expected that the gas content of ruthenium would have an important effect on its ductility. Of the methods of preparation so far investigated electron bombardment has reduced oxygen content to the minimum value, but this value is still sufficiently high to be suspect in producing ar

References p. 291

adverse effect on the properties of the metal. Control of atmosphere during both solidification and subsequent forming processes are therefore both aspects that warrant careful control in future investigations.

ACKNOWLEDGEMENTS

Acknowledgement is made to The Mond Nickel Co. Ltd., for permission to publish this paper; to Mr. A. R. RAPER and Mr. F. S. CLEMENTS, Manager and Assistant Manager of The Precious Metal Refinery of the Mond Nickel Co. for supplying the ruthenium powders and analyses; and to Dr. G. L. J. BAILEY, Superintendent of the Precious Metal Research Laboratories for advice and encouragement at all times.

REFERENCES

1 C. S. SIVIL, *Am. Inst. Mining Met. Engrs., Inst. Metals Div.*, 93 (1931) 244.
2 A. JOLY, *Compt. rend.*, 116 (1893) 430.
3 C. JOHNSON AND R. ATKINSON, *Trans. Inst. Chem. Engrs. (London)*, 15 (1937) 131.
4 C. GILCHRIST, *Chem. Revs.*, 32 (1943) 227.
5 M. DAVIS, C. E. DENSEM AND J. H. RENDALL, *J. Inst. Metals*, 84 (1955) 160.
6 A. CALVERLEY, M. DAVIS AND R. F. T. LEVER, *J. Sci. Instr.*, 34 (1957) 142.
7 F. M. JAEGER AND E. ROSENBOHM, *Proc. Acad. Sci. Amsterdam*, 34 (1931) 815.
8 F. M. JAEGER AND E. ROSENBOHM, *Rec. trav. chim.*, 51 (1932) 37.
9 F. M. JAEGER AND E. ROSENBOHM, *Z. anorg. u. allgem. Chem.*, 203 (1931) 98.
10 F. M. JAEGER AND E. ROSENBOHM, *Proc. Acad. Sci. Amsterdam*, 144 (1941) 44.
11 F. HALL AND J. CRANGLE, *Acta. Cryst.*, 10 (1957) 240.
12 J. BAIRD AND G. A. GEACH, *Private communication.*
13 W. P. ALLRED, R. C. HIMES AND H. L. GOERING, *S.E.R.L. Symposium on Electron Bombardment Melting*, Baldock, Gt. Brit., March 1959.

THE SYSTEMS PALLADIUM - INDIUM AND PALLADIUM - TIN

J. R. KNIGHT

Baker Platinum Division, Engelhard Industries Ltd., London (Great Britain)

AND

D. W. RHYS

The Mond Nickel Company Ltd., Research and Development Department, London (Great Britain)

(Received May 22nd, 1959)

SUMMARY

The equilibrium diagrams of palladium–indium and palladium–tin alloys have been investigated by thermal analysis, metallographic and X-ray methods. Intermediate phases based on Pd_3In, Pd_2In, PdIn, $PdIn_2$ and $PdIn_3$ have been found in the palladium–indium system and phases Pd_3Sn, Pd_2Sn, Pd_3Sn_2, PdSn, Pd_3Sn_4, and $PdSn_2$ in the palladium–tin system. The solid solubilities of indium and tin in palladium are appreciable but palladium has very low solid solubility in both indium and tin. The properties of the palladium–rich solid solutions have been compared with those of other palladium alloys.

INTRODUCTION

The formation of coloured alloys from white metals is not unique, but it was this comparatively unusual property that focussed interest on the palladium–indium alloys. A brief reference to the fact that an attractive rose-coloured finish can be obtained by the electrodeposition of alternate layers of silver, palladium and indium followed by a diffusion treatment, is made in the Metals Industry Handbook 1944, though this information was deleted from subsequent editions. A few brief experiments only were necessary to establish that this colour is due to a red alloy formed in the palladium–indium system.

In addition, there was interest in both the palladium–indium and the palladium–tin system from the point of view of the possible phases that might be formed in more complex systems.

Palladium is face-centred cubic at all temperatures up to its melting point at 1552°C the closest approach of atoms being 2.75 Å. In the solid state, the outer electrons of palladium are usually thought to occupy overlapping 4d and 5s bands with 0.6 holes in the 4d band.

Indium is face-centred tetragonal, with a small axial ratio (c/a = 1.078), and therefore approximates very closely to a face-centred cubic metal; the closest distance of approach of atoms is 3.24 Å (17.8% larger than for palladium) and the metal has an estimated atomic diameter of 3.14 Å for co-ordination number 12.

References p. 303

The size factor in palladium–indium alloys cannot therefore be considered as favourable. Indium has a melting point of 156.4°C.

Tin exists in two allotropic forms; grey tin is the stable form below 13.2°C and has a diamond-type structure, with minimum distance between atoms of 2.80 Å; white tin, stable between 13.2 and 231.9°C the melting point of tin, may be described as having a distorted form of diamond, or tetragonal structure with c/a ratio 0.5456. The minimum interatomic distance in white tin is 3.02 Å, 9.8% larger than palladium.

Indium and tin resemble one another chemically in that they form compounds in which each has two valencies: tri and monovalent indium and quadri and di-valent tin. This is considered as being due to the relative inertness of the $(5s)^2$ electrons in each case, and it is probable that the stability of this electron pair is responsible for an incomplete ionisation of the metals in the solid form and consequently the abnormal crystal structures and low melting points of the metals.

Previous work on the palladium–indium and palladium–tin systems has been limited to X-ray examination of certain of the phases. Thus HELLNER AND LAVES[1] report the existence of Pd_3In, Pd_2In, PdIn, Pd_2In_3 and $PdIn_3$. The structures of these compounds, according to HELLNER AND LAVES are given in Table I. NOWOTNY, SCHUBERT AND DETTINGER[2] report an order-disorder transformation based on Pd_3Sn in the palladium-rich solid solution and compounds Pd_2Sn, Pd_3Sn_2, PdSn, $PdSn_2$ and $PdSn_4$, while NIAL[3] found compounds Pd_3Sn_2, PdSn and $PdSn_2$. The structures of these compounds are also given in Table I.

TABLE I

COMPARISON OF PHASES FORMED IN PALLADIUM–INDIUM AND PALLADIUM–TIN ALLOYS

Palladium–indium			*Maximum melting temp. °C*	*Maximum melting temp. °C*	*Palladium–tin*		
Composition	*Structure*	*How formed*			*How formed*	*Structure*	*Composition*
Pd_3In	f.c. Tetragonal	Peritectic	1360	1326	Liquidus maximum	f.c.c.	Pd_3Sn
Pd_2In	Not identified	Liquidus maximum	1323	1287	Liquidus maximum	Not identified	Pd_2Sn
—	—	—	—	929	Peritectic	Hexagonal partially filled NiAs type	Pd_3Sn_2
PdIn	Ordered b.c.c.	Liquidus maximum	1285	825	Peritectic	Orthorhombic	PdSn
—	—	—	—	617	Peritectic	Not identified	Pd_3Sn_4
Pd_2In_3	Ni_2Al_3 type	Peritectic	709	—	—	—	—
—	—	—	—	348	Peritectic	f.c. Orthorhombic	$PdSn_2$
$PdIn_3$	Partly filled γ-brass	Peritectic	664	—	—	—	—

References p. 303

EXPERIMENTAL PROCEDURE

(*a*) *Materials*

The palladium and indium used were of 99.9% + purity. The tin was 'Chempur' quality.

(*b*) *Preparation of alloys*

Alloys of lower melting point were melted in a platinum -wound resistance furnace using a graphite crucible with a tightly fitting graphite lid.

Melting in graphite crucibles was found to be unsuitable for alloys containing palladium-rich primary solid solutions as these dissolve carbon when liquid. These higher melting point alloys were melted in an induction furnace using alumina crucibles and an atmosphere of argon.

Under the conditions of melting employed the ingots obtained were clean and free from apparent oxidation. Any change in weight during melting was attributed to loss by evaporation of indium or tin, this amounting to less than 0.2 per cent of the indium or tin content of the alloy except in a few of the higher melting point alloys. This hypothesis was confirmed by chemical analysis of some of the alloys.

Consequently it was usually unnecessary to analyse the alloy compositions prepared. Analysis was carried out only of a few critical alloys and in these composition was found to be very close to nominal.

Two hundred gram quantities of palladium–tin alloys and one hundred gram quantities of palladium–indium alloys were prepared.

(*c*) *Thermal analysis*

The liquidus and solidus temperatures (where the latter formed part of an eutectic or peritectic horizontal) of each alloy were determined by means of inverse-rate cooling curves. Thermal analysis was carried out in alumina crucibles under argon, for alloys prepared in this way; the remainder being contained in graphite crucibles.

Temperature measurements were made with platinum/platinum–10% rhodium thermocouples, contained in thin-walled alumina sheaths, calibrated at the melting temperatures of indium, tin, antimony, silver, gold, copper and palladium.

Some of the indium and tin-rich alloys were prone to under-cooling but this was prevented by thorough stirring during thermal analysis.

Owing to the wide temperature range over which thermal analysis was carried out (100–1600°C), it was not possible to use a single design of furnace which would give the necessary cooling rate (2–3°C per minute) at all the arrest points. High thermal capacity furnaces were used for the palladium-rich alloys, and low thermal capacity furnaces for indium and tin-rich alloys; all the furnaces were of the electric resistance type and had a thermal gradient not greater than 5°C over the ingot length at the relevant temperatures.

(*d*) *Solidus determinations*

Determination of the solidus temperature of alloys not showing eutectic or peritectic arrests was carried out by quenching and microscopical examination. The heating and quenching techniques were as described in the following section. In general alloys were heated to successive temperatures differing by 2.5°C, and the

References p. 303

solidus was taken as the mean between successive temperatures showing melting and no melting respectively. Heating rates were adjusted so that the last 1°C increase in temperature took approximately 5 minutes.

Alloys examined were either in the worked condition, or had been given long homogenising anneals in vacuo.

(e) Microscopical examination

Alloy ingots, after thermal analysis, were remelted and cast into $\frac{1}{4}$-in. diameter rods in a graphite mould. Sections cut from these rods were used for microscopical examination, all heat treatments being carried out in evacuated silica capsules. A vertical tube furnace was used and the capsules were contained in a platinum carrier, maintained in contact with two alumina-sheathed thermocouples. One of the thermocouples was connected to a temperature controller and the other to a slidewire potentiometer, by means of which the effectiveness of temperature control could be assessed. At temperatures of the order of 1200°C temperatures were controlled to $\pm$ 2°C, whilst at lower temperatures control was better. The pointed sealed end of the

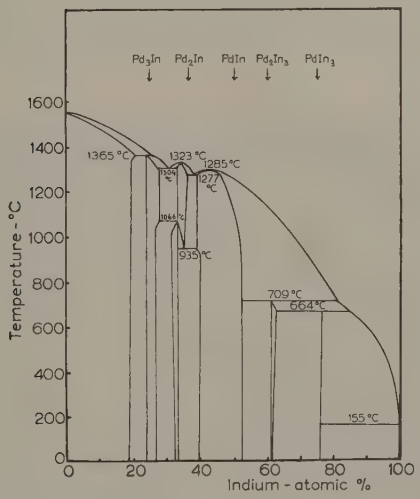

Fig. 1. Equilibrium diagram of the system palladium–indium.

silica capsule protruded from the bottom of the platinum carrier so that when the carrier was released, the mass of the platinum was sufficient to break the end of the capsule when it struck the bottom of the quenching bath, thus flooding it with water and ensuring rapid cooling.

Alloys were homogenised at temperatures just below the solidus temperature before further heat treatment and furnace cooled to the appropriate heat treatment temperature, being maintained thereat for the requisite period before quenching.

References p. 303

Etching was carried out by means of potassium cyanide-ammonium persulphate solution mixtures, and ferric chloride solutions at strengths up to 25%.

THE PALLADIUM–INDIUM SYSTEM

The equilibrium diagram as deduced from the results of thermal analysis and microscopic examination is reproduced in Fig. 1. The phases so observed agree in number and composition with those indicated by HELLNER AND LAVES.

(*a*) *Solid solution of indium in palladium*

The solid solubility of indium in palladium has been found between 20 atomic percent and 21 atomic percent at temperatures just below the solidus. There is some decrease in the solubility with decrease in temperature, and at 600°C it is between 17 and 18 atomic percent.

A peritectic reaction occurs between the solid solution and the phase Pd_3In at 1360°C.

(*b*) *Compound Pd_3In*

Between the primary solid solution and 24.8 atomic percent indium is a duplex region containing this compound which also exists as a single phase between 24.8

Fig. 2. Slowly cooled 69% palladium–31% indium alloy (×75).

atomic percent and about 27 atomic percent indium near the solidus temperature. At about 1066°C however, this homogeneous region decreases abruptly by about 1 percent on the indium-rich boundary due to a transformation in the adjoining phase Pd_2In, and thereafter the boundary is vertical. Between Pd_3In and the adjoining Pd_2In an eutectic occurs at about 31 atomic percent indium and 1304°C. The structure of this eutectic is shown in Fig. 2, which is the slowly cooled 31 atomic percent alloy.

References p. 303

(c) Compound Pd_2In

This occurs as a maximum on the liquidus curve of 1323°C at 33.3 atomic percent indium and is homogeneous at temperatures just below the solidus from about 32.8

Fig. 3. 67.7% Palladium–33.3% indium alloy, water quenched from 1040°C (× 75)

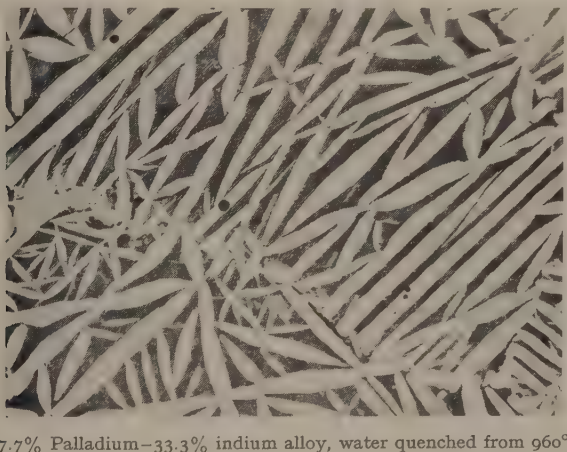

Fig. 4. 67.7% Palladium–33.3% indium alloy, water quenched from 960°C (× 75).

to 36.5 atomic percent. At lower temperatures this phase undergoes a transformation which starts at 1066°C at the palladium-rich boundary and is complete at 936°C as the result of an eutectoid. Figures 3 and 4 illustrate the process of separation in the 33.3 atomic percent alloy after homogenisation at 1250°C followed by cooling to and maintaining at 1040°C and 960°C respectively. The light etching needles of the transformation product can be observed in the primary matrix.

References p. 303

It was not found possible to suppress this transformation entirely by quenching, signs of incipient transformation invariably being present. Fig. 5 is a higher magnification of the area shown in Fig. 3 in which the typical Widmanstatten structure associated with this incipient change is clearly seen.

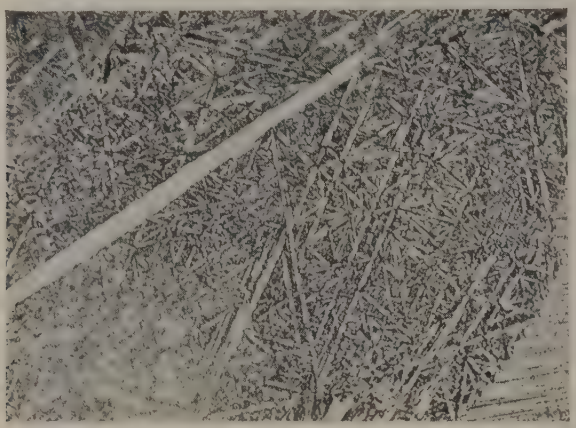

Fig. 5. 67.7% Palladium–33.3% indium alloy, water quenched from 1040°C (×500).

The small region of homogeneous transformation product shown on Fig. 1 is in accordance with X-ray measurements. Preliminary observation suggested a face-centred tetragonal structure for this phase but other lines were present and it is possibly more complex. It was observed, however, that the X-ray pattern of the 31.4 atomic percent indium alloy (Pd_3In + Pd_2In) and 39.3 atomic percent indium alloy (Pd_2In + PdIn) gave slightly different values for the parameters of this phase, suggesting a small homogeneity range.

The exact composition of the phase is not known but it is probably a polymorphic modification of Pd_2In.

(d) Compound PdIn

The liquidus curve rises to a shallow peak at 1285°C at 46 atomic percent indium, the solidus and liquidus being very close to one another up to 48 atomic percent after which the solidus decreases sharply to 709°C at 52 atomic percent.

The homogeneous PdIn phase, which occurs in this region, extends, at the solidus temperature, from about 38.5 to 52 atomic percent indium whilst at low temperatures the range is narrowed somewhat on the palladium-rich side as a result of the Pd_2In transformation.

PdIn is a 3:2 type electron compound having an ordered body-centred cubic structure. There is no evidence of any transformation in this phase and it seems likely

References p. 303

that the ordered structure is very stable and is preserved at temperatures up to the melting point. It is of interest that the maximum on the liquidus curve does not correspond to the PdIn composition at which the liquidus temperature is 1265°C.

(e) Compound Pd_2In_3

This phase is formed by a peritectic reaction at 709°C and seems to have a very limited range of homogeneity arround the theoretical composition.

(f) Compound $PdIn_3$

This phase is formed by a peritectic reaction at 664°C.

Between this phase and indium an eutectic is formed which melts and has a composition very close to that of pure indium. The solubility of palladium in indium is low and even 0.1 percent additions result in a two phase alloy.

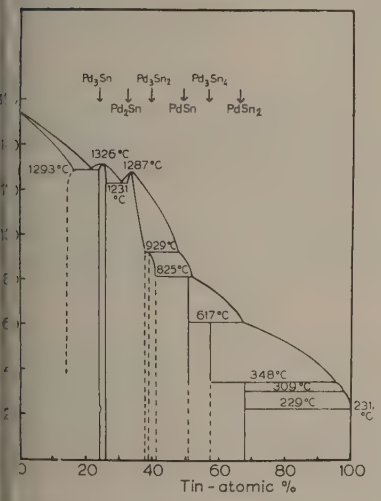

Fig. 6. Equilibrium diagram of the system palladium–tin.

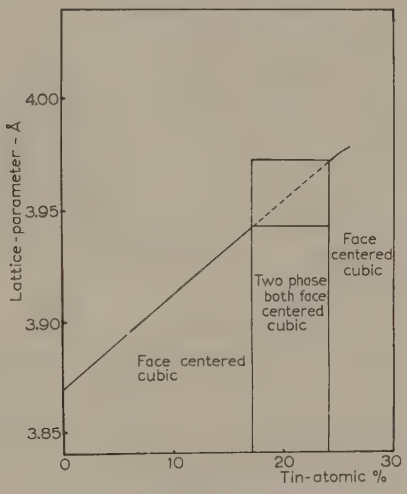

Fig. 7. Lattice parameters of palladium–tin alloys.

THE PALLADIUM–TIN SYSTEM

The general features of the equilibrium diagram as revealed in this investigation are illustrated in Fig. 6. The phases agree with those of previous investigators with the exception that no compound $PdSn_4$ was found. It is probable that this reported phase in is fact a polymorph of $PdSn_2$.

(a) Solid solubility of tin in palladium

The solid solubility of tin in palladium has been found to be approximately 17 atomic percent at the solidus temperature. The solid solubility appears to decrease

only slightly with temperature and while this phase boundary has not been determined accurately, the solubility is greater than 16 atomic percent at 600°C.

The palladium-rich solid solution forms an eutectic at 21.2 atomic percent tin and 1293°C with the compound Pd_3Sn.

(*b*) *Compound Pd_3Sn*

The palladium solid solution and the compound Pd_3Sn coexist over the approximate range 17–24 atomic percent tin. Pd_3Sn has a small homogeneous range that is apparently little affected by temperature. The compound has a maximum freezing temperature at 1326°C and forms another eutectic at 30.2 atomic percent tin and 1231°C with the compound Pd_2Sn.

Previous investigators have reported Pd_3Sn as being formed as the result of a superlattice change in the primary solid solution, but no evidence has been obtained that the compound is ordered. It has a face-centred cubic structure and it is of interest that its lattice parameter can be obtained by extending the parameter composition curve of the primary palladium rich solid solution, Fig. 7. No solid transformations involving Pd_3Sn were found.

(*c*) *Compound Pd_2Sn*

The compounds Pd_3Sn and Pd_2Sn coexist at higher temperatures over the range 26–32 atomic percent tin, and the compound Pd_2Sn has an appreciable homogeneous range on either side of its stoichiometric composition; at temperatures just below the solidus, this extends from 32 to 42 atomic percent tin.

The compound has a maximum melting point at 1287°C and some solid transformations at lower temperatures were observed in this phase but phase boundaries were not determined.

(*d*) *Compound Pd_3Sn_2*

It is probable that this phase which is formed as the result of a peritectic reaction at 929°C can exist as a single phase over a small range. The duplex region Pd_2Sn–Pd_3Sn_2 is narrow but the Pd_3Sn_2–PdSn range is much wider. Solid transformations involving Pd_3Sn_2 were not fully investigated but none was detected above 600°.

(*e*) *Compound PdSn*

This is formed as the result of a peritectic reaction at 825°C. Solid transformations in this phase were not investigated.

(*f*) *Compound Pd_3Sn_4*

This is formed as the result of a peritectic reaction at 617°C. Low temperature modifications of this phase were not investigated.

(*g*) *Compound $PdSn_2$*

This is formed as the result of a peritectic reaction at 348°C. Before solidification of this phase is complete it undergoes a transformation to a polymorphic form by a peritectic change at 309°C. This modification forms an eutectic with tin at 229°C and a tin content of the alloy greater than 99.9 atomic percent.

References p. 303

PROPERTIES OF THE PALLADIUM-RICH PRIMARY SOLID SOLUTIONS

The palladium-rich primary solid solutions containing indium are appreciably harder than pure palladium. Nevertheless, indium is not a particularly potent hardener being less effective than tin. Hardness of the alloys is recorded graphically in Fig. 8.

The resistivity of the palladium–tin solid solution alloys shows an interesting feature in that there is a maximum at about 13 atomic percent tin and a subsequent minimum at about 14 atomic percent tin. This is a phenomenon which has also been

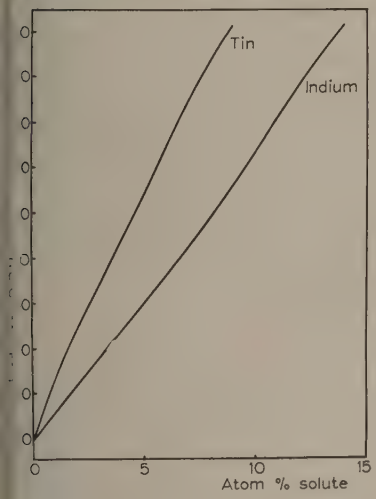

Fig. 8. Hardness of annealed palladium–indium and palladium–tin alloys.

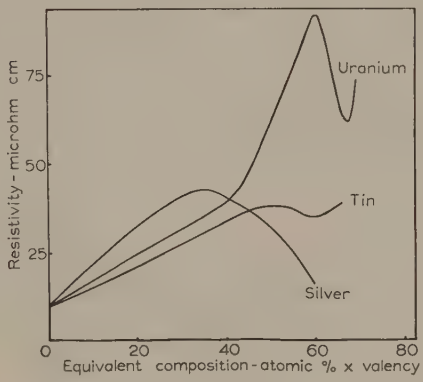

Fig. 9. Electrical resistivity of some palladium alloys at 20°C.

observed by CATTERALL[4] in palladium–uranium alloys and the maximum has been attributed by him to the filling of the vacancies in the d-band of palladium. Equivalent composition–resistivity curves for palladium–silver[5], palladium–tin and palladium–uranium alloys are shown in Fig. 9, assigning valencies of one, four and six to silver, tin and uranium respectively.

Assuming that there are 0.6 holes in the d-band of palladium and that all valency electrons from the solute elements go into this band, it would be completely filled at equivalent concentrations of 37.5 silver, 52 tin and 55 uranium, which are in good agreement with silver and tin but slightly low for uranium. Catterall considers this as due to the uranium at higher concentrations entering solution in an incompletely ionised form. No resistivity measurements have been made on palladium–indium solid solution alloys but it might be expected that similar phenomena would be observed.

Figure 10 indicates the lowering of the liquidus temperature of palladium by the elements immediately following it in the second long period. The figures for antimony were obtained from GRIGOJEV[6] and for silver from RUER[7]; but information on

References p. 303

cadmium is unfortunately not available. These curves have also been adjusted to equivalent electron concentration by assigning valencies of one, three, four and five to silver, indium, tin and antimony respectively. The maximum lowering of liquidus is obtained with silver followed by antimony, tin and indium in that order. If, as appears likely, these elements are exerting maximum valency in solution, it would appear that electron concentration has little effect on the lowering of the liquidus and on the nature of the adjoining compounds.

Silver is mutually soluble in palladium in all proportions and the maximum solubilities of indium, tin and antimony in palladium are 20, 17 and 13 atomic percent

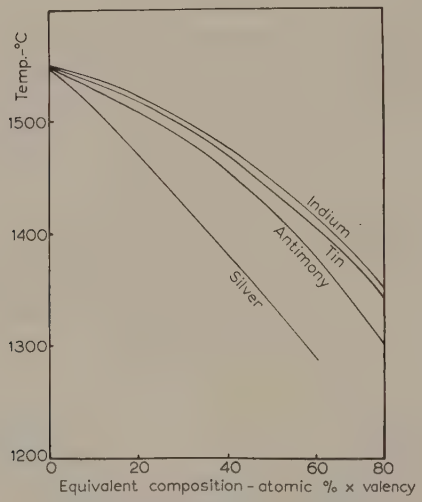

Fig. 10. Depression of freezing temperature of palladium by alloying additions.

respectively or equivalent concentrations 60, 68 and 65. The respective eutectic compositons for tin and antimony are both about 21 atomic percent and the eutectic or peritectic horizontals involving the primary solid solutions are indium 1354°C, tin 1293°C, antimony 1070°C, all being in equilibrium with a phase of general formula Pd_3X.

Of the four elements under consideration silver has the most favourable size factor followed by tin, indium and antimony in that order. Electrochemically palladium is nearest to silver followed by antimony, tin and indium and depression of freezing point is in the reverse of this order.

From the above it would appear that the nature and extent of the solid solution is governed to an appreciable extent by the electronegativity of the solute elements, though size factor may also have an important bearing in some instances.

An interesting feature in the palladium–tin system is the fact that both the

References p. 303

primary solid solution and the adjacent phase Pd_3Sn have face-centred cubic structures with very similar lattice parameters. It might thus appear probable that the solubility of tin in palladium is governed by size factor considerations and that possibly Pd_3Sn has an ordered structure. Owing to the similar scattering power of the two components this has not been observed.

INTERMEDIATE PHASES

It is of interest that both tin and indium form phases based on compositions Pd_3X, Pd_2X, PdX and PdX_2, the maximum melting temperatures of the indium phases, as indicated in Table I being higher than those of the corresponding tin phases.

In both instances the Pd_3X phase has a face centred structure, though Pd_3Sn is cubic and Pd_3In tetragonal. The axial ratio (0.93) of Pd_3In is sufficiently close to unity however for these two phases to be of similar type.

Pd_2Sn and Pd_2In have unidentified structures but the two PdX phases are of different type.

The PdIn phase is of particular interest because of its colour. This phase has a body-centred cubic structure which is ordered up to its melting point. There is little doubt that electron concentration is the principal factor in the formation of this phase.

ACKNOWLEDGEMENTS

Acknowledgement is made to the Mond Nickel Company Limited, in whose laboratories these researches were carried out, for permission to publish this contribution; to Dr. E. C. RHODES who was Superintendent of the Laboratory when the major part of the investigation was made; and to Dr. G. L. J. BAILEY for his help and criticisms in the preparation of the text.

REFERENCES

1 E. HELLNER AND F. LAVES, *Z. Naturforsch.*, 2a (1947) 177.
2 H. NOWOTNY, K. SCHUBERT AND U. DETTINGER, *Z. Metallkunde*, 37 (1946) 137.
3 O. NIAL, *Inaugural Ph.D Dissertation*, University of Stockholm (1945).
4 J. A. CATTERALL, *Phil. Mag.*, 48 (1957) 491.
5 W. R. G. KEMP, P. G. KLEMENS, A. K. SREEDHAR AND G. K. WHITE, *Proc. Roy. Soc.*, 233A (1956) 480.
6 A. I. GRIGORJEV, *Z. anorg. u. allgem. Chem.*, 209 (1932) 308.
7 R. RUER, *Z. anorg. u. allgem. Chem.*, 51 (1906) 315.

THE COMPOUND Bi_4Rh

R. G. ROSS AND W. HUME-ROTHERY

Department of Metallurgy, University Museum, Oxford (Great Britain)

(Received July 3rd, 1959)

SUMMARY

Previous work suggested that the compound Bi_4Rh existed in three modifications with transformation temperatures α/β 310°C and β/γ 390°C. Diffraction films taken in a high temperature X-ray camera show that only one structure exists between room temperature and 460°C, the temperature of the $Bi_4Rh \rightleftarrows Bi_2Rh$ + Liq. peritectic horizontal. The crystal structure of this one modification is body-centred cubic, space group No. 230, lattice parameter 14.9274 ± 0.0002 Å at 20°C, and is identical with the α-Bi_4Rh modification of previous investigators.

The liquidus curve of Bi-rich BiRh alloys has been redetermined and the most probable equilibrium diagram is reproduced.

INTRODUCTION

The phase diagram of the BiRh system determined by RODE[1] by thermal and microscopic methods is shown in Fig. 1, which is reproduced from HANSEN[2]. The compound Bi_4Rh was found to have a narrow range of composition, and to be

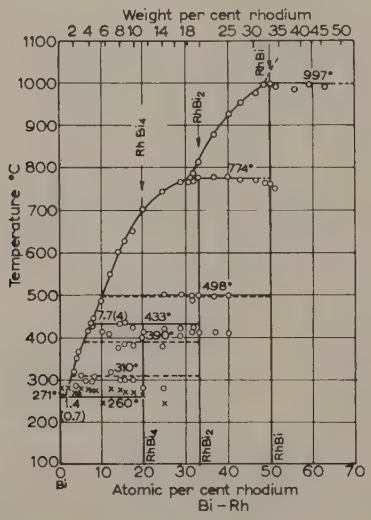

Fig. 1. The system Bi–Rh (HANSEN).

References p. 308

formed by a peritectic transformation at 433°C. Weak arrests were found in the vicinity of the compound which indicated polymorphic transformations at $\sim$ 310° and $\sim$ 390°C.

ZHURAVLEV AND ZHDANOV[3,4] accepted RODE's value of the peritectic transformation temperature, and that the arrests at $\sim$ 310° and $\sim$ 390°C. indicated polymorphic transformations in Bi_4Rh. They claimed to have obtained three modifications of the compound, and some of the properties they found are shown in Table I.

TABLE I

Modification	*Temp. range*	*Crystal structure*
α-Bi_4Rh	up to 310°C	body-centred cubic, space group No. 230 (Intern. Tables, 1952), lattice parameter $a = 14.928 \pm 0.005$Å[3]
β-Bi_4Rh	310—390°C	orthorhombic, $a = 11.4$, $b = 4.25$, $c = 9.0$Å[4]
γ-Bi_4Rh	390—433°C	hexagonal(?), from observation of the plate-like external shape of the crystals, and of well-developed lines of cleavage at angles close to 120° [3]

Their conclusion that three distinct structures exist was based on observation of the properties: external shape of crystals, microhardness and powder X-ray pattern.

Details of their experimental method are relevant to a discussion of these phases. ZHURAVLEV AND ZHDANOV[3] found that annealing and quenching of either pure Bi_4Rh or Bi_4Rh + excess Bi alloys resulted in the structure α-Bi_4Rh. β- and γ-Bi_4Rh modifications were obtained from a 6.9 at.% Rh (*i.e.* excess Bi) alloy only if the alloy was given the preliminary treatment of heating above 433°C before quenching from the desired temperature. (The exact temperature to which the alloys were heated was not stated.) It was definitely stated[3] that crystals of α-Bi_4Rh were extracted from a 6 at.% Rh alloy by dissolving the excess Bi in dilute nitric acid. Probably, crystals of β and γ modifications were extracted from a 6.9 at.% Rh alloy in a similar manner.

WOOLMINGTON[5], working in this Laboratory, determined the liquidus up to about 35 at.% Rh, and found the peritectic temperature for the formation of Bi_4Rh to be 445°C. He found the variation in composition of the compound to be small, and to include the exact whole number ratio Bi_4Rh. In these circumstances, complete re-examination of the compound has been made.

EXPERIMENTAL DETAILS

The bismuth used was specially pure metal kindly presented by the Atomic Energy Research Establishment, Harwell. The rhodium was introduced in the form of a master alloy prepared by Messrs. Johnson, Matthey & Co., Ltd., from high purity metals and containing 52.2 at.% Rh.

The alloys were prepared by melting appropriate amounts of the master alloy and the pure bismuth in an evacuated silica tube, quenching and annealing for 2 weeks at 240°C. The resultant specimen appeared homogeneous when examined microscopically.

To determine the peritectic transformation temperature, lumps of this pure homo-

References p. 308

geneous specimen were sealed in evacuated glass tubes, annealed at the desired temperature for about 20 hours, and quenched in ice water.

The X-ray work was done using a modified[6] Unicam high temperature X-ray camera operated with an atmosphere of hydrogen gas. Temperature calibration of the camera was done using a specimen of pure Ag, and the lattice spacing *vs.* temperature for Ag as determined by HUME-ROTHERY AND REYNOLDS[7] and OWEN AND ROBERTS[8]. Filtered Cu radiation ($K\alpha_1 = 1.54050$ Å) was used for all exposures. All X-ray specimens were contained in evacuated silica capillaries. Lattice parameters were determined by extrapolation to $\theta = 90°$ against the Nelson-Riley function.

EXPERIMENTAL RESULTS

The annealing and quenching experiments established the temperature for the peritectic formation of Bi_4Rh as 460 ± 3°C. This work appeared conclusive and all specimens quenched from below 460°C were homogeneous whilst those quenched from higher temperatures either showed chilled liquid or shattered on quenching.

The high temperature X-ray experiments showed that the compound retained the same structure at all temperatures between 20°C and the peritectic transformation temperature. At low temperatures, the powder film contained 115 lines. On raising the temperature, the high angle lines gradually diminished in intensity, but at 370°C 110 lines persisted and were those of the room temperature pattern. Immediately below the melting point 95 lines were still present, and were again those of the room temperature structure.

The reaction:

$$Bi_4Rh \rightarrow Bi_2Rh \text{ (high temperature modification)} + \text{liquid alloy}$$

has been confirmed by a high temperature X-ray investigation of Bi_2Rh which showed Bi_2Rh to have a structural change at about 430°C.

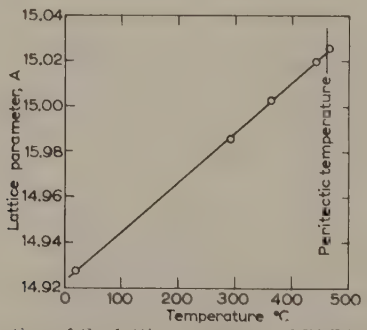

Fig. 2. The variation of the lattice parameter of Bi_4Rh with temperature.

All lines of the Bi_4Rh powder pattern were indexed in agreement with space group No. 230 (International Tables, 1952), which has bodycentred cubic symmetry. This is the structure given by ZHURAVLEV AND ZHDANOV[9] for α-Bi_4Rh. The lattice spacing

References p. 308

was determined as 14.9274 ± 0.0002 Å at 20°C and Fig. 2 shows the variation with temperature.

DISCUSSION

Fig. 3 shows the equilibrium diagram of bismuth-rich BiRh alloys as determined by the present work and the thermal analyses of WOOLMINGTON.

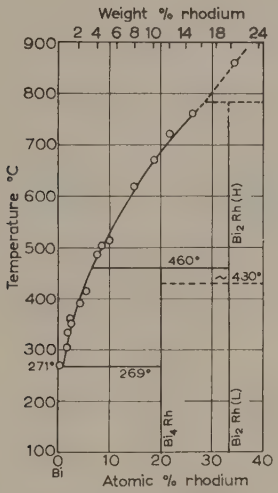

Fig. 3. The system Bi–Rh (present authors).

So far as conditions of true equilibrium are concerned, the diagram appears to be very much more simple than that previously accepted. WOOLMINGTON[5] obtained evidence of slight thermal arrests on some alloys at 325° and 390°C. These, however, were very ill-defined and were regarded as uncertain. The present work established conclusively that one form of Bi_4Rh is stable up to the melting point and no explanation can be offered of the method by which the supposed β and γ modifications were produced.

ACKNOWLEDGEMENTS

One of us (W.H.-R.) acknowledges with thanks the receipt of a grant from the United Kingdom Atomic Energy Authority towards the cost of the research programme.

R.G.R. is indebted to the United Kingdom Atomic Energy Authority for the award of a research bursary.

The authors must also express their thanks to Mr. K. G. WOOLMINGTON for the determination of the liquidus points which are included in Fig. 3.

References p. 308

REFERENCES

[1] E. J. RODE, *Izvest. Inst. Izucheniyu Platiny i Drug. Blagorod. Metal.*, No. 7, (1929) 21 (in Russian). Original paper not available, information taken from ref.[2].
[2] M. HANSEN AND K. ANDERKO, *Constitution of Binary Alloys*, McGraw-Hill Book Company, Inc., New York, 1958.
[3] N. N. ZHURAVLEV AND G. S. ZHDANOV, *Zhur. Eksper. i Teoret. Fiz.* 28, (1955) 228 (in Russian). Translation from *Soviet Phys. JETP*, 1 (1955) 91.
[4] N. N. ZHURAVLEV AND G. S. ZHDANOV *Izvest. Akad. Nauk S.S.S.R., Ser. Fiz.*, 20 (1956) 708 (in Russian). Original paper not available, abstract from *Abstr. J. Met.(U.S.S.R.)(English translation)*, No. 10, 11, 12 (1957) Abstract No. 44, p. 16.
[5] K. G. WOOLMINGTON, unpublished work.
[6] Z. S. BASINSKI, W. B. PEARSON AND J. W. CHRISTIAN, *J. Sci. Instr.*, 29 (1952) 154.
[7] W. HUME-ROTHERY AND P. W. REYNOLDS, *Proc. Roy. Soc.*, A 167 (1938) 25.
[8] E. A. OWEN AND E. W. ROBERTS, *Phil. Mag.*, 27 (1939) 294.

Note added in proof:

The complete structural determination of Bi_4Rh (*i.e.* the α-Bi_4Rh of Ref. 3) is given in G. S. ZHDANOV, *Trudy Inst. Krist. Akad. Nauk S.S.S.R.*, 10 (1954) 99.

A NOTE ON TRANSFORMATIONS IN METALLIC CERIUM

R. T. WEINER AND G. V. RAYNOR

Department of Physical Metallurgy, The University, Edgbaston, Birmingham (Great Britain)

(Received July 11th, 1959)

SUMMARY

Experiments on two samples of metallic cerium, respectively 99% and 99.95% pure, have failed to produce transformation from the normal face-centred cubic structure ($a_0 = 5.1502$ kX) to the close-packed hexagonal modification to which references appear in the literature. A possible new phase has, however, been observed after annealing the normal face-centred cubic modification for periods of 24 hours to one week at temperatures above 500°C, followed by slow cooling. The new structure, which is face-centred cubic, has a lattice spacing $a_0 = 5.112$ kX, and after annealing at 700°C, is admixed with only very small amounts of the initial face-centred cubic structure with $a_0 = 5.1502$ kX. The latter may possibly be metastable at room temperature in samples solidified from the melt. The new structure may, however, be connected with the presence of small amounts of hydrogen in the samples, as evidenced by the detection in diffraction patterns of very weak lines due to CeH_2.

INTRODUCTION

Confusion exists in the literature of the subject with regard to the room temperature structure of cerium, and the structural changes which may occur on alteration of temperature or annealing. Though many authorities agree that at room temperature cerium is face-centred cubic, with a_0 lying between 5.140 and 5.1502 kX[1-6], there are also references to the existence of a close-packed hexagonal phase ($a_0 = 3.65$ kX; $c_0 = 5.96$ kX) in addition to the cubic modification[7,8]. Above approximately 700°C (or 730°C according to SPEDDING, DAANE AND HERMANN[6]) a high-temperature modification of unknown structure exists. Interesting transformations occur below room temperature; thus on rapid cooling to the temperature of liquid air, a face-centred cubic structure of lattice spacing $a_0 = 4.82$ Å may be produced[9], and the same structure has been observed on compression to 12,430 kg/cm^2 [10,11]. Examinations of certain physical properties as functions of temperature have, however, revealed complicating anomalies. Thus, FOËX AND TROMBE[12], in the course of a dilatometric study of cerium of purity 99.6%, found that cooling to liquid nitrogen temperatures after quenching to room temperature from 400°C produced a marked contraction at —160° to —170°C, presumably owing to the formation of the structure with $a_0 = 4.82$ Å; similar treatment following slow cooling to room temperature, however, gave rise to a small increase in length at —50°C, the contraction at —160°C being very much reduced. This work suggested that a modification (γ), presumably stable at 400°C, is retained by quenching, and can subsequently be transformed at low temperatures into the contracted face-centred cubic structure (α); on slow cooling to room temperature, the γ phase appears to transform into another phase (β), from which it is not

References p. 313

possible to produce α at low temperatures. Support for these suggestions has been obtained from work on electrical resistance[13] and magnetic susceptibility[14] as functions of temperature. According to MAHN[15] the effect of magnesium is to stabilise β at the expense of γ, while further dilatometric work by TROMBE AND FOËX[16] on metal of commercial purity (major impurities calcium and iron) indicates that the $\gamma \rightarrow \alpha$ change occurs at lower temperatures, and the $\beta \rightarrow \alpha$ change at higher temperatures, than in the pure metal. Further, the $\gamma \rightarrow \beta$ change has been shown to occur slowly in specimens cooled slowly to room temperature and held there for 5 months. The transformations are thus impurity sensitive, and this may explain why other workers[17,18] have failed to observe physical property anomalies at low temperatures attributable to the formation of α; owing to the impurity contents, the metal used was probably in the form denoted β by FOËX AND TROMBE[12].

Further complications have been noted. According to DIALER AND ROTHE[19], who worked mainly on the cerium–hydrogen system, the two forms of cerium which can be obtained at ordinary temperatures are both face-centred cubic. One, with $a_0 = 5.142$ kX, does not react with hydrogen at room temperature, whereas conversion to the other form ($a_0 = 5.126$ kX) allows reaction to take place. JAMES, LEGVOLD AND SPEDDING[20], however, while generally agreeing with the electrical resistance work of FOËX[13], found the diffraction pattern of a specimen containing the β form of cerium to contain lines due to a close-packed hexagonal structure in addition to those due to a face-centred cubic structure. Evidence was also found for a transformation from β to α at lower temperatures (11° to 14°K) than that of γ to α.

The most plausible interpretation of previous work is that, at temperatures considerably above room temperature, cerium exists in the γ state but undergoes a sluggish change at lower temperatures to a β modification. Cooling of γ to liquid air temperatures produces α (face-centred cubic, $a_0 = 4.82$ Å), but the $\beta \rightarrow \alpha$ change if possible at all, can occur only at still lower temperatures. Owing to the very slow $\gamma \rightarrow \beta$ change, most specimens of cerium are probably in the γ state at room temperature, from which it may be inferred that γ is the face-centred cubic form with $a_0 = 5.1202$ kX[5,6]. The nature of β appears uncertain, both face-centred cubic and close-packed hexagonal structures having been reported, with the latter more probable.

The present note describes further experiments undertaken in an attempt to gain further information with regard to the structure of cerium.

EXPERIMENTAL RESULTS

Two samples of metallic cerium were available. Sample 1 was 99% pure and contained 0.9% iron and 0.1% other rare earths; sample 2 was 99.95% pure, containing only 0.002% iron, $<$ 0.05% lithium and traces of silicon, manganese, sodium, molybdenum, copper and aluminium.

Filings of sample 1, annealed in evacuated pyrex tubes at temperatures from 450° to 650°C and rapidly cooled, gave diffraction patterns in which the main lines corresponded to a face-centred cubic structure of lattice spacing $a_0 = 5.1508$ kX, in good agreement with the work of SPEDDING *et al.*[5,6]. Extra lines were present, which were indexed in terms of a face-centred cubic unit cell of lattice spacing $a = 5.57$ kX. This corresponds with the structure of CeH_2[21], indicating that, at the annealing temperature, the filings had reacted with water vapour originating from the glass. To minimise hydrogen contamination, new experimental arrangements

References p. 313

were made which allowed the filings to be annealed at a pressure of $< 10^{-6}$ mm Hg in a transparent silica tube which had been outgassed at 950°C for 2 days with continuous pumping. By these means the CeH_2 lines on diffraction photographs were reduced to very low intensities. Whether quenched from 500°C or slowly cooled to room temperature over 12 h the cerium structure observed for sample 1 proved to be face-centred cubic (Fig. 1(a)), with $a_0 = 5.1508$ kX. Corresponding experiments for fine wires of sample 2 indicated the same face-centred cubic structure, with $a_0 = 5.1501$ kX. If this structure is identified with γ, the experiments gave no indication of the formation of β on slow cooling.

In order to approximate to conditions used in the experiments of FOËX AND TROMBE[12], slowly cooled filings of sample 1 and fibres of sample 2 were cooled to the temperature of liquid air, and in some cases cycled between room temperature and that of liquid nitrogen. The resulting room temperature diffraction patterns contained diffuse lines corresponding in position with those of the γ modification, and no indication of a second structure. Though no survival of the α structure would be expected, the work of FOËX AND TROMBE suggests that the β modification should be present. It was, however, not observed in the present work.

In the hope of producing β by other heat treatments, filaments of sample 2 were annealed, at a pressure of $< 10^{-6}$ mm Hg, at 600°, 650° and 700°C for periods of 24 h, 1 week, and 24 h respectively, and cooled to room temperature over periods of 16 h. In all three cases the diffraction patterns contained sharp lines corresponding to the presence of γ ($a_0 = 5.1508$ kX), together with rather more diffuse lines due to another face-centred cubic structure with $a_0 = 5.112$ kX, which may be denoted γ'. The γ' content was much greater after annealing at 650°C than after treatment at 600°C (Fig. 1(b)); in the specimen annealed at 700°C, the γ modification had almost disappeared (Fig. 1(c)). The specimen slowly cooled from 700°C, consisting mainly of γ', showed no change in diffraction pattern after cooling to liquid nitrogen temperatures; the γ' lines remained sharp, suggesting that no transformation to α had taken place at the lower temperatures.

Further attempts to produce β by the deformation of cerium at the temperatures of solid carbon dioxide or liquid nitrogen were unsuccessful; subsequent room temperature diffraction patterns showed only diffuse lines due to the γ structure.

DISCUSSION

In no experiments of the present work was any indication of the existence of a close-packed hexagonal β structure obtained. It may be suggested, therefore, either that this structure does not exist as a modification of cerium, or that the particular impurities in the samples used in the present work (especially hydrogen) suppress the $\gamma \rightarrow \beta$ change. The production of the γ' phase (face-centred cubic, $a_0 = 5.112$ kX) is unexpected; this phase may, however, correspond with the modification denoted β in work on electrical resistance and magnetic susceptibility changes with change in temperature, although the conditions of its formation do not support this view.

The present work suggests that the γ' structure corresponds with a new phase not previously reported, which is formed by long annealing of the γ structure at temperatures in excess of 500°C. The γ structure which is observed at room temperature in metal solidified from the melt would thus appear to be metastable; annealing at 500°C, followed by quenching or slow cooling, does not suffice to change this struc-

References p. 313

Fig. 1(a). Heated to 500°C, and cooled to room temperature in 12 hours.

Fig. 1(b). Annealed 24 hours at 600°C, and cooled to room temperature in 16 hours.

Fig. 1(c). Annealed 24 hours at 700°C, and cooled to room temperature in 16 hours.

ture, whereas annealing at 600°, 650° and 700°C leads to a progressive development of γ', which remains unchanged on slow cooling. It is thus possible that γ is in reality a high temperature modification of cerium, the transformation of which to γ' is so sluggish that the latter can be obtained only by long annealing and not during cooling of the solidified metal to room temperature. It appears improbable that γ' is a high temperature form to which γ changes on heating; if this were so, and in view of the fact that γ is obtained at room temperature after normal solidification, γ' would not be expected to survive the slow cooling from the temperature of annealing to room temperature over 16 h.

It is of interest to note that a face-centred cubic form of lanthanum with a spacing 0.5 to 1% smaller than the normal face-centred cubic lanthanum structure has also been detected, admixed with the normal face-centred cubic structure at room temperature[22], following annealing of the close-packed hexagonal material at 350° to 400°C for two to four days.

Metallic cerium therefore may show one or other, or a mixture, of two face-centred cubic phases with slightly different parameters according to heat treatment. The γ' phase ($a_0 = 5.112$ kX) appears to be the stable modification, but the possibility that it occurs only in the presence of traces of hydrogen should be considered. Thus, according to MULFORD AND HOLLEY[23] the solubility of hydrogen in cerium is negligible at temperatures below 500°C; it is only above 500°C that the cerium γ-phase can be made to change into γ' by annealing, and it may be that a small solution of hydrogen is necessary for the formation of γ'. If this is true, the necessary amount of hydrogen must be very small, in view of the good vacua attained in the present work.

ACKNOWLEDGEMENTS

The authors gratefully acknowledge the financial support of the United Kingdom Atomic Energy Authority for the work reported, which forms a part of a more general programme.

REFERENCES

1 L. L. QUILL, *Z. anorg. u. allgem. Chem.*, 208 (1932) 273.
2 E. E. SCHUMACHER AND F. F. LUCAS, *J. Am. Chem. Soc.*, 46 (1924) 1167.
3 L. F. AUDREITH, *Metallwirtschaft*, 14 (1935) 3.
4 W. KLEMM AND H. BOMMER, *Z. anorg. u. allgem. Chem.*, 231 (1937) 138.
5 F. H. SPEDDING, A. H. DAANE AND K. W. HERMANN, *Acta Cryst.*, 9 (1956) 559.
6 F. H. SPEDDING, A. H. DAANE AND K. W. HERMANN, *J. Metals*, 9 (1957) 895.
7 A. W. HULL, *Phys. Rev.*, 18 (1921) 88.
8 E. ZINTL AND S. NEUMAYR, *Z. Elektrochem.*, 39 (1933) 84.
9 A. F. SCHUCH AND J. H. STURDIVANT, *J. Chem. Phys.*, 18 (1950) 145.
10 P. W. BRIDGMAN, *Proc. Am. Acad. Arts Sci.*, 76 (1948) 71.
11 A. W. LAWSON AND TING-YUAN TANG, *Phys. Rev.*, 76 (1949) 301.
12 M. FOËX AND F. TROMBE, *Compt. rend.*, 217 (1943) 501.
13 M. FOËX, *Compt. rend.*, 219 (1944) 117.
14 F. TROMBE, *Compt. rend.*, 219 (1944) 90.
15 F. MAHN, *Compt. rend.*, 223 (1946) 78.
16 F. TROMBE AND M. FOËX, *Compt. rend.*, 223 (1946) 949.
17 C. STARR AND A. R. KAUFMANN, *Phys. Rev.*, 58 (1940) 657.
18 L. F. WERESCHTSCHAGIN, L. W. SCHUBNIKOW AND B. G. LASAREW, *Physik. Z. Sowjetunion*, 10 (1936) 618.
19 K. D. DIALER AND W. ROTHE, *Z. Elektrochem.*, 59 (1955) 970.
20 N. R. JAMES, S. LEGVOLD AND F. H. SPEDDING, *Phys. Rev.*, 88 (1952) 1092.
21 C. E. HOLLEY, R. N. R. MULFORD, E. H. ELLINGER, W. C. KOEHLER AND W. H. ZACHARIESEN, *J. Phys. Chem.*, 59 (1955) 1226.
22 W. T. ZIEGLER, R. A. YOUNG AND A. L. FLOYD, *J. Am. Chem. Soc.*, 75 (1953) 1215.
23 R. N. R. MULFORD AND C. E. HOLLEY, *J. Phys. Chem.*, 59 (1955) 1222.

SOME OBSERVATIONS ON THORIUM-RICH THORIUM–INDIUM ALLOYS

J. R. MURRAY

Metallurgy Division, U.K. Atomic Energy Research Establishment, Harwell, Berks. (Great Britain)

(Received July 28th, 1959)

SUMMARY

Thorium–indium alloys containing 0–33 at.% indium have been studied by metallographic and X-ray methods. Within this composition range one compound, Th_2In, occurs; this melts at 1170 ± 10°C and forms a eutectic with α-thorium at approximately 18 at.% indium and 1160 ± 10°C. Th_2In has the tetragonal $CuAl_2$ (C16) structure, $a = 7.787$, $c = 6.113$ Å, and is isostructural with Th_2Al, Th_2Ag etc. The solubilities of indium in α-thorium at 1160° and 800°C are approximately 9.2 at.% and 1.7 at.% respectively; solubility of indium increases the room temperature hardness of thorium and age-hardening has been observed at 600°C in an 8.6 at.% indium alloy. Within the solid solubility range, indium enhances the oxidation resistance of thorium at room temperature but the intermetallic compounds oxidise readily to form indium and thorium oxide.

INTRODUCTION

The constitution of thorium–indium alloys has been investigated at the Atomic Energy Research Establishment as part of a general programme for the study of the alloying behaviour of thorium. GOLDHOFF, OGDEN AND JAFFEE[1,2] examined the mechanical properties of thorium alloys containing up to 5 at.% of various alloying additions and found that indium was one of the few elements which increased the yield strength of "Ames" thorium*. They also observed that indium produced a significant increase in the hardness, both at room temperature and at 300°C and suggested that thorium–indium alloys may exhibit age-hardening but make no mention of the constitution of these alloys. FERRO[3] recently published information on the crystal structure of an intermetallic compound $ThIn_3$ which has the cubic LI_2 structure and is isostructural with $ThHg_3$, $ThTl_3$, $ThSn_3$, $ThPb_3$ and UIn_3 etc.; he found that "the alloys are rather oxidisable".

EXPERIMENTAL METHODS

Electrolytic thorium was used throughout, this contained carbon 100–150 p.p.m., oxygen 2000–3000 p.p.m. and total metallic impurities of less than 300 p.p.m.; the indium was supplied by Messrs. Johnson Matthey & Co. Ltd. Alloys were prepared by arc-melting in a zirconium-gettered argon atmosphere when some weight loss

* A typical analysis of Ames material is Fe 250–350 p.p.m., Al 100–1000 p.p.m., Cr 120 p.p.m., Ni 78 p.p.m., Si 80 p.p.m, Be 250 p.p.m., C 500–1000 p.p.m., N 80 p.p.m., O 1700 p.p.m.

References p. 320

occurred; the nominal compositions were calculated after melting on the assumption that any loss of weight was due to volatilization of indium.

For solid solubility determinations, specimens containing less than 12.5 at.% indium were cold-worked in a vice, wrapped in tantalum foil and sealed in silica capsules under a vacuum of better than 10^{-5} mm Hg; alloys with higher indium contents were too brittle to be cold-worked. Melting points were determined by annealing and quenching specimens wrapped in tantalum foil as for solid solubility studies; the alloys did not wet the tantalum when melting occurred. Conventional methods of mounting and polishing were employed in the preparation of sections for metallographic examination and air tarnishing proved a satisfactory method of differentiating between phases. The hardness was determined using a standard Vickers pyramid hardness tester with a 10 kg load; all results are the average of at least three values.

Powders for X-ray studies were prepared by crushing or filing under CCl_4 depending on the brittleness of the particular material. Powder patterns were obtained with a Guinier focussing camera, equivalent in size to a standard 19 cm diameter camera, using monochromatised copper radiation. The calculated intensities were obtained from the expression

$$I_c \propto \frac{1 + \cos^2 2\theta \cos^2 2\alpha}{(1 + \cos^2 2\alpha) \sin^2 \theta \cos \theta} pF^2$$

where I_c is the calculated intensity, θ the Bragg angle, α the angle which the X-ray beam from the anticathode makes with the monochromator (for Cu K_α radiation $2\alpha = 26°40'$) p the multiplicity and F the structure factor. Lines due to the small amount of ThO_2 which was present in all specimens, have been ignored except those which were superimposed on lines due to the intermetallic compound. The weighted mean wavelength for Cu K_α radiation has been taken as 1.54180 Å.

RESULTS

In general, alloys containing more than 33 at.% indium corroded in moist air too rapidly to be investigated by the methods outlined above and no effort was made to develop equipment suitable for handling these materials. An effect noted on several of these indium-richer alloys was the growth of "whiskers" when the specimens were stored in dry air (Fig. 1); X-ray examination showed that they were indium. Alloys which crumbled on storage in air or under oil or CCl_4 gave X-ray patterns of ThO_2 $a = 5.60$ Å and indium $a = 3.25$, $c = 4.95$ Å. Metallography was possible on an alloy containing 74 at.% indium which was found to be essentially single phase (Fig. 2) in agreement with FERRO[3]. Specimens with 40–66 at.% indium crumbled much more rapidly, suggesting the occurrence of at least one other readily oxidisable compound in this composition range.

Results on alloys containing 0–33 at.% indium are summarized in Fig. 3. No attempt was made to determine the effect of indium on the face-centred cubic (α) to body-centred cubic (β) phase change in thorium. The solid solubility of indium in α-thorium was determined primarily by metallographic methods but lattice parameters were calculated from X-ray powder patterns of filings from alloys containing 5.6 and 12.4 at.% indium annealed at temperatures up to 1150°C. Solution of indium

References p. 320

Fig. 1. Whiskers grown on thorium–75 at.% indium alloy during storage in a bottle.

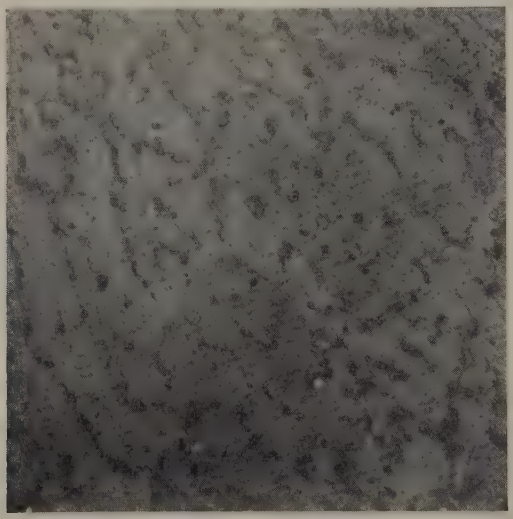

Fig. 2. Thorium–75 at.% indium alloy as arc-melted. Mechanically polished and air tarnished. Essentially single phase $ThIn_3$.

caused a contraction of the thorium lattice. The change in atomic volume with composition was calculated assuming Vegard's law to be obeyed and using this graph an estimate of the solubility/temperature relationship was made from the observed

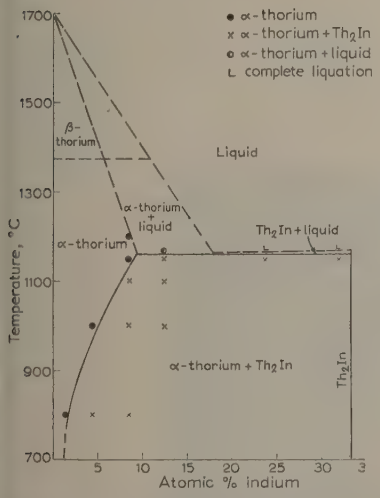

Fig. 3. Phase diagram of thorium–indium alloys containing 0.33 at.% indium.

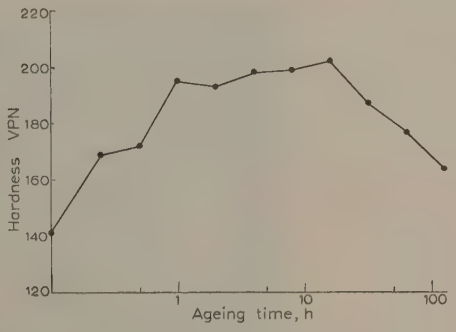

Fig. 4. Ageing curve at 600°C for thorium–8.6 at.% indium alloy.

lattice parameters; solubilities determined in this way agreed well with those obtained metallographically. A plot of the logarithm of the metallographic values for the solubilities against the reciprocal of the absolute temperatures gave a straight line relationship.

Solution of indium increased the hardness of thorium from 65 VPN for the unalloyed material to 141 VPN for the specimen containing 8.6 at.% indium after solution treatment at 1100°C. Age-hardening was observed in this alloy on subsequent annealing at 600°C and the results are shown in Fig. 4; a maximum hardness of 202 VPN was observed after 16 hours. Metallographic examination after ageing for 128 hours showed that precipitation of Th_2In had occurred mainly at the grain boundaries.

Within the solid solubility range, additions of indium enhanced the tarnishing resistance of thorium to air at room temperature but if the solubility limit was exceeded the rate of oxidation of alloys containing up to 33 at.% indium increased with increasing indium content due to oxidation of the second phase.

The intermetallic compound richest in thorium was Th_2In which solidified directly from the liquid and melted at 1170 ± 10°C; it formed a eutectic with α–thorium at approximately 18 at.% indium and 1160 ± 10°C and Fig. 5 shows the microstructure of a segregated alloy containing 24 at.% indium. The X-ray powder pattern of Th_2In could be indexed on the basis of a tetragonal unit cell $a = 7.787$, $c = 6.113$ Å, calculated and observed values of $\sin^2\theta$ are given in Table I. The compound has four units of Th_2In per unit cell giving a calculated density of 10.36 g/c.c., the density could not be measured directly since the specimen reacted rapidly with all available liquids.

References p. 320

The observed intensities compare well with those for the $CuAl_2$ (C 16) structure, space group D_{4h}^{18} – 14/mcm as shown in Table I. The nearest neighbour distances are:

Th –	4In	3.308 Å
	1Th	3.473
	2Th	3.667
	4Th	3.924
In –	2In	3.051
	8Th	3.308

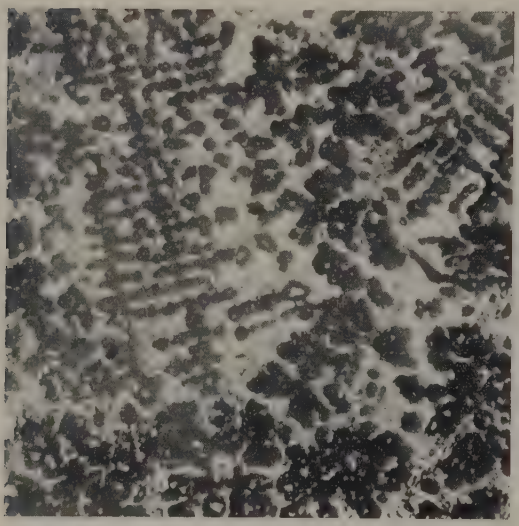

Fig. 5. Thorium–24 at.% indium alloy as arc-melted. Alloy showed some segregation, indium-richer area as mechanically polished and air-tarnished dendrites of Th_2In in thorium–Th_2In eutectic.

DISCUSSION

The electronic structures of aluminium and indium in the free atom have some similarity since each has two '*s*' and one '*p*' electron in the outer shell and this similarity is reflected in the binary alloys of the elements with thorium. In both the thorium–aluminium[4–8] and thorium–indium systems several intermetallic compounds occur and the compounds richest in thorium are isostructural, having the $CuAl_2$ (C16) structure. In each case there is a temperature dependant solubility of the second element in thorium[5] and, after suitable heat treatment, precipitation hardening has been obtained[9]. It is possible that gallium and thallium might behave similarly although the smaller size of the gallium atom might lead to a lower solubility than that of aluminium.

In the pure metals the atomic diameters for twelvefold co-ordination for aluminium, indium and thorium are 2.80, 3.14 and 3.59 respectively and, if aluminium and indium

References p. 320

TABLE I

COMPARISON OF OBSERVED AND CALCULATED $\sin^2\theta$ VALUES AND LINE INTENSITIES FOR Th_2In

hkl	$\sin^2\theta_{obs}$	$\sin^2\theta_{calc}$	I_{obs}	I_{calc}
110	—	0.0196	—	0.1
200	0.0392	0.0392	vvw	1.9
002	0.0633	0.0636	wm	11.9
211	0.0647	0.0649	ss	100
220	0.0784	0.0784	w	5.8
112	0.0830	0.0832	m	19.2
310	0.0981	0.0980	s	31.7
202	0.1028	0.1028	m	20.8
222	—	0.1420	—	0.2
321	0.1434	0.1433	vvw	1.4
400	0.1569	0.1568	vw	2.4
312	0.1616	0.1616	vw	4.3
330	0.1764	0.1764	w	5.7
411	0.1825	0.1825	m	15.3
213	0.1920	0.1921	m	22.2
420	0.1961	0.1960	w	5.1
402	0.2203	0.2204	m	13.0
332	0.2401	0.2400	m	19.8
004 510	0.2548	{0.2544 0.2548	vw	{4.7 0.1
422	—	0.2596	—	0
431	—	0.2609	—	0.3
323	—	0.2705	—	0.5
114	—	0.2740	—	0
204	—	0.2936	—	0.2
521	0.3001	0.3001	m	14.6
413	0.3095	0.3097	vw	6.6
512	0.3185	0.3184	vvvw	2.5
440	—	0.3234	—	1.9
224 530	0.3332	{0.3328 0.3332	vvvw	{1.3 1.9
314 600	0.3528	{0.3524 0.3528	mw	{9.0 5.2
611	0.3787	0.3785	m*	1.0
442	—	0.3870	—	0.3
433	—	0.3881	—	0.2
620	—	0.3920	—	0.1
532	—	0.3968	—	0
404	—	0.4112	—	1.1
602	—	0.4164	—	2.9
541	0.4180	0.4177	vw	5.8
523	0.4276	0.4273	w	8.9
334	—	0.4308	—	3.0
215	0.4451	0.4465	vvw	6.1

* ThO_2 line.

do not change their effective diameter (d) on solution in thorium, indium has a more favourable size factor ($d_{Th}/d_{In} = 1.14$) than aluminium ($d_{Th}/d_{In} = 1.28$). Its high solubility in thorium may be explained in this way (the maximum solubility of aluminium and of indium in α-thorium are approximately 0.9 at.% and 9.2 at.% respectively).

RAYNOR[10], in a survey of the compounds crystallizing in the $CuAl_2(BA_2)$ structure,

References p. 320

has suggested that for this structure to be assumed $d_A/d_B \sim 1.2$ where d_A and d_B are the atomic radii of the larger and smaller atoms respectively. For Th_2In $d_A/d_B = 1.14$ which is fairly close to 1.2. The contraction in the larger atom (thorium) nearest neighbour distance is characteristic of the $CuAl_2$ structure as is the small volume expansion on formation (approximately 1%).

The hardness values of 70 and 91 VPN obtained on the 1.5 and 4.6 at.% indium alloys respectively after annealing for three weeks at 800°C show fair agreement with values of 88 and 115 VPN quoted by GOLDHOFF, OGDEN AND JAFFEE[2] for 1 and 5 at.% indium alloys which had been worked at 300°C and annealed for two hours at 850°C. The considerable precipitation hardening observed in an 8.6 at.% indium alloy aged at 600°C, confirmed the tentative conclusion of GOLDHOFF, OGDEN AND JAFFEE[2] that age-hardening had occurred in a 4.6 at.% indium alloy which was annealed at 300° and 400°C. The hardness values obtained with the 8.6 at.% indium alloy were higher, after ageing at 600°C for times of up to 64 h, than those observed previously in thorium–aluminium and thorium–uranium alloys[9]. As with thorium–aluminium alloys there is a slight kink in the hardness curve after ageing for $\frac{1}{2}$ h at 600°C which suggests that precipitation of Th_2In from face-centred-cubic α–thorium might be multi-stage as is the case for precipitation of the isostructural compound $CuAl_2$ from face-centred-cubic aluminium.

ACKNOWLEDGEMENT

The author would like to thank Mr. C. H. THOMAS for assistance with the melting and heat treatment.

REFERENCES

1 R. M. GOLDHOFF, H. R. OGDEN AND R. I. JAFFEE, *U.S. Atomic Energy Comm., Report*, BMI. 720 (1951).
2 R. M. GOLDHOFF, H. R. OGDEN AND R. I. JAFFEE, *U.S. Atomic Energy Comm. Report*, BMI. 776 (1952).
3 R. FERRO, *Acta Cryst.*, 11 (10) (1958) 737.
4 J. R. MURRAY, *J. Inst. Metals*, 84 (1955–56) 91.
5 J. R. MURRAY, *J. Inst. Metals*, 87 (1958–59) 349.
6 P. B. BRAUN AND J. H. N. VAN VUCHT, *Acta Cryst.*, 8 (2) (1955) 117.
7 P. B. BRAUN AND J. H. N. VAN VUCHT, *Acta Cryst.*, 8 (4) (1955) 246.
8 A. F. ANDRESEN AND J. A. GOEDKOOP, *Acta Cryst.*, 8 (2) (1955) 118.
9 G. H. BANNISTER AND J. R. MURRAY, *Atomic Energy Research Establ. (G. B.), Report*, 2951 (1959).
10 G. V. RAYNOR, Progress in Metal Physics, Vol. 1, Butterworths, London, 1949, p. 1.

THE ELECTRODEPOSITION OF BERYLLIUM FROM NON-AQUEOUS SOLUTIONS

I. A. MENZIES*, D. L. HILL** AND L. W. OWEN

United Kingdom Atomic Energy Authority, A.W.R.E., Aldermaston, Berks. (Great Britain)

(Received July 29th, 1959)

SUMMARY

Electrolyses of solutions of beryllium chloride in anhydrous liquid ammonia have been carried out at —33°C using platinum and beryllium anodes and copper and beryllium cathodes. Gassing occurred at both anode and cathode in all electrolyses but no metal was deposited at the cathode.

The anodic dissolution and cathodic re-deposition of beryllium in fused-salt baths at 400–500°C has been studied. Beryllium dissolves anodically in eutectic mixtures of LiCl–KCl and NaCl–$BeCl_2$ and metal of 99.5% purity is obtained at the cathode. The general features of such systems and the effect of complex ion formation on the possible deposition mechanisms are discussed.

INTRODUCTION

Beryllium is of interest in the atomic energy field because of its low absorption and high scattering cross section for thermal neutrons. The metallurgical properties and nuclear applications of this metal have been reviewed recently[1–3].

The electrodeposition of beryllium from solutions of its compounds in organic solvents has been studied[4–6]. Several workers have claimed successful deposition of metal from solutions of beryllium chloride, beryllium acetylacetonate and other beryllium compounds in solvents such as aniline, pyrrole, and piperidine. More recent work in the United States[7] and by the present authors[8] indicates that many of these early claims cannot be confirmed. Metallic beryllium has, however, been obtained[7,8] by electrolysing beryllium chloride etherate at 150°C and also by electrolysing mixtures of beryllium chloride and beryllium dimethyl in ethyl ether at 20°C.

Although several workers have claimed the deposition of beryllium from solutions of its compounds in liquid ammonia[9–12] little information as to the purity and form of the metal obtained has been given. There is a large volume of literature[13–22] concerning the extraction of beryllium by the electrolysis of beryllium chloride in fused alkali metal chloride baths, but the possibility of refining beryllium in such baths by anodic dissolution and cathodic deposition of pure metal has not been investigated. In the present investigation the electrolysis of solutions of beryllium chloride in liquid ammonia, and the anodic dissolution and cathodic re-deposition of beryllium have been studied.

* Now at Research and Development Branch U.K.A.E.A (I.G.) Springfields Works, Preston, Lancs.

** Now at Rensselaer Polytechnic Institute, Troy, N.Y., U.S.A.

References p. 329/330

EXPERIMENTAL

(a) *Purification of beryllium chloride*

Beryllium chloride of commercial grade which contained iron and hydrolysis products was purified before use. A sample of the chloride was heated to 300°C in a "Pyrex" glass still and hydrogen passed over it for one hour to convert volatile ferric chloride to non-volatile ferrous chloride. The temperature of the still was then

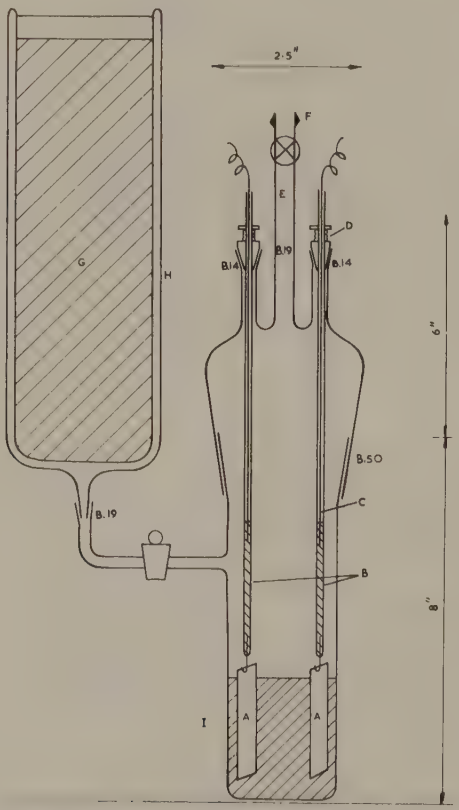

Fig. 1. Liquid ammonia electrolysis cell. A. Electrodes. B. Electrode supports filled with mercury. C. Copper wires. D. 'O' ring seal. E. Connecting arm to vacuum system. F. Spherical ground glass joint. G. Solid carbon dioxide-acetone freezing mixture. H. Dewar flask. I. Etched volume calibration marks.

raised to 450–500°C and pure beryllium chloride distilled into a water-cooled receiver as a fine snow-white powder. This receiver was transferred to an argon-filled glove box, without allowing ingress of air, and the beryllium chloride removed and stored in sealed polythene bottles in the box.

References p. 329/330

(b) Purification of ammonia

Synthetic ammonia gas was passed through three drying towers containing calcium oxide before condensation over metallic sodium. The anhydrous ammonia thus obtained was distilled directly into the electrolysis cell.

(c) Purification of fused-salt melts.

Lithium chloride–potassium chloride melts were prepared from recrystallised materials which had been oven dried at 300°C for several hours. The eutectic mixture containing 60 mole % LiCl was made up from the dried powders, and melted and filtered in air at ∼ 400°C. The solid eutectic was then placed in the electrolysis cell (Fig. 2) and heated to ∼ 400°C in a vacuum of 10^{-3}–10^{-4} mm Hg. Hydrochloric acid gas was bubbled through the molten eutectic for one hour, the cell re-evacuated,

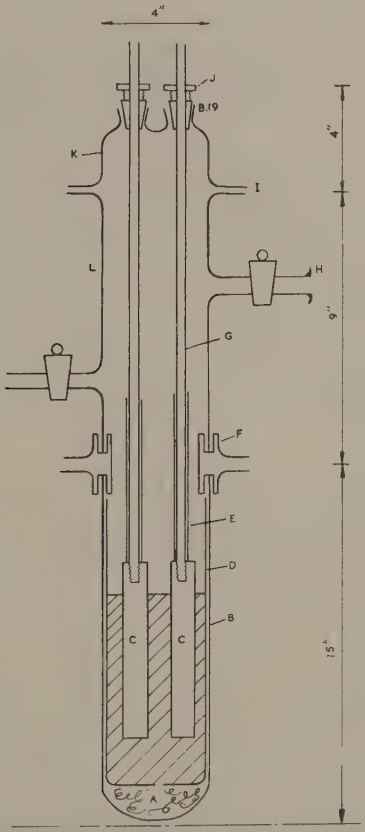

Fig. 2. Fused-salt electrolysis cell. A. Vitreosil wool pad. B. "Pyrex" glass test-tube. C. Graphite or beryllium electrode. D. Crucible. E. Alumina sheath. F. Water-cooled brass union. G. Stainless-steel electrode shaft. H. Spherical ground glass joint. I. Ground glass flange. J. 'O' ring seal. K. "Pyrex" glass dome. L. "Pyrex" glass cell body.

References p. 329/330

argon admitted, and pre-electrolysis carried out using a graphite anode and a nickel cathode at a voltage just below the decomposition voltage of the eutectic to remove final traces of moisture and metallic impurities such as iron. Pre-electrolysis was normally carried out overnight with argon flowing.

The sodium chloride–beryllium chloride eutectic mixture containing 50 mole % $BeCl_2$ was similarly purified except that this eutectic was not pre-melted in air and was heated in the electrolysis cell in argon not under vacuum.

(d) Purification of gases

"Lead-seal" argon of 99.95% purity was dried by passage through phosphorus pentoxide and purified by passage through titanium sponge at 1000°C.

(e) Liquid ammonia electrolysis cell and electrolysis procedure

The electrolysis cell shown in Fig. 1 was constructed of "Pyrex" glass. The cell was attached to a high vacuum system and to an anhydrous ammonia reservoir. The electrodes could be moved in a vertical direction by slightly loosening the screw caps on the 'O' ring seals D. The electrodes were strips of copper or platinum sheet 1.0 cm broad and 4.0 cm long or discs of beryllium 1 inch in diameter and 0.1 inches thick.

The electrolysis cell, filled with argon and loaded with beryllium chloride with the electrodes sealed in position in the head of the cell, was evacuated, and the required volume of anhydrous ammonia condensed on top of the beryllium chloride. Solution was assisted by means of a magnetic stirrer. The electrodes were lowered into the solution with a voltage applied and electrolysis commenced. During electrolysis the pressure of ammonia gas in the system was maintained at one atmosphere. At the end of the electrolysis the cold trap G was removed and the ammonia allowed to evaporate to waste through a CaO drying tower. The cell was then transferred to the glove box and the electrodes removed. The cathodes with their deposits were washed in acetone, dried and transferred to polythene bottles to await analysis.

(f) Fused-salt electrolysis cell and electrolysis procedure

The electrolysis cells used in this work are shown in Fig. 2. The water-cooled brass union facilitated replacement of the test-tube section B of the cell. There were five outlets on the cell head to accommodate the pre-electrolysis and electrolysis electrode assemblies and a thermocouple pocket. The cell was connected to a high vacuum system and a source of purified argon. The cell, with four electrodes and the thermocouple pocket in position, could be maintained at a vacuum of 10^{-5}–10^{-6} mm Hg at operating temperature.

After pre-electrolysis the cell was evacuated and purged with argon. The electrolysis electrodes were slid down into the melt and electrolysis commenced with a 300 ml/min flow of argon through the cell. At the end of the electrolysis the electrodes and thermocouple were withdrawn up into the cell body, and the apparatus allowed to cool to room temperature. All taps were then closed and the cell removed to the glove box for dismantling.

The deposited beryllium was leached with dilute caustic soda solution to remove aluminium, then washed with dilute nitric acid, water and finally acetone. The metal was then air dried on a filter pad.

References p. 329/330

(g) Analysis of cathode products

A number of deposits were subjected to particle size analysis through B.S.S. 410 (1943) Mesh sieves. All chemical analyses were carried out on flake or powder metal without compacting or melting.

The total beryllium was determined by precipitation as beryllium ammonium phosphate and subsequent ignition to beryllium pyrophosphate[23-25]. Interfering ions were removed from the solutions, before precipitation of beryllium ammonium phosphate, by sequestration with the disodium salt of ethylenediaminetetra-acetic acid (EDTA). These determinations are considered to be accurate to within $\pm$ 0.5%.

Oxygen was determined by the vacuum fusion method[26-28] and results are probably accurate to within $\pm$ 0.1% (as BeO) at the levels of the determinations. Molybdenum was determined spectrographically.

RESULTS

(a) Electrolyses in liquid ammonia solutions

The results of these experiments are given in Table I.

TABLE I

ELECTROLYSES IN SOLUTIONS OF BERYLLIUM CHLORIDE IN LIQUID AMMONIA AT —33°C

Wt. of $BeCl_2$ in solution g/l	*Anode*	*Cathode*	*Cathodic current density Amp. dm^{-2}*	*Notes*
30	Pt	Cu	0.1	Powdery black deposit
30	Be	Be	0.1	Loose black deposit–treeing at anode
30	Be	Cu	0.1	Powdery grey deposit
35	Pt	Cu	1.0	Powdery grey deposit
35	Be	Be	1.0	Black deposit–treeing at anode
35	Be	Cu	1.0	Black deposit–treeing at anode
40	Pt	Cu	3.0	Black deposit–treeing at anode
40	Be	Be	3.0	Grey deposit–treeing at anode
40	Be	Cu	3.0	Black semi-adherent deposit
45	Pt	Cu	5.0	Patchy deposit
45	Be	Be	5.0	Local spots of black deposits
45	Be	Cu	5.0	Powdery deposit

No satisfactory deposits were obtained in any of the above electrolyses. Violent gassing occurred at both electrodes and many of the deposits reacted with acetone yielding a white powder. The deposits did not exhibit any metallic lustre when examined microscopically although spectrographic analyses of a number of the deposits indicated the presence of beryllium.

There was no systematic variation of the form of deposit with variation of electro-

References p. 329/330

lysis conditions and it is therefore assumed that deposition of metal did not occur. The beryllium content of all of the deposits was 1–5%. It is possible that some compound of beryllium is deposited rather than metal.

(b) Electrolyses in fused-salt systems

The anodic dissolution of beryllium in lithium chloride–potassium chloride and sodium chloride–beryllium chloride melts was studied at 400–500°C. The results are given in Table II.

It is evident from these results that beryllium dissolves anodically in both molten salt baths and that high purity metal is deposited at the cathode. The dissolution process proceeds smoothly and the anode dissolves uniformly. Typical cell current–voltage curves obtained during the electrolyses are shown for the $\overset{+}{Be}/LiCl\text{-}KCl/\overset{-}{Be}$ system in Fig. 3 and for the $\overset{+}{C}/BeCl_2\text{–}NaCl/\overset{-}{Ni}$ system in Fig. 4.

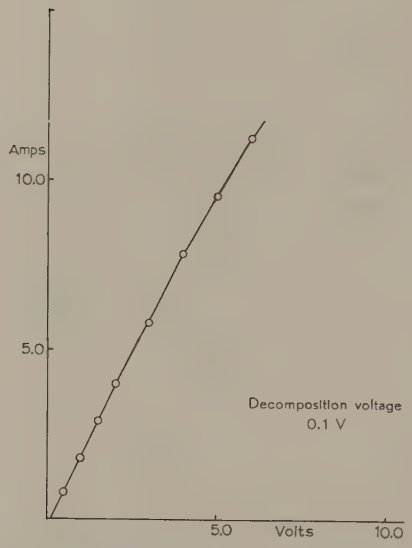

Fig. 3. Current–voltage curve in the system $\overset{+}{Be}/LiCl\text{–}KCl/\overset{-}{Be}$ at 550°C.

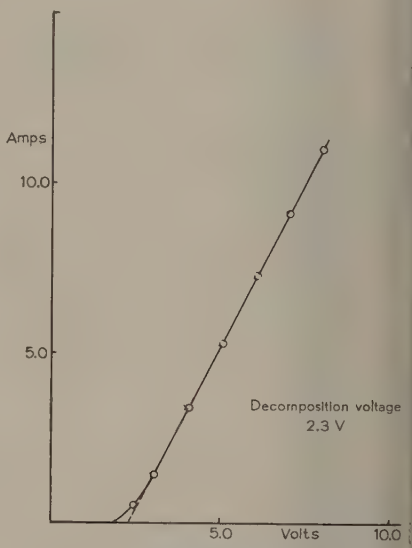

Fig. 4. Current–voltage curve in the system $\overset{+}{C}/BeCl_2\text{–}NaCl/\overset{-}{Ni}$ at 350°C.

The anodic current efficiencies are reasonable as the anodic current densities are high. In the $\overset{+}{Be}/LiCl\text{–}KCl/\overset{-}{Ni}_{Be}$ systems the only beryllium which can deposit cathodically is derived from the anode; hence it is to be expected that the cathodic efficiencies will be lower than the anodic efficiencies in these systems. There is some evidence that the anodic current efficiency decreases at higher current densities in the range 30.0–85.0 amp.dm^{-2}.

The purest metal produced by the process contained 99.5% beryllium. The metal purity was dependent on the length of time of electrolysis as shown by the results of

References p. 329/330

TABLE II

ANODIC DISSOLUTION AND CATHODIC DEPOSITION OF BERYLLIUM FROM LiCl–KCl AND NaCl–$BeCl_2$ MELTS

Run No. 1. 400°C; Be anode and cathode; stainless steel electrode supports in alumina sheaths.

Amp. h	*V*	*A.C.D.**	*C.C.D.**	*A.C.E.**	*C.C.E.**
20	3.0–1.0	50	70	70	63

Product: non-adherent grey powder containing 85% beryllium.

Run No. 2. 460°C; Be anode; Ni cathode; stainless steel electrode supports in alumina sheaths.

Amp. h	*V*	*A.C.D.*	*C.C.D.*	*A.C.E.*	*C.C.E.*
56	5.0–2.0	50	50	66	51

Adherent cathode deposit. Total Be content of metal 99.0%, BeO content 0.5%. Mesh analysis of deposit indicated:

+85	+300 — 85	—300
68%	29%	3%

Run No. 3. 500°C; Be anode and cathode; unprotected Mo electrode supports.

Amp. h	*V*	*A.C.D.*	*C.C.D.*	*A.C.E.*	*C.C.E.*
38	5.1–3.0	31	94	64	56

The cathode product was non-adherent and traces of alkali metal were found in the melt during leaching operations. The product was impure. Total Be content was 95%, BeO content 2.8% and Mo content 700 p.p.m. Mesh analysis indicated:

+85	+300 — 85	—300
70%	28.5%	1.5 %

Run No. 4. 550°C; Be anode; stainless steel cathode; electrode shafts protected by alumina sleeves.

Amp.h	*V*	*A.C.D.*	*C.C.D.*	*A.C.E.*	*C.C.E.*
140	3.0–1.0	85	170	40	31

The non-adherent cathode product consisted of flakes of beryllium up to 0.6 in. long. The total Be content of the metal was 99.5%. Mesh analysis indicated:

+85	+300 — 85	—300
65%	32%	3%

Run No. 5. 500°C. Bath containing equimolar amounts of $BeCl_2$ and NaCl. Be anode; Ni cathode; electrode shafts protected by alumina sheaths.

Amp.h	*V*	*A.C.D.*	*C.C.D.*	*A.C.E.*	*C.C.E.*
50	2.6–1.2	40	100	66	63

Adherent deposit. Large flake of pure beryllium. Total Be content of metal 99.3%.

Run No. 6. 350°C. Bath containing equimolar amounts of $BeCl_2$ and NaCl. Graphite anode; Ni cathode; electrode shafts protected by alumina sheaths.

	Amp. h	*V*	*C.C.D.*	*C.C.E.*[a]*
(1)	8.5	3.5	20	28
(2)	10.0	3.5	20	52

First product from electrolysis No. 1 consisted of shiny, adherent flakes of beryllium. The product of the second electrolysis was of larger particle size and had a total Be content of 99.4%.

* A.C.D.: anodic current density, amp.dm^{-2}.
C.C.D.: cathodic current density, amp.dm^{-2}.
A.C.E. and C.C.E.: anodic and cathodic current efficiencies based on the reactions $Be^{\circ} \rightarrow Be^{2+} + 2e$ and $Be^{2+} + 2e \rightarrow Be^{\circ}$.
C.C.E.[a]: cathodic current efficiency based on weight of adherent deposit only.

References p. 329/330

Run 6. Most runs produced metal 60–70% which was of + 85 mesh size, and generally less than 4% was —300 mesh.

The deposits consisted of a mixture of powder, needles, dendrites and flake metal. Long leaf-like needles similar to those deposited from the system $\overset{+}{Ti}/LiCl\text{-}KCl/\overset{-}{Ti}$ under similar conditions of electrolysis were obtained. Growth lines on the basal planes of the hexagonal crystal flakes were similar to those observed on electrolytic titanium crystals[29].

The electrolysis technique adopted in this work was essential if pure metal was to be obtained. In other electrolyses in which an argon leak occurred or if the technique for purification of the melts was not rigorously adhered to, only impure metal was obtained.

DISCUSSION

Preliminary experiments concerned with the electrodeposition of silver from liquid ammonia solutions indicated that the apparatus functioned satisfactorily[30]. The results of the electrolyses in liquid ammonia, although disappointing, are in agreement with the observations of WOOD AND BRENNER[7]. It now seems unlikely that beryllium can be deposited from solutions of its chloride in liquid ammonia. The use of anhydrous beryllium nitrate as the solute in liquid ammonia baths, however, seems worthy of re-investigation as it has been claimed[31] that this bath may be used for the electrolytic refining of beryllium.

The investigations of the anodic dissolution and cathodic deposition of beryllium from fused-salt systems reported in this paper must be regarded as being of a preliminary nature. No detailed study of the factors affecting the form in which the metal is produced has been made. This would, however, depend on metal ion concentration, current density and temperature. Deposits containing metal of large particle size would, for example, be favoured by operation of the cell at low current density and high temperature.

Any choice as to which of the two fused-salt baths would be preferable for large scale operation would depend on economic factors and the form in which the product was required. Since the beryllium ion concentration in the LiCl–KCl bath must be built up by dissolution of metal from the anode this bath would normally operate at a comparatively low metal ion concentration which would restrict operation of the bath to low current densities. This factor and the high cost and deliquescent nature of LiCl suggests that the NaCl–$BeCl_2$ bath would probably be the more suitable for large scale operation.

The form of the metal deposited may also depend on the mechanism of the deposition process. It has been suggested[32] that the complex beryllium compound Na_2BeCl_4 and also eutectic structures are present in $BeCl_2$–NaCl melts at temperatures not far above the melting point of the bath. The formation of such complex compounds would influence the nature of the beryllium bearing ions present.

In a simple uncomplexed halide system a significant concentration of Be^{2+} ions would be expected and hence primary deposition of metal by the reaction $Be^{2+} + 2e \rightarrow Be^{\circ}$. Such a process would be controlled by the current density and metal ion concentration in the melt. The lower the degree of ionisation of the beryllium halide the more negative will be the cathodic deposition potential. The formation of ionic

References p. 329/330

complexes containing beryllium can only reduce the activity of the beryllium ions and displace the cathodic deposition potential to even more negative values. The working cathode potential may even exceed that for alkali metal deposition (*cf.* Run 3). The effective complexing of the beryllium ion can therefore lead to a change of cathodic process from primary to secondary. The degree of complexing will be sensitive to temperature and a process which is principally secondary at one temperature may be primary at another.

Little is known concerning the reduction of complex anions, even in aqueous systems but it is possible that direct electrochemical reduction of such ions could take place. Secondary reduction of beryllium compounds in solution would probably lead to powdery, partially adherent deposits. Such deposits were obtained from the system $\overline{Be}$/LiCl–KCl/$\overline{Be}$ in the early stages of deposition when the beryllium ion concentration in the melt was low. The large flake metal was always found on the outside surface of the cathode and was deposited at a later stage in the electrolyses. Such large particles are more typical of those to be expected of a product produced by a primary deposition reaction.

The change in particle size as deposition proceeds could also be due simply to a decrease in current density as the surface area of the deposit increases during electrolysis at constant current. Detailed studies of this system using, for example, polarographic and e.m.f. methods would be necessary in order to determine the deposition mechanism.

Although further work would be required to optimise the process and to establish the deposition mechanism the present work indicates that such a process could be used for the recovery of scrap beryllium[33]. This may become an important problem if beryllium is used as a canning material in advanced gas-cooled reactor systems as has been proposed[34].

ACKNOWLEDGEMENTS

The authors wish to thank the United Kingdom Atomic Energy Authority for permission to publish this work.

REFERENCES

1 L. R. Williams and P. B. Eyre, *Nuclear Eng.*, 3 (1958) 9.
2 I. E. Newnham, *Research (London)*, 11 (1958) 185.
3 G. C. Ellis, *Metallurgia*, 58 (1958) 243, 265.
4 J. M. Tien, *Trans. Electrochem. Soc.*, 89 (1946) 237.
5 T. P. Dirkse and H. T. Briscoe, *Metal Ind.*, 36 (1938) 284.
6 H. S. Booth and G. G. Torrey, *J. Phys. Chem.*, 35 (1931) 2464, 2492.
7 G. B. Wood and A. Brenner, *J. Electrochem. Soc.*, 104 (1957) 29.
8 I. A. Menzies, D. L. Hill and L. W. Owen, *Nature*, 183 (1959) 816.
9 H. S. Booth and G. G. Torrey, *J. Phys. Chem.*, 35 (1931) 3111.
10 H. S. Booth and M. Merlub-Sobel, *J. Phys. Chem.*, 35 (1931) 3303.
11 H. S. Booth, G. G. Torrey and M. Merlub-Sobel, *U.S.Pat.*, 1,893,221 (1933).
12 M. A. Klochko, *Light Metals*, 6, 64 (1943) 254; 65 (1943) 269.
13 W. Borchers, *Z. Elektrochem.*, 2 (1895) 39.
14 Kemet Laboratories Co, *French Pat.* 633,491 (1927).
15 Beryllium Development Corporation, *Brit. Pat.*, 377,858.
16 B. R. Kjellgren and C. B. Sawyer, *U.S.Pat.* 2,188,904; *Canadian Pat.* 429,726; *U.S.Pat.* 2,311,257; *Canadian Pat.* 371,194.
17 G. Jaeger, *U.S.Pat.* 1,041,131.
18 C. L. Mantell, *Industrial Electrochemistry*, 3rd Ed., McGraw-Hill, New York, 1950, p. 540.

[19] D. W. WHITE AND J. E. BURKE, *The Metal Beryllium*, American Society for Metals, Cleveland, Ohio, 1955, p. 114.
[20] G. A. MEYERSON, *Proc. Conf. on the Peaceful Uses of Atomic Energy*, New York, 1956, Vol. 8, p. 588.
[21] P. S. BRYANT, *Symposium on the Extraction Metallurgy of some of the Less Common Metals*, Inst. of Mining and Metallurgy, London, 1957, Paper No. 17.
[22] M. C. KELLS, R. B. HOLDEN AND C. WHITMAN, *Second Intern. Conf. on the Peaceful Uses of Atomic Energy*, Geneva, 1958, Paper No. 717.
[23] J. HURE, M. KREMER AND F. LE BERGUIER, *Anal. Chim. Acta*, 7 (1952) 37.
[24] R. AIROLDI, *Ann. Chim. (Rome)*, 41 (1951) 487.
[25] R. PRIBIL AND J. KUCHARSKY, *Collection Czechoslov. Chem. Communs.*, 15 (1950) 132.
[26] J. N. GREGORY, D. MAPPER AND J. S. WOODWARD, *Analyst*, 78 (1953) 414.
[27] J. N. GREGORY AND D. MAPPER, *Analyst*, 80 (1955) 225.
[28] J. N. GREGORY AND D. MAPPER, *Analyst*, 80 (1955) 230.
[29] I. A. MENZIES, *Thesis*, London, 1957.
[30] I. A. MENZIES AND L. W. OWEN, *Chem. and Ind. (London)*, 537 (1959).
[31] G. JAEGER, *Metall*, 4 (1950) 183.
[32] YU. K. DELIMARSKII, I. N. SHEIBO AND V. G. FESHCHENKO, *Zhur. Fiz. Khim*, 29 (1955) 1499.
[33] I. A. MENZIES, D. L. HILL AND L. W. OWEN, *Pat. Applic.* No. 34712/58.
[34] R. V. MOORE, H. KRONBERGER AND L. GRAINGER, *Second Intern. Conf. on the Peaceful Uses of Atomic Energy*, Geneva, 1958, Paper No. 312.

Short Communication

Seebeck coefficient of yttrium from 0° to 1000°C

The Seebeck coefficient of yttrium metal does not appear to have been previously reported*. A specimen of yttrium-swaged rod 1/16 in. in diameter and 16 in. long was made available for examination by the U.S. Bureau of Mines Station at Albany, Oregon. The rod was swaged from material with an yttrium analysis of about 99.7%. The principal impurities were oxygen, iron, chromium, and copper.

A schematic diagram of the experimental apparatus is shown in Fig. 1.

The hot junction consisted of a Pt–Pt10%Rh couple (Baker C.P. grade) twisted tightly about the yttrium rod. The connections at the cold junction were made to copper wires and placed in a bath so that all three cold junctions were at the same

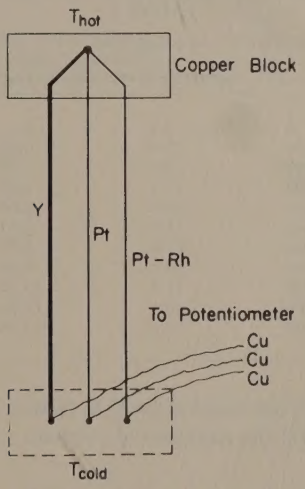

Fig. 1. Experimental apparatus, schematic.

* Two tables giving the Seebeck coefficient of yttrium are cited by A. JOFFE in *Semiconductor Thermoelements and Thermoelectric Cooling*, Infosearch, London, 1957, p. 5. One table is attributed to "JUSTI (1948)," and this has been traced to the book by E. JUSTI, *Leitfähigkeit und Leitungsmechanisms fester Stoffe*, Vendenhoeck & Ruprecht, Göttingen, 1948, p. 88. The entry of Y in JOFFE's book is an error. The entry should be Ir. Correspondence with the translator of JOFFE's book confirmed this.

The other table is attributed to MEISNER (1955), and we have been unable to find this reference. However, since the Y occurs in the same position in both JUSTI's and MEISNER's tables, it is strongly suspected that the same substitution of yttrium for iridium has been made by JOFFE.

known temperature. The hot junction was maintained in a flow of argon which was purified by passing over heated zirconium turnings.

Measurements were taken with a Leeds & Northrup Type K3 potentiometer and a Leeds & Northrup box-type galvanometer. Hot junction temperature equilibrium was checked by reading Y–Pt, Pt–PtRh, and PtRh–Y e.m.f.'s in quick succession. A reading was taken as stable when the sum of the readings came within a microvolt of zero. Both ascending and descending temperature readings were obtained.

The data were examined by the method of least squares. In the region from 50°–1000°C the dependence was found to be

$$E = -0.0244 + 4.486 \cdot 10^{-3}T + 1.318 \cdot 10^{-5}T^2 - 5.568 \cdot 10^{-9}T^3 + 3.109 \cdot 10^{-12}T^4$$

for the region 0°– 60°C the data fitted the polynomial

$$E = 3.12 \cdot 10^{-3}T - 3.60 \cdot 10^{-4}T^2 + 4.05 \cdot 10^{-7}T^3$$

where E is in mV and T is in °C.

The values of the thermal e.m.f. and the Seebeck coefficient obtained by differentiation of the above expression for the range 0° to 1000°C are shown in Table I. The e.m.f. data are probably accurate to $\pm$ 10 μV/°C.

TABLE I

SEEBECK COEFFICIENT AND THERMAL E.M.F. OF YTTRIUM

T(°C)	*a(μV/°C) vs. Pt*	*E$_s$(mV) vs. Pt*
0	+ 3.1	0
100	7.0	+ 0.55
200	9.2	1.36
300	11.2	2.38
400	13.2	3.60
500	15.0	5.01
600	17.0	6.61
700	19.0	8.41
800	21.2	10.42
900	23.7	12.67
1000	26.5	15.81

The authors wish to thank personnel of the U.S. Bureau of Mines Station at Albany, Oregon, for kindly furnishing the specimen of yttrium.

Westinghouse Research Laboratories,
Pittsburgh, Pa. (U.S.A.)

H. A. JOHANSEN
R. C. MILLER

Received June 20th, 195

CONTENTS

The solution chemistry of rhodium(III) in 6 *N* HCl
by A. M. KRISTJANSON AND M. LEDERER (Paris) 245

The study of rhodium(III) complexes by paper electrophoresis and ion exchange chromatography. IV. The solution chemistry of rhodium sulphates
by S. K. SHUKLA AND M. LEDERER (Paris) 255

Reactions of ortho-esters of titanium. Part I. Reactions between isopropyl titanate and acetyl bromide
by I. D. VERMA AND R. C. MEHROTRA (Gorakhpur) 263

The fabrication and properties of ruthenium
by D. W. RHYS (London) 269

The systems palladium–indium and palladium–tin
by J. R. KNIGHT AND D. W. RHYS (London) 292

The compound Bi_4Rh
by R. G. ROSS AND W. HUME-ROTHERY (Oxford) 304

A note on transformations in metallic cerium
by R. T. WEINER AND G. V. RAYNOR (Birmingham) 309

Some observations on thorium-rich thorium–indium alloys
by J. R. MURRAY (Harwell) 314

The electrodeposition of beryllium from non-aqueous solutions
by I. A. MENZIES, D. L. HILL AND L. W. OWEN (Aldermaston) 321

Short Communication

Seebeck coefficient of yttrium from 0° to 1000°C
by H. A. JOHANSEN AND R. C. MILLER (Pittsburgh, Pa) 331

All rights reserved

ELSEVIER PUBLISHING COMPANY, AMSTERDAM

Printed in The Netherlands by

NEDERLANDSE BOEKDRUK INRICHTING N.V., 'S-HERTOGENBOSCH

FILED IN STACKS

ELSEVIER'S

SCIENTIFIC JOURNALS

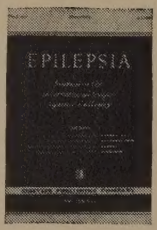

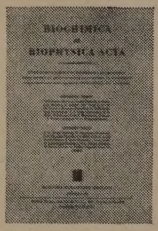

ANALYTICA CHIMICA ACTA

BIOCHIMICA ET BIOPHYSICA ACTA

JOURNAL OF CHROMATOGRAPHY

CLINICA CHIMICA ACTA

JOURNAL OF ELECTROANALYTICAL CHEMISTRY

EPILEPSIA

ICSU REVIEW

TROPICAL AND GEOGRAPHICAL MEDICINE

WEAR - USURE - VERSCHLEISS

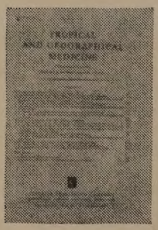

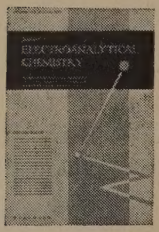

Specimen copies are available

ELSEVIER PUBLISHING COMPANY
110-112 SPUISTRAAT — AMSTERDAM — THE NETHERLANDS